

# The role of macrophages and apoptotic cell clearance in the maintenance of liver tolerance

Dissertation with the aim of achieving a doctoral degree (Dr. rer. nat) at the Faculty of  
Mathematics, Informatics and Natural Sciences

Department of Biology

University of Hamburg

Submitted by Amirah Al jawazneh

Hamburg, June 2022

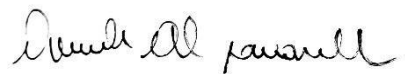
Day of oral defence: 28.9.2022

Gutachter: Prof. Tim Gilberger

Gutachter: PD Dr. Thomas Jacobs

## **Statutory declaration / Eidesstattliche Versicherung**

Hiermit erkläre ich an Eides statt, dass ich die vorliegende Dissertationsschrift selbst verfasst und keine anderen als die angegebenen Quellen und Hilfsmittel benutzt habe.

A handwritten signature in black ink, appearing to read "David Al. Jansell". The signature is written in a cursive style with some loops and flourishes.

Hamburg, den 13.06.2022

## Nachweis über die Korrektheit der Sprache

Hiermit bestätige ich, Madeleine Hamley, geb. 02.10.1991 in London, dass die vorliegende Dissertation „The role of macrophages and apoptotic cell clearance in the maintenance of liver tolerance“ sprachlich korrekt ist.

Hamburg, den 10.06.2022

A handwritten signature in black ink, appearing to read 'M. Hamley', written over a horizontal line.

(Ort, Datum und Unterschrift)

## Acknowledgment

I would like to thank Prof. Tim Gilberger for the work of supervision during my PhD, without which it would not have been possible to write my doctoral thesis. I want to thank Thomas Jacobs for the great opportunity to work at the BNITM, the support and discussion of my work.

My thanks go to all the members of my lab, especially Imke Liebold and Madeleine Hamley, who supported me during all the stages of my PhD. A special thanks goes to Imke Liebold for all the scientific discussions, the emotional support and the friendship that we created during these years. Thanks also to Stephanie Leyk and Clarissa Lanzloth for their help during all the experiments.

I would like to thank Lidia Bosurgi for the opportunity to work in her group, the freedom to develop my project and the all her supervision during all the steps of my PhD. Grazie per aver creduto in me.

Many thanks go to my colleagues at the BNITM, who made me feel welcome from the first day. Especially to Ulricke Richards, Cari Lehmann and Mathias Riehn for the answers to all my questions. Furthermore, I would like to thank Johannes Brandi and Birgit Hüsing for the technical support.

Special thanks go to Stella, Cassandra and all my friends in Italy and in Hamburg that were always there for me when I needed them. In particolare ci tengo a ringraziare mia madre che mi e sempre stata vicino in tutte le fasi della mia vita. Ringrazio di cuore Luigi e mia sorella Sibilla per essere sempre stati al mio fianco.

---

## Table of contents

Statuary declaration / Eidesstattliche Versicherung .....	I
Nachweis über die Korrektheit der Sprache .....	II
Acknowledgment .....	III
Abbreviations .....	VI
List of figures .....	VIII
List of Tables .....	IX
Abstract.....	X
1. Introduction .....	1
1.1 The immune system – a general overview .....	1
1.2 Macrophages .....	2
1.2.1 Macrophage distribution in the tissues .....	2
1.2.2 Polarization of macrophages .....	4
1.2.3 Phagocytosis .....	6
1.2.3.1 The phosphatidylserine-dependent phagocytosis of apoptotic cells .....	8
1.3 Apoptosis .....	10
1.4 The liver as an immunogenic organ .....	12
1.4.1 Anatomy of the liver .....	12
1.4.2 Bile acids .....	13
1.4.3 Kupffer cells – the liver-resident macrophages .....	14
Aim of the study .....	20
2. Material .....	21
2.1 Laboratory equipment .....	21
2.2 Chemical reagents .....	21
2.3 Glass and plastic consumables .....	22
2.4 Media and buffer .....	23
2.5 Commercially available kits .....	24
2.6 Software .....	24
2.7 Antibodies .....	25
2.7.1 Antibodies .....	26
2.8 Primer sequences for qPCR .....	27
2.9 Cell lines .....	27
2.10 Mice strains .....	28
3. Methods .....	29
3.1 Cell culture .....	29
3.2 Hepa 1-6 culture .....	29
3.3 Jurkat cell culture .....	29
3.4 H69 cell culture .....	29
3.5 Cell count .....	30

---

3.6 Isolation of bone marrow-derived macrophages .....	30
3.7 Isolation of neutrophils.....	30
3.8 Induction of apoptosis.....	30
3.9 Apoptotic cell staining with Annexin V and PI.....	31
3.10 Phagocytosis assay.....	31
3.11 Apoptotic cell dyes.....	31
3.12 Flow cytometry.....	32
3.13 Fluorescence-activated cell sorting (FACS) .....	32
3.14 t-distributed stochastic neighbour embedding (tSNE) .....	33
3.15 Competitive phagocytosis assay .....	33
3.16 Imaging and quantification.....	33
3.17 RNA isolation and quantitative real-time PCR analysis.....	34
3.18 Mice .....	35
3.19 Genotyping of <i>Mdr2</i> <sup>-/-</sup> and <i>Mdr2</i> <sup>+/+</sup> mice .....	35
3.20 Cell isolation from different organs .....	36
3.21 Isolation of macrophages from the liver.....	36
3.22 Kupffer cell isolation.....	37
3.23 Isolation of peritoneal macrophages.....	37
3.24 Isolation of macrophages from the spleen.....	37
3.25 Bile acid measurement .....	38
3.26 Isolation of peripheral blood mononuclear cells (PBMCs) using Ficoll density gradient. ....	38
3.27 Purification of CD14 <sup>+</sup> cells from PBMCs.....	38
3.28 Statistics .....	39
4. Results .....	40
4.1 Phagocytic receptor expression is downregulated in liver MOs from <i>Mdr2</i> <sup>-/-</sup> mice and correlates with an impaired ability to phagocytose apoptotic cells.....	40
4.2 The uptake of apoptotic cells with different identities is mediated by distinct phagocytic receptors .....	47
4.3 Bile acids can modulate the phagocytic receptor expression and the phagocytosis capacity in liver MOs.....	50
4.4 Bile acids accumulate in liver MOs and impair their ability to phagocytose apoptotic cells .....	52
4.5 Characterization of phagocytic receptor expression on human monocytes during primary sclerosing cholangitis.....	58
5. Discussion .....	62
5.1 The downregulation of phagocytic receptors leads to an accumulation of apoptotic cells.....	62
5.2. The engagement of phagocytic receptors is mediated by the identity of the apoptotic cell .....	68
5.3 Bile acids can alter the phagocytic ability of macrophages .....	70
5.4 The relevance of proper phagocytosis in the liver of PSC patients.....	73
6. Future perspectives .....	75
References .....	77

## Abbreviations

AC: Apoptotic cells

aH: Apoptotic hepatocyte

AM: Axl and MERTK

aN: Apoptotic neutrophil

APC: Antigen-presenting cell

Arg1: Arginase 1

aT: Apoptotic thymocytes

ATP: Adenosine triphosphate

BMDMs: Bone marrow-derived macrophages

CD: Cluster of differentiation

Cre: Cre-recombinase

CSF1/CSF1-R: Colony stimulation factor 1 /-Receptor

DAMPs: Damage-associated molecular patterns

DC: Dendritic cell

DNA: Deoxyribonucleic acid

Ear2 Eosinophil cationic protein 2

f/f: Flox/flox

Fas-L: Fas ligand (CD95L)

Fc: Fragment crystallisable region

FGF: Fibroblast growth factor

FSC: Forward scatter

G: Gravitational force equivalent

H: Hours

IFN $\gamma$ : Interferon gamma

IL: Interleukin

iNOS: Inducible nitric oxide synthase

KC: Kupffer cell

MERTK: Mer tyrosine kinase

Min: Minutes

mL: Millilitre

mRNA: Messenger ribonucleic acid

MS: Multiple sclerosis

MO: Macrophage

Nf- $\kappa$ B: Nuclear factor-kappa B



## Abbreviations

---

NK: Natural killer cell  
PAMPs: Pathogen-associated molecular patterns  
PBMC: Peripheral blood mononuclear cells  
PBS: Phosphate buffered saline  
PCR: Polymerase chain reaction  
PDGF: Platelet-derived growth factor  
PI: Propidium Iodide  
PROS1: Protein s1  
PRR: Pattern recognition receptors  
PSC: Primary sclerosing cholangitis  
PtdSer: Phosphatidylserine  
PtdSer-R: Phosphatidylserine- Receptor  
qPCR: Quantitative real time PCR  
RNA: Ribonucleic acid  
RNase2: Ribonuclease A family member 2  
Sec: Seconds  
SEM: Standard error of the mean  
SOCS: Suppressor of cytokine signalling  
SSC: Side scatter  
TF: Transcription factor  
TFG $\beta$ : Transforming growth factor beta  
Th: T helper cell  
TSP1: Thrombospondin 1  
TIM-4: T cell immunoglobulin and mucin domain containing 4  
TLR: Toll like receptor  
TNF $\alpha$ : Tumor necrosis factor  $\alpha$   
Treg: Regulatory T cell

## List of figures

### Introduction

Fig.1: Apoptotic cell “eat me signals” and phagocytic receptors.....	11
Fig.2: The role of Kupffer cells during liver disease.....	17
Fig.3: General overview of the pathophysiology of primary sclerosing cholangitis.....	18

### Results

Fig.1: The frequencies of resident and infiltrating macrophages is comparable between <i>Mdr2</i> <sup>-/-</sup> and <i>Mdr2</i> <sup>+/+</sup> mice.....	41
Fig. 2: Phenotypical characterization of resident and infiltrating liver MOs in 8-weeks old <i>Mdr2</i> <sup>-/-</sup> mice compared to the controls ( <i>Mdr2</i> <sup>+/+</sup> ) .....	42
Fig. 3: Phenotypical characterization of resident and infiltrating liver MOs in 12-weeks old <i>Mdr2</i> <sup>-/-</sup> mice compared to the controls ( <i>Mdr2</i> <sup>+/+</sup> ) .....	43
Fig. 4: Phenotypical characterization of resident and infiltrating liver MOs in 25-weeks old <i>Mdr2</i> <sup>-/-</sup> mice compared to the controls ( <i>Mdr2</i> <sup>+/+</sup> ) .....	44
Fig. 5: Apoptotic cells are present in the liver of <i>Mdr2</i> <sup>-/-</sup> mice during the course of the disease. ....	45
Fig. 6: MOs isolated from the liver of <i>Mdr2</i> <sup>-/-</sup> have a reduced capacity to phagocytose apoptotic T cells <i>in vitro</i> .....	46
Fig. 7 The phagocytosis of apoptotic cells is mediated by different phagocytic receptors <i>in vitro</i> .....	48
Fig. 8: When exposed concomitantly to apoptotic cells with different identities, MOs preferentially phagocytose one type of apoptotic cell at the time .....	49
Fig. 9: TLCA treatment downregulates the phagocytic receptor expression without affecting their viability <i>in vitro</i> .....	51
Fig. 10: Liver MOs show a reduced phagocytic capacity after TLCA treatment <i>in vitro</i> .....	51
Fig. 11: The bile acid receptors <i>Fxr</i> and <i>Tgr5</i> are downregulated in liver macrophages of <i>Mdr2</i> <sup>-/-</sup> mice.....	52
Fig. 12: Bile acids accumulate in phagocytic receptor-enriched <i>Mdr2</i> <sup>-/-</sup> mice liver MOs .....	53
Fig. 13: Characterization of the bile acid profile in phagocytic receptor-enriched and -deficient <i>Mdr2</i> <sup>-/-</sup> mice liver MOs .....	54
Fig. 14: Bile acids can accumulate inside MOs that have been phagocytosed bile acid-treated-aH.....	56
Fig. 15: MOs exposed to TLCA-treated hepatocytes are shown to have a decreased phagocytic rate.....	57
Fig. 16: Frequencies of classical and non-classical monocytes in PBMCs isolated from PSC patients and healthy donors .....	59
Fig. 17: Phagocytic receptor expression in classical and non-classical monocytes in PSC patients and HDs.....	59
Fig. 18: The phagocytic capability of peripheral monocytes is not impaired in PSC patients .....	60

## List of Tables

### Material and methods

Table 1: Laboratory equipment and companies .....	21
Table 2: Chemical and molecular biology reagents.....	21
Table 3: Plastic and glass consumables .....	22
Table 4: Media and buffers.....	23
Table 5: Kits.....	24
Table 6: Software.....	24
Table 7: Mouse antibody specifications.....	25
Table 8: Human antibody specifications.....	26
Table 9: Mouse primers.....	27
Table 10: Eukaryotic cell lines .....	27
Table 11: Mouse strains .....	28

## Abstract

Phagocytosis is a process that contributes to the maintenance of homeostatic conditions in the body via the recognition and engulfment of apoptotic cells generated under physiological conditions or as result of tissue damage. Macrophages are professional phagocytic cells adorned with a variety of phagocytic receptors which guarantee the proper clearance of dying cells. However, dysregulation in the phagocytic receptor expression can lead to failure in the process of dead cell clearance and is associated with the exacerbation of several autoimmune diseases. Phagocytosis of apoptotic cells by macrophages constitutes a critical immune signal, not only for dying cells and debris, but, most importantly, for regulating macrophage function and the re-establishment of homeostasis upon different types of tissue damage. The liver is an immunologically tolerant organ in which macrophages are defined as a heterogenous population of immune cells that account for the largest non-parenchymal cell population. Changes in the regulation of the functional activity of liver macrophages are associated with chronic inflammation and several liver diseases, including NASH, liver fibrosis and hepatocellular carcinoma. The present study demonstrates that an alteration in the phagocytic capacity of macrophages occurs in the liver of *Mdr2*<sup>-/-</sup> mice, a model of primary sclerosing cholangitis (PSC), a cholestatic autoimmune disease characterised by progressive inflammation and fibrosis. PSC patients are reported to have altered levels and composition of bile acids, which characterise the course of the disease. Here, a connection is formed between the dysregulated bile acid pool and the reduction in the phagocytic capacity of liver macrophages. Furthermore, the bile acid profile of *Mdr2*<sup>-/-</sup> mice was investigated and an innovative phagocytosis-dependent mechanism of bile acid accumulation inside macrophages was demonstrated. The data in this thesis also demonstrate that the accumulation of bile acids inside macrophages significantly decreased their ability to further uptake apoptotic cells, thereby contributing to the presence of unremoved apoptotic bodies in the liver and sustaining the inflammation. In addition, in order to validate the data obtained in the mouse model in a human context, PBMCs were isolated from PSC patients and healthy donors as controls, and the phagocytic receptor expression and phagocytic capacity was assessed in the monocyte subset. However, no differences were found in the frequency of phagocytic receptors in monocytes from PSC patients. Accordingly, the normal expression of phagocytic receptors correlates with a functional phagocytic capability in circulation, suggesting the alteration in the macrophage phagocytosis is liver-related.

In conclusion, the present data indicate that in the liver, a bile acid-mediated alteration in the phagocytic machinery operated by macrophages occurs during the course of PSC. This results in defective apoptotic cell clearance, thereby contributing to progressive liver inflammation. These findings reveal the importance of proper phagocytosis in the maintenance of liver tolerance and lay the foundations for a deeper analysis on the role of macrophages during cholestatic diseases.

# 1. Introduction

## 1.1 The immune system – a general overview

The innate immune system is defined as an evolutionarily conserved host defence system <sup>1</sup>. It provides an immediate and non-specific defence against pathogens, including the identification of foreign antigens and the clearance of dead cells. Innate defence mechanisms are activated in the early phase of the immune response to respond to perturbations like infections, genotoxic insults and tissue damage via germline-encoded receptors known as pattern recognition receptors (PRRs e.g. Toll-like receptors-TLRs) <sup>2</sup>. When a pathogen persists, the adaptive immune system is recruited, providing highly specific and long-lasting immunity. PRRs are expressed on innate immune cells, such as dendritic cells (DCs), macrophages, neutrophils and epithelial cells, and allow the recognition of two distinct classes of molecules: damage-associated molecular patterns (DAMPs), mainly associated with cell death or damage in host structures (e.g. ATP, uric acid, heparin sulfate) and pathogen-associated molecular pattern (PAMPs) related to pathogens with microbial origins (e.g. microbial nucleic acids, including DNA and double-stranded RNA (dsRNA)) <sup>3</sup>. Toll-like receptors (TLRs) are transmembrane proteins responsible for the recognition of DAMPs, the subsequent secretion of cytokines and activation of both the innate and adaptive immune responses <sup>4</sup>. Innate immune cells, both of lymphoid and myeloid origin, can orchestrate the immune response and exert antimicrobial and tissue protective functions <sup>5</sup>. In general, macrophages, neutrophils, DCs and innate lymphoid cells (ILCs) are considered to be an integral part of the innate immune system. Natural killer (NK) cells are classified as group I ILCs, owing to their immunological function of recognising virally infected and tumour cells. <sup>6</sup>

Phagocytosis is a specific tissue protective function that encompasses the recognition, engulfment and digestion of pathogens and dying cells and promotes the secretion of anti-inflammatory cytokines <sup>7 8</sup>. Macrophages, neutrophils and DCs not only take part in phagocytosis, but can also act as antigen-presenting cells (APCs) and therefore trigger the activation of the adaptive immune system. APCs can process a protein antigen via its fragmentation into peptides and present it to other cells in conjunction with major histocompatibility complex (MHC) molecules. On the one hand, antigen presentation via MHC class II molecules allows the interaction with CD4<sup>+</sup> helper T cells, leading to T cell activation and the release of IL-2. On the other hand, presentation via MHC class I molecules leads to an interaction with cytotoxic CD8<sup>+</sup> T cells. Other APCs include B cells, keratinocytes, endothelial cells and Kupffer cells. In

this group of APCs, the antigen is processed in the endosomal compartment and presented via MHC II molecules <sup>9</sup>.

The immune system is able to activate tolerogenic pathways in order to prevent immune responses against self-antigens that may lead to autoimmunity <sup>10</sup>. Macrophages exert a key role in this process, preventing the accumulation of free apoptotic material, suppressing inflammatory cytokine production and interacting with other immune cells in order to maintain homeostatic conditions in the body.

### **1.2 Macrophages**

#### **1.2.1 Macrophage distribution in the tissues**

Macrophages are widely distributed throughout the body and are present in all vertebrate tissues. Their functions do not only extend to the engulfment and processing of apoptotic cells, but also to tissue repair and the maintenance and re-establishment of tissue homeostasis in response to external stimuli. Macrophages arise from myeloid cells from primary lymphoid organs during both embryonic and adult haematopoiesis, and are classified accordingly as yolk-sac-derived macrophages (YS-MOs) during the embryonic phase, fetal liver monocytes (FL-MOs), and bone marrow-derived monocytes (BMDMs). YS-MOs and FL-MOs can spread throughout all tissues during the embryonic phase and give rise to populations of self-maintaining, resident macrophages. BMDMs originate from the stem cells in the bone marrow and they continuously replenish blood monocytes during the life span <sup>11</sup>. In the adult phase, BMDMs can be recruited after inflammation and secure the turn-over of different macrophage niches in the tissues <sup>12</sup>. In line with this, Lavin and colleagues have shown that transplanted adult BMDMs can acquire a tissue-specific epigenomic profile in different organs of the host after engraftment, highlighting the role of the tissue microenvironment in the establishment of the macrophage identity <sup>13</sup>. In the intestine, circulating monocytes can maintain the resident macrophages in a CCR2-dependent-manner and *Ccr2*<sup>-/-</sup> mice show a reduction in these macrophage populations <sup>14</sup><sup>15</sup>. However, in other tissues, such as the liver (Kupffer cells), brain (microglia) and epidermis (Langerhans cells), macrophages do not undergo external replacement in steady state conditions after birth <sup>16</sup> <sup>17</sup>.

Macrophages in different organs can be identified through the expression of different surface molecules, as a consequence of the heterogeneous expression of antigens <sup>18</sup>. In the spleen, macrophages can be identified depending on the different organ compartments and zonation, which give rise to a specific microenvironment. Red pulp macrophages specifically express F4/80<sup>+</sup>VCAM1<sup>+</sup>CD11b<sup>lo</sup> and one of their

main functions is to clear senescent red blood cells and take part in the defence against circulatory bacterial infections<sup>19 20</sup>. In the white pulp, macrophages are known for their phagocytic capabilities. Here, macrophages are F480<sup>neg</sup>CD68<sup>+</sup> and express high levels of phagocytic receptors such as MERTK, TIM4 and CD36, enhancing their role as homeostatic regulators.<sup>19 21</sup> Furthermore, after myocardial infarction (MI), the observation of an increased number of spleen-derived Ly6C<sup>high</sup> monocytes in the blood suggests that this organ plays a key role as a reservoir for recruitable monocytes at distant sites, sustaining both the innate and adaptive immunity throughout the body<sup>22</sup>.

Intestinal macrophages are present in the whole gastrointestinal tract, in which complex interactions with the microbial flora occur. This symbiotic interaction allows macrophages and other APCs to interact with the content in the gut lumen to elicit tissue-protective responses.<sup>23</sup> Gut-resident macrophages (gMacs) are a highly heterogeneous group of cells, located in different layers of the intestine and characterised by the expression of CX3CR1. In the lamina propria (LP), macrophages are known for their high phagocytic ability and subsequent IL-10 production in order to maintain gut homeostasis. Indeed, IL-10<sup>-/-</sup> mice spontaneously develop intestinal inflammation and resident CX3CR1<sup>high</sup> macrophages gain migratory and pro-inflammatory signatures in an IL-10-deficient environment<sup>24</sup>. However, other populations of macrophages which are functionally distinct depending on the niche in where they reside also exist. CD169<sup>+</sup> macrophages, located at the bottom end of the LP, recruit inflammatory monocytes in a CCL8-dependent fashion and the selective depletion of these macrophages ameliorates the symptoms of dextran sodium sulfate (DSS)-induced colitis in mice<sup>25</sup>. Of note, single cell transcriptional profile analysis has shown the unique expression of genes related to tissue support processes, such as angiogenesis and epithelial cell differentiation, in self-maintaining gMacs compared to monocyte-replaced ones<sup>26</sup>.

In the mouse peritoneal cavity, two different subsets of macrophages coexist. These subsets, defined as small peritoneal macrophages (SPMs) and large peritoneal macrophages (LPMs) are phenotypically distinct based on the expression of the classical macrophage markers CD11b and F4/80. Specifically, SPMs are characterised by a lower expression of these markers, but instead express MHCII, which is not present on LPMs<sup>27</sup>. Microarray analysis revealed a unique regulator of anatomical localisation in peritoneal macrophages, the zinc finger transcription factor GATA6. Gata6 depletion in mouse macrophages resulted in a dramatic reduction in LPMs without affecting their proliferative status<sup>28</sup>.



LPMs expressing GATA-6 are maintained in the peritoneal cavity through self-renewal and can be recruited to the liver after injury. Here, they acquire a tissue remodelling phenotype and function as a reservoir for hepatic macrophages <sup>29 30 31</sup>.

In the lung, high oxygen levels can contribute to local injury and inflammation. Lung macrophages have been shown to have specific functions in the removal of dust, pollutants and microbes through the expression of the mannose receptors CD206, which recognises microbial carbohydrates, and MARCO (macrophage receptor with collagenous structure) for particle clearance <sup>32 33</sup>. Lung macrophages express high levels of CD11c and are CD11b<sup>low</sup>F4/80<sup>hi</sup>MHCII<sup>low</sup>SIRP $\alpha$ <sup>hi</sup>CD64<sup>hi</sup> and Ly6C<sup>low</sup> <sup>34</sup>. The granulocyte macrophage colony-stimulating factor (GM-CSF) and the autocrine production of transforming growth factor-beta (TGF- $\beta$ ) induce the transcription factor PPR gamma (PPR- $\gamma$ ), which is crucial for the development of fetal monocytes to alveolar macrophages (AM). Indeed, the conditional knock-out of TGF- $\beta$ R leads to impaired differentiation of AMs without affecting the interstitial population of macrophages in the lung <sup>35 36</sup>. AMs are responsible for the immune response against inhaled pathogens and the subsequent production of pro-inflammatory cytokines and neutrophil recruitment. However, in order to prevent injury, AMs are able to establish an immunosuppressive intercommunication in the lung epithelium via connexin 43 (Cx43)-containing gap junctional channels (GJCs) and the depletion of Cx43 in AMs increases the level of lung inflammation and injury following intranasal administration of LPS, highlighting the protective role of AM-epithelium GJCs <sup>37</sup>.

### 1.2.2 Polarization of macrophages

In different tissues, macrophages are able to maintain and re-establish homeostasis through the production of cytokines and chemokines, and exert their function and phenotype depending on the surrounding environment <sup>38</sup>. Mills and colleagues described two different subsets of macrophages that had two opposing functional peculiarities: killing and healing <sup>39 40 41</sup>. Depending on the stimuli, described in more detail below, classically activated macrophages can induce the inducible NO synthase (iNOS) that leads to the production of citrulline and toxic NO. In humans, iNOS expression is especially strong in inflamed tissues, while the levels of monocyte-derived macrophages in the blood are low. <sup>42 43 44</sup>. Classically activated macrophages are defined according to their prototypical inflammatory response. Three main categories of stimuli are responsible for triggering this phenotype: interferon-gamma (IFN- $\gamma$ ), LPS and GM-CSF. IFN- $\gamma$ , recognised by IFN- $\gamma$  receptors (IFNR) on the macrophage surface, recruits

the Janus kinases (JAK) 1 and 2, that in turn activate STAT1 (signal transducers and activators of transcription) and regulate the expression of cell activation markers (e.g. CD38), cell adhesion molecules (e.g. ICAM-1, VLA-4) and cytokine receptors (e.g. GM-CSF-receptor, IFNR)<sup>45</sup>. LPS is the best characterised pro-inflammatory stimulus of microbial origin. It leads to the activation of a variety of pro-inflammatory cytokines (e.g. TNF, IL-6, IL-12) in a TLR4-dependent (classical activation) or independent manner (via inflammasomes)<sup>46</sup>. Finally, GM-CSF, which is produced by a wide variety of cells, enhances not only the activity of macrophages against microbes, but also adhesion, antigen presentation and the upregulation of the activation markers CD86 and F4/80. This in turn, downregulates the expression of CD11b via the recruitment of JAK2 and the activation of STAT5<sup>47</sup>. Alternatively activated macrophages metabolise L-arginine into ornithine and urea via the arginase pathway, and mediate many repair processes, cell proliferation and collagen biosynthesis<sup>40</sup>. IL-4, IL-13, glucocorticoids and IL-10 positively polarise the macrophages to antagonise inflammation<sup>48</sup>. IL-4 and IL-13 are the prototypical signals that shape the macrophages into an anti-inflammatory phenotype<sup>49</sup>. Specifically, IL-4, which is produced by Th2 cells, basophils and eosinophils, is recognised by receptor complexes and mediates its effect via several downstream signalling events<sup>50</sup>, supporting tissue integrity and healing<sup>48</sup>. IL-4 can bind three different receptor pairs on the macrophage surface. IL-4R $\alpha$ 1 can bind IL-4 via the common gamma chain ( $\gamma$ c) or IL-4 or IL-13 can bind by pairing with the IL13R $\alpha$ 1 chain. IL-4-receptor binding activates JAK1 and JAK3 and induces the translocation of STAT6. The result is the upregulation of anti-inflammatory genes including *transglutaminase 2* (TGM2), *Mrc1*, the transcription factors *Irf4* and Krüpper-like factor 4 (*Klf4*), as well as other signalling modulators such as *Socs1* in humans and genes such as *Chil3*, *Retnla* and *Arg1* in mouse<sup>51</sup>. IL-13, mainly secreted by activated Th2 cells, mediates its effect via a complex receptor system comprised of IL-4 $\alpha$ 1 and the IL-13 binding proteins IL-13 $\alpha$ 1 and IL-13 $\alpha$ 2<sup>52</sup>. IL-13 triggers the upregulation of the mannose receptor CD206 and can sustain the anti-inflammatory phenotype of macrophages via the induction of *Arg1 in vitro*. Nevertheless, IL-13 cannot compensate for the induction of *Arg1* by IL-4 *in vivo*, as shown in IL-4-deficient mice<sup>49</sup>. Glucocorticoids and IL-10 also play a role in shaping the alternatively activated phenotype in macrophages. Glucocorticoids induce the expression of anti-inflammatory-related genes like *Cd163*, *Mrc1* and *Il-10* and can antagonise the LPS and IFN- $\gamma$  pathways after long term exposure<sup>53</sup>, while IL-10 mediates the inhibition of a pro-inflammatory cytokine profile in macrophages. Indeed, IL-10-deficient mice spontaneously develop inflammatory bowel disease<sup>54</sup>. However, high resolution

approaches on human macrophages with diverse activation signals suggest that the complexity of the macrophage activation status cannot be defined by a dichotomous approach alone <sup>55</sup>. The outcome is dependent on cytokines and growth factors released into the local tissue microenvironment in an input-specific fashion <sup>56,29</sup>. Interestingly, studies on different tissue macrophages have shown that their activation status is not only dependent on the surrounding environment, but also their ontogeny. In the intestine, LPS-stimulated monocyte-derived macrophages maintain an immunosuppressive profile and express IL-10-related genes <sup>57</sup>. In contrast, LPS-activated fetal liver-derived alveolar macrophages lose their ability to suppress T cell proliferation <sup>58</sup>. Hence, macrophages can be defined as a plastic and heterogeneous group of cells based on their ability to shape their phenotype and function.

### 1.2.3 Phagocytosis

Phagocytosis is a process that mediates the engulfment and internalisation of particles larger than 0.5  $\mu\text{m}$  via a membrane-bound vesicle, the phagosome. Phagocytes are divided into “professional phagocytic cells”, such as macrophages, dendritic cells and neutrophils, and “nonprofessional phagocytic cells” like epithelial cells, which can also mediate the engulfment of the apoptotic meal in tissues <sup>59</sup>. This process encompasses the *in situ* migration of phagocytes to the target and its recognition via a broad range of phagocytic receptors and “eat me” signals on the surface of apoptotic cells. Phagocytosis is normally considered a silent immunological process, characterised by its non-inflammatory features. However, an imbalance between tolerogenic and immunogenic cell clearance results in the manifestations of several autoimmune diseases, as rheumatoid arthritis (RA), diabetes type 1, systemic lupus erythematosus (SLE) and multiple sclerosis (MS) <sup>60 61</sup>. This underlines the importance of phagocytosis for a proper functionality of the immune system.

Phagocytosis is not only carried out by tissue-resident cells, but also by circulatory phagocytes. The regulation of the phagocytes' migration is based on “find me” signals released by the apoptotic meal. Several “find me” signals have been reported up to now, including fractalkine, sphingosine-1-phosphate (S1P), lysophosphatidylcholine (LPC) and the nucleotides ATP and UTP <sup>62 63 64 65</sup>. Fractalkine, a chemokine and intracellular adhesion molecule, can be released by apoptotic cells and efficiently induce chemotaxis in macrophages via the fractalkine receptor CX3CR1 <sup>64</sup>. S1P and LPC are bioactive lipids that stimulate the expression of the G-protein-coupled receptors S1P-R1 and G2A, respectively, that promote the attraction of the phagocytes <sup>66 67</sup>. The nucleotides ATP and UTP, which are released during

the early phase of apoptosis by dying cells, can create a gradient that attracts monocytes via the ATP/UTP receptor P2Y<sub>2</sub><sup>65</sup>. The effect of ATP, however, is not only driven by direct action on the phagocytes, but also via its catabolic derivatives (e.g. ADP, AMP) that exert their immunoregulatory role via activation of the G-protein-coupled adenosine receptors A<sub>2a</sub>, A<sub>2b</sub> and A<sub>3</sub>, which are abundantly expressed by macrophages<sup>68 69</sup>. Specifically, Murphy and colleagues studied the role of CD73, a 5'-ecto-nucleotidase which is expressed in lung and peritoneal macrophages, in the conversion of AMP to adenosine. AMP is released by apoptotic cells, and its conversion to adenosine leads to a suppression of TNF production during efferocytosis.<sup>70</sup> After attracting the phagocyte, apoptotic cells express several "eat me" signals that are recognised via phagocytic receptors on the macrophage surface and lead to the phagocytosis of the apoptotic cell. The best characterised "eat me" signal on the apoptotic cell surface is phosphatidylserine (PtdSer)<sup>71 72</sup>. PtdSer is stored in the inner leaflet of the lipid bilayer and becomes exposed on the outer leaflet of the membrane during the apoptosis process.<sup>73 74</sup> The mechanism of the PtdSer exposure is partially mediated by Ca<sup>2+</sup>-dependent phospholipid scramblases that allow the transport of phospholipids in two directions. Once PtdSer is exposed on the cell membrane, it can be recognised either directly via PtdSer-dependent receptors or indirectly via bridging molecules (e.g. GAS6, PROS1). Furthermore, the presence of the intracellular proteins Annexin I and Calreticulin can colocalise with PtdSer in order to trigger a more efficient phagocytosis<sup>75 76</sup>. Other "eat me" signals can be expressed on the apoptotic cell surface as the expression of the intercellular adhesion molecule 3 (ICAM3), oxidised low-density lipoprotein (LDL)-like moiety<sup>77 78</sup>, the change in cell-surface charge or the binding of plasma protein on the cell membrane<sup>79</sup>. This leads to downstream signalling events essential for the cytoskeletal rearrangement, engulfment and digestion of the apoptotic cell<sup>8</sup>. After engulfment, phagocytes enforce an immunological procedure to maintain or re-establish tissue homeostasis upon damage and to contain the inflammatory response via the production of anti-inflammatory cytokines (e.g. TGF $\beta$ , IL-10, platelet-activating factor (PAF) and prostaglandin E<sub>2</sub> (PGE<sub>2</sub>)<sup>80 81</sup>, which in turn leads to a suppression of the production of pro-inflammatory cytokines (e.g. TNF- $\alpha$ , IL-1 and IL-12)<sup>82</sup>. Anti-inflammatory cytokines can induce a specific T-cell response, such as the differentiation of regulatory T cell and Th<sub>2</sub> cells. The recognition of PtdSer on the apoptotic cell surface leads to an anti-inflammatory response in macrophages after engulfment. When PtdSer is not present during apoptosis, as is the case for PLB-985 cells, the production of TG $\beta$ 1 is impaired. The transfer of PtdSer onto the cell surface membrane of PBL-985 cells or the use of PtdSer-coated liposomes can

restore the TGF- $\beta$ 1 secretion.<sup>83</sup> TGF- $\beta$ 1, in turn, stimulates the migration of monocytes, the production of growth factors and the release of other anti-inflammatory mediators such as PGE2, PGI2 and LipoxinA4<sup>84 85</sup>. The loss of TGF- $\beta$ 1 in mice triggers inflammatory cell activation and tissue necrosis, which leads to an organ failure and death 20 days after birth<sup>86</sup>. Thus, the expression of PtdSer receptors (e.g. stabilin-2) on the phagocytes also transmits an anti-inflammatory response in macrophages via the release of TGF- $\beta$ 1<sup>87</sup>. Also, the PtdSer-receptor MERTK has been shown to be involved in the anti-inflammatory signalling pathway by suppressing nuclear factor-kappa B (Nf- $\kappa$ B). However, treatment of the macrophage cell line RAW264.7 with Calphostin C (Cal-C) and Gas-6, which effectively inhibits the phagocytosis, does not affect the capability of MERTK to suppress Nf- $\kappa$ B, suggesting that phagocytosis is not necessary in the MERTK-mediated anti-inflammatory effect<sup>88</sup>.

The complexity of the regulation of the apoptotic cell clearance is also underlined by the presence of “don’t eat me” signals. Among others, the most prominent one is the integrin associated protein CD47<sup>89</sup>. The binding of this molecule to the macrophage signal regulatory protein alpha (SIRP $\alpha$ , CD172) inhibits phagocytosis via the modulation of cytoskeletal rearrangement<sup>90</sup>. Indeed, the blocking of CD47 on the surface of the apoptotic cell can restore phagocytosis and allow their clearance by macrophages<sup>91</sup>.

### **1.2.3.1 The phosphatidylserine-dependent phagocytosis of apoptotic cells**

As mentioned above, phagocytosis is not only important for the uptake of the apoptotic cargo that is continuously produced under physiological conditions by the body, but is also able to prevent inflammasome activation and the subsequent production of pro-inflammatory cytokines. TAM receptors are well-established phagocytic surface receptor tyrosin kinases (RTKs) in macrophages. They comprise three constituents: Tyro3, Axl and MERTK. The TAM receptors don’t bind PtdSer directly, instead relying on activating ligands: the growth arrest-specific gene 6 (Gas6) and Protein S (PROS1)<sup>92</sup>. GAS6 can bind all three receptors and is AXL-dependent for its expression in tissues *in vivo*<sup>93</sup>, whereas PROS1 can bind only MERTK and Tyro3<sup>92</sup>. GAS6 and PROS1 activate the tyrosine kinase function in TAM receptors and bind to PtdSer via  $\gamma$ -carboxyglutamic acid (GLA) domains. Both AXL and MERTK have been shown to be expressed under basal/steady state conditions, while TYRO3 is poorly expressed in macrophages. However, the expression of MERTK is associated with homeostasis and tissue turn-over, while the expression of AXL is strongly upregulated in the presence of inflammatory stimuli such as IFN- $\gamma$  or LPS<sup>93 94</sup>. The PtdSer-dependent phagocytosis of the apoptotic cells in

combination with IL-4 and IL-13 is also responsible for the tissue remodelling phenotype in macrophages. Indeed, blocking PtdSer sensing via Annexin V or the depletion of *Axl* and *Mertk* in BMDMs significantly reduces the expression of tissue remodelling-associated genes (e.g. *Retnla*, *Arg1*) upon IL-4 stimulation<sup>95</sup>. Moreover, the depletion of these receptors is strongly associated with the development of several autoimmune diseases and defects in multiple organs and systems<sup>96 97 98</sup>. In the liver, it has been reported that TAM-deficient mice develop immune liver damage resembling autoimmune hepatitis (AIH), accompanied by an increase in serum levels of non-organ-specific autoantibodies<sup>99</sup>. The hepatoprotective role of MERTK in the liver has also been shown by Tryantafyllou and colleagues in a model of acute liver failure (ALF). During the resolution phase of ALF, a subset of KCs expressed high levels of MERTK and HLA-DR and showed enhanced efferocytic capability, thereby acting as important mediator during the restoration of liver homeostasis. On the contrary, *Mertk*<sup>-/-</sup> mice exhibit persistent liver inflammation, characterised by an increase in the neutrophil compartment and a decrease in the population of KCs<sup>100</sup>. Although the transcriptional pathways that allow the recognition of apoptotic cells have yet to be unveiled, signalling via the liver X receptors (LXR $\alpha$  and LXR $\beta$ ) and oxysterol-activated transcription factors was found crucial for the expression of *Mertk* and the subsequent maintenance of immune tolerance<sup>101</sup>. Apart from the TAM receptors, other well-characterised PtdSer-dependent receptors are also known to play a role in apoptotic cell clearance: T cell Ig mucin domain protein-4 (TIM4) is a phagocytic receptor expressed in both dendritic cells and macrophages. TIM4 expression in liver macrophages has been shown to be induced in murine models of non-alcoholic fatty liver disease (NAFLD), leading to an inhibition in the NLRP3 inflammasome activation, inducing autophagy and slowing down the disease progression<sup>102</sup>. Stabilin-2, expressed on human monocyte-derived macrophages, also participates in the recognition of apoptotic and aged cells.<sup>87</sup> Furthermore, Stabilin-1 and Stabilin-2 are also critical for the removal of aged erythrocytes by hepatic sinusoidal endothelial cells (HSECs) in the mouse liver<sup>103</sup>. Brain-specific angiogenesis inhibitor 1 (BAI1), a scavenger receptor that is expressed not only in the brain glia and neuronal cells<sup>104</sup>, but also in other immunological tissues such as the spleen and bone marrow, can bind PtdSer via thrombospondin type 1 repeats<sup>105</sup> and participate in the phagocytic process. However, the interaction with apoptotic cells can also be orchestrated by different scavenger receptors synergistically. Thus, macrophages, dendritic cells and other endothelial cells can express several scavenger receptors, such

as integrins and the fatty acid transporter CD36, that are able to form multi-ligand-dependent interactions via the engagement of bridging molecules such as milk-fat-globule EGF factor-8 and TSP-1 <sup>106</sup>.

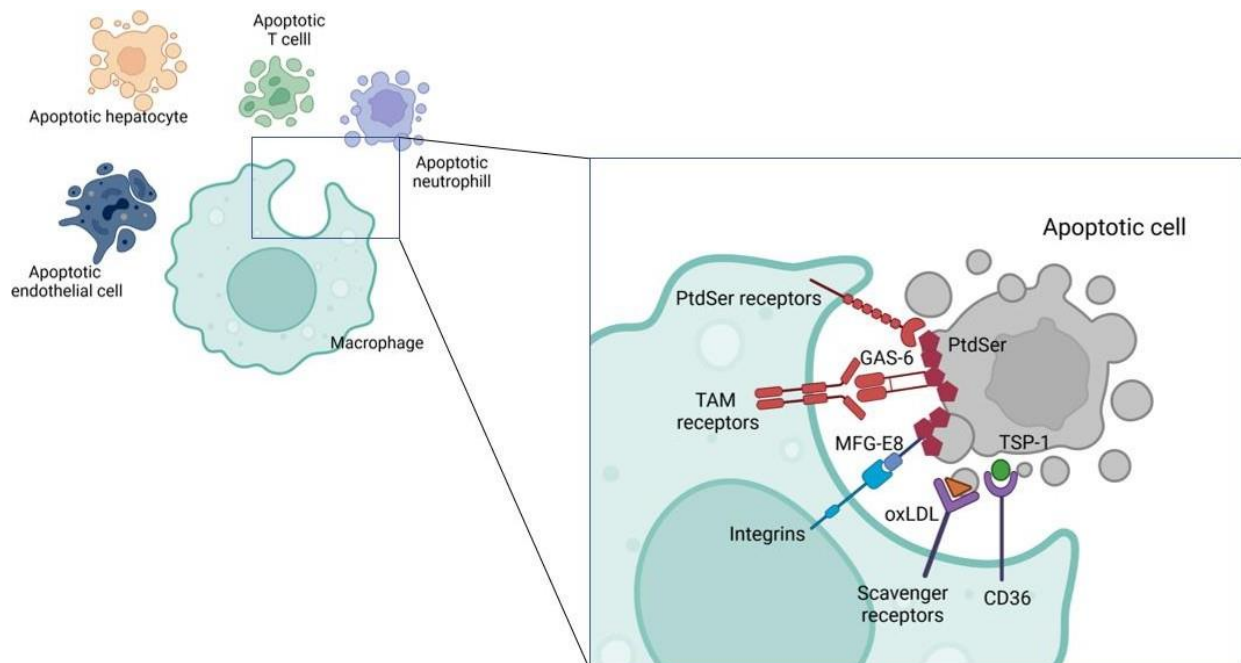


**Fig 1: Apoptotic cell “eat me signals” and phagocytic receptors**

When a cell undergoes apoptosis, it begins to expose “eat me” signals on the cell surface. Phosphatidylserine (PtdSer) is the best characterised “eat me” signal and is recognised by a broad range of phagocytic receptors expressed by phagocytes. The phagocytic receptors can recognise “eat me” signals either directly (e.g. the PtdSer receptors TIM4, BAI1 and Stabilin-2) or indirectly via accessory or bridging molecules (e.g. TAM receptors in combination with GAS6). PtdSer: Phosphatidylserine; GAS6: growth-arrest-specific 6; MFG-E8: Milk-fat-globule EGF factor 8 protein; oxLDL: oxidised low-density lipoprotein; TSP-1: Thrombospondin-1. Figure created with Biorender.com

### 1.3 Apoptosis

Apoptosis is commonly defined as “programmed cell death” and occurs during various processes, including normal cell turnover, embryonic development and chemical-induced cell-death. Although apoptosis occurs during physiological conditions, a wide range of pathological stimuli can trigger cell death, such as inflammation, hypoxia, toxins, heat or the use of corticosteroids, Irradiation and chemotherapy can result in DNA damage, also leading to apoptotic death. Apoptosis has to be distinguished from necrosis and other forms of cell death that can occur independently of apoptosis, but trigger a pro-inflammatory response <sup>107</sup>. Apoptotic bodies are tightly packed organelles with an intact plasma membrane. This configuration prevents the release of cellular debris into the surrounding environment and induces a quick phagocytosis, preventing secondary necrosis and inflammation <sup>108 109</sup>.

The mechanism of apoptosis involves caspase-dependent molecular events, mainly divided into two pathways: the mitochondrial (intrinsic) or the death receptor (extrinsic) pathway. The intrinsic pathway is a series of non-receptor-mediated stimuli that encompass a cascade of mitochondria-initiated intracellular events. Stimuli such as radiation, toxins, hormones and viruses cause an imbalance in the mitochondrial membrane, followed by the formation of mitochondrial permeability transition (MPT) pores and the release of pro-apoptotic proteins, which activate a caspase-dependent pathway<sup>110</sup>. Cytochrome c is one of the first mitochondrial proteins released into the cytoplasm upon apoptosis and induces the formation of an “apoptosome” via the activation of protease-activating factor-1 (Apaf-1) and procaspase-9<sup>111 112 113</sup>. Other mitochondrial factors, like Smac/DIABLO and HtrA2/OMI, can contribute to the apoptotic process in both a caspase-dependent or independent manner<sup>114 115</sup>. However, the regulation of the mitochondrial events is defined by the Bcl-2 family of proteins that controls mitochondrial permeability and determines the anti-apoptotic or pro-apoptotic cell fate<sup>116</sup>.

The extrinsic pathway encompasses death receptors, such as members of the tumour necrosis factor (TNF) receptor gene superfamily<sup>117</sup>. The best characterised death receptors and ligands are FasL/FasR, TNF- $\alpha$ /TNFR1 and TNF-related apoptosis induced ligand-receptor 1 and 2/ TNF-related apoptosis induced ligand (TRAIL-R1/R2/TRAIL)<sup>118 119 120</sup>. The binding of FasL and FasR and of the TNF ligand with the TNF receptor results in the binding of the adapter protein FAS-associated death domain (FADD) and tumour necrosis factor receptor type 1-associated death domain (TRADD) respectively<sup>121 122</sup>. This signal results in the activation of caspase-8 via the death-inducing signalling complex (DISC)<sup>123</sup>. This leads to the common morphological features of apoptosis, including DNA fragmentation, cell shrinkage, chromatin condensation, formation of apoptotic bodies and exposure of “eat me” signals (e.g. PtdSer).

Both the extrinsic and intrinsic pathway converge in the execution phase of apoptosis that results from caspase activity. The initiator caspases (caspase-8, caspase-9, or caspase-10) are responsible for the activation of the execution caspases (caspase-3, caspase-6, and caspase-7), which act on cytoplasmic endonucleases and proteases that in turn degrade both nuclear and cytoskeletal proteins<sup>124</sup>.

If apoptotic cells are not cleared by phagocytes, they can accumulate in the tissues and promote inflammation and alterations to homeostasis. In contrast, sustained apoptosis due to long-lasting exposure to stimuli is an important source of self-antigens. In SLE, an increased number of apoptotic



lymphocytes has been reported and deficiency in the apoptotic cell clearance was proposed to be the cause<sup>125 126</sup>, whereas in RA, resident synovial cells and infiltrating lymphocytes exerted Fas-mediated apoptosis, both *in vivo* and *in vitro*<sup>127128</sup>. Here, the regression of the synovium, a hallmark of the disease, was proposed to be due to the interaction of the synovial-expressing Fas cells and the FasL-expressing T cells, which induce apoptosis in the synovial cells. Hence, defects in the apoptotic pathways and/or abnormal processing of apoptotic cells could lead to a sustained autoimmune response, playing a pivotal role in the pathogenesis of several autoimmune diseases.

### **1.4 The liver as an immunogenic organ**

#### **1.4.1 Anatomy of the liver**

The liver is an immunologically tolerant organ which counteracts gut-derived pathogens and, thanks to its unique architecture, can mount quick and specific immune surveillance. The liver is supplied by both the oxygen-rich arterial blood and the nutrition-rich portal venous blood. Although both the hepatic artery and the portal vein contribute to the total blood influx to the liver, the majority of the total blood volume is portal venous blood that carries gut-derived nutrients and pathogen-associated molecules<sup>129</sup> which bypass other immune organs, such as the lymph nodes and spleen. The complex network of tubular conducts (ducts) is referred to as the biliary tree, anatomically divided into intra- and extra-hepatic compartments. The extrahepatic biliary tree includes the common hepatic duct, the cystic duct, the gallbladder and the bile duct, while the intrahepatic biliary tree is formed by small and large bile ducts<sup>130</sup>. Cholangiocytes line the bile ducts and represent a dynamic population of epithelial cells. Once the bile enters the hepatic lumen and diffuses within the biliary tree, cholangiocytes execute a series of processes to secrete  $\text{Cl}^-$ , bicarbonate ( $\text{HCO}_3^-$ ) and water and reabsorb bile acids, amino acids and glucose<sup>131 130</sup>. Bile acids are mainly secreted into bile canaliculi by hepatocytes and can be delivered to the intestine (enterohepatic circulation) or be absorbed by cholangiocytes and return to hepatocytes (cholehepatic shunt)<sup>131</sup>. The liver is mainly composed of hepatocytes (60-80%) that regulate the synthesis and processing of small and complex molecules and form the structure of the organ. Hepatocytes are also involved in the presentation of antigens to liver-infiltrating T cells, but are more commonly regarded as targets for cellular immune responses<sup>132</sup>. The remaining population of nonparenchymal cells is diverse and includes LSEC, Kupffer cells, biliary cells, stellate cells and intrahepatic lymphocytes. Kupffer cells are resident antigen-presenting cells and are part of the reticuloendothelial system alongside liver sinusoidal endothelial cells (LSEC), which represent an

unusual type of vascular endothelial cells, and dendritic cells (DC) <sup>133 134</sup>. These cell types are considered to be essential for the maintenance of tolerance under noninflammatory conditions. During pathology, a wide variety of cells, including neutrophils, T cells and macrophages, colonise the liver, in turn enabling a quick and effective response against pathogenic stimuli and maintaining the turnover of resident liver cells. The response to pathogens is also associated with a strong CD4 and CD8 T cell activation and proliferation that results in the production of cytokines such as IFN- $\gamma$  and TNF- $\alpha$  <sup>135</sup>. Therefore, both adaptive and innate immunity contribute to the maintenance of liver tolerance, pathogen clearance and repair/restoration of the tissue, while maintaining a status of immune hyporesponsiveness.

### 1.4.2 Bile acids

Bile acids (BAs) are the end product of the cholesterol metabolism in the liver. They are transported and assembled as primary conjugated BAs in the canalicular membrane of the hepatocytes before being transferred to the gut, where further enzymatic modifications occur. The enterohepatic circulation of BAs via the portal blood, from the ileum to the liver, plays a key role in nutrient absorption and inhibits “*de novo*” bile acid synthesis in the liver. In the human liver, the major primary BAs are cholic acid (CA) and chenodeoxycholic acid (CDCA), subsequently conjugated into taurine or glycine prior to their secretion into the bile <sup>136 137</sup>. BAs are able to activate nuclear receptors and G protein-coupled receptors (GPCR) in order to regulate the metabolic homeostasis. The best characterised target of bile acid-modulated effects are the nuclear receptors FXR and the bile acid-activated membrane G protein-coupled receptor (TGR5). These bile acid ligands, also expressed by macrophages, are known to be involved in the energy metabolism and homeostasis <sup>138 139</sup>. Specifically, in gut and liver, the activation of FXR $\alpha$  protects from the toxic accumulation of bile acids and increases bile acid conjugation, promoting bile flow <sup>140 141</sup>. Once activated, the bile acid receptor TGR5, highly expressed in the gallbladder, spleen, liver, intestine, adipose tissue and immune cells, stimulates the synthesis of c-AMP, which activates PKA <sup>142</sup>. The expression of TGR5 in liver sinusoidal cells suggests a hepatoprotective role, since it has been reported that bile acids can induce nitric oxide synthase in these cells in a c-AMP-dependent fashion <sup>143</sup>. The metabolic regulation of bile acids via nuclear receptors and cell signalling triggers an overall physiological response and regulates biosynthetic and metabolic pathways in the liver. Dysregulation in the metabolic pathway involved in the synthesis or recognition of BAs has been shown to influence liver inflammatory processes and cholestasis. <sup>144</sup>

### 1.4.3 Kupffer cells – the liver-resident macrophages

Kupffer cells (KCs) represent the main macrophage population in the liver and make up 35% of the non-parenchymal cells<sup>145</sup>. They are present throughout the liver, in the lumen of the liver sinusoids and in contact with the endothelial cells, but are able to extend their processes through the endothelial blood vessels to interact with cells located in the space of Disse<sup>134</sup>. KCs are composed of a limited fraction of self-renewing cells, tightly controlled by repressive transcription factors (*MafB* and *cMaf*)<sup>146</sup>, and of yolk sac-derived cells and circulating monocytes that migrate through the blood and acquire tissue-resident features<sup>147</sup>. Indeed, recruited monocyte-derived macrophages were able to differentiate into functional KCs and restore the hepatic macrophage population after depletion of *Clec4E*-expressing KCs<sup>148</sup>. Depending on the different zones of the hepatic acinus, KCs can show different morphologies and functions: midzonal and perivenous KCs produce higher levels of NO with lower phagocytic and lysosomal activity compared to the large periportal KCs<sup>145</sup>. Furthermore, large KCs produce higher levels of prostaglandin E2 (PGE2), interleukin-1 (IL-1) and TNF<sup>149</sup>. Although the morphology of the KCs can change according to the different zones across the sinusoid, an unbiased cytometry by time of flight (CyTOF) approach revealed two distinct populations that differ with regard to their expression of CD11c, without influencing their ability to remove pathogens<sup>150</sup>.

The contact with KCs or LSECs and pathogens is optimised by the reduced flow of the blood once it enters the sinusoidal cavities of the liver. Both Kupffer cells and LSECs filter the blood and detect pathogens and bacteria, in turn activating the immune response via the production of cytokines and promoting the recruitment of other immune cells. The complement receptor of the immunoglobulin superfamily (CRIg) is mainly expressed in KCs and is able to bind bacteria via the complement C3b and inactivated C3b (iC3b) under shear conditions<sup>151</sup>. KCs are able to express an array of well-known scavenger receptors, antibody receptors and TLRs that effectively detect and remove pathogens. However, the phagocytic ability of KCs is not only restricted to bloodstream-derived pathogens, but also contributes to the effective clearance of platelets, red blood cells and apoptotic cells<sup>152</sup>. Approximately a third of all aged neutrophils is removed in the liver via the interaction of Fc receptors and integrin-CD36 complexes that allow the internalization and subsequent production of anti-inflammatory cytokines

<sup>153</sup> <sup>154</sup>.

MacParland and colleagues, via single-cell RNA-sequencing analysis on human cells, investigated the heterogeneity of KC subpopulations<sup>155</sup>. CD68<sup>+</sup> MARCO<sup>+</sup> macrophages are involved in the suppression of inflammation via the expression of genes such as CD163 and HMOX1 (hemoxygenase) and in the maintenance of immune tolerance. CD68<sup>+</sup> MARCO<sup>-</sup> cells, although they share a similar transcriptomic profile, secrete more TNF- $\alpha$  after LPS stimulation, suggesting that they play a more pro-inflammatory role in the liver<sup>155</sup>. In mice, hepatic macrophages can be distinguished based on the expression of several surface markers: KCs are CD11b<sup>low</sup>, F4/80<sup>high</sup> and CLEC4F<sup>+</sup>, while monocyte-derived macrophages are CD11b<sup>+</sup>, F4/80<sup>int</sup>, LY6C<sup>+</sup> and CSF1R<sup>+</sup><sup>156 157 148</sup>. Monocyte-derived macrophages in mice can be further divided into two subpopulations, depending on their LY6C expression. Notably, a population of macrophages resident in the hepatic capsule has been reported. These liver capsular macrophages (LCMs) phenotypically differ from both KCs and monocyte-derived macrophages, are CD11b<sup>+</sup>F4/80<sup>+</sup>CD11c<sup>+</sup>MHC-II<sup>+</sup>CSF1R<sup>+</sup>LY6C<sup>-</sup>CLECF<sup>-</sup>TIM4<sup>-</sup> and can promote the recruitment of neutrophils<sup>158</sup>.

Due to their location and enhanced capacity to phagocyte foreign or familiar targets, KCs and liver macrophages play a key role in severe liver diseases. During the development of liver fibrosis, KCs recruit pro-inflammatory monocytes via the secretion of CCL2<sup>159</sup> and interact with hepatic stellate cells (HSCs) via the release of growth factors (e.g. TGF- $\beta$ , PDGF) and pro-inflammatory cytokines (TNF $\alpha$ , IL-6), which in the end leads to a pro-fibrogenic milieu and the establishment of the liver fibrosis niche<sup>160</sup><sup>161</sup>. However, macrophages can also have a protective function and promote the resolution of fibrosis via the loss of pro-fibrogenic signals during fibrogenesis<sup>162 163</sup>. Notably, Kalmark and colleagues have shown that CX3CL1 produced by hepatocytes and HSCs can recruit macrophages to the liver in a CX3CR1-dependent manner, both inducing macrophage survival and an anti-inflammatory phenotype that limits inflammation and fibrosis<sup>164</sup>. In contrast, dysregulation of their function can exacerbate and increase the development of the pathology. In a mouse model of non-alcoholic steatohepatitis (NASH), it was shown that KCs undergo LXR-mediated reprogramming that leads to a loss of the specific cell identity and to a scar-associated phenotype, underlining their role in the disease pathogenesis<sup>165</sup>.

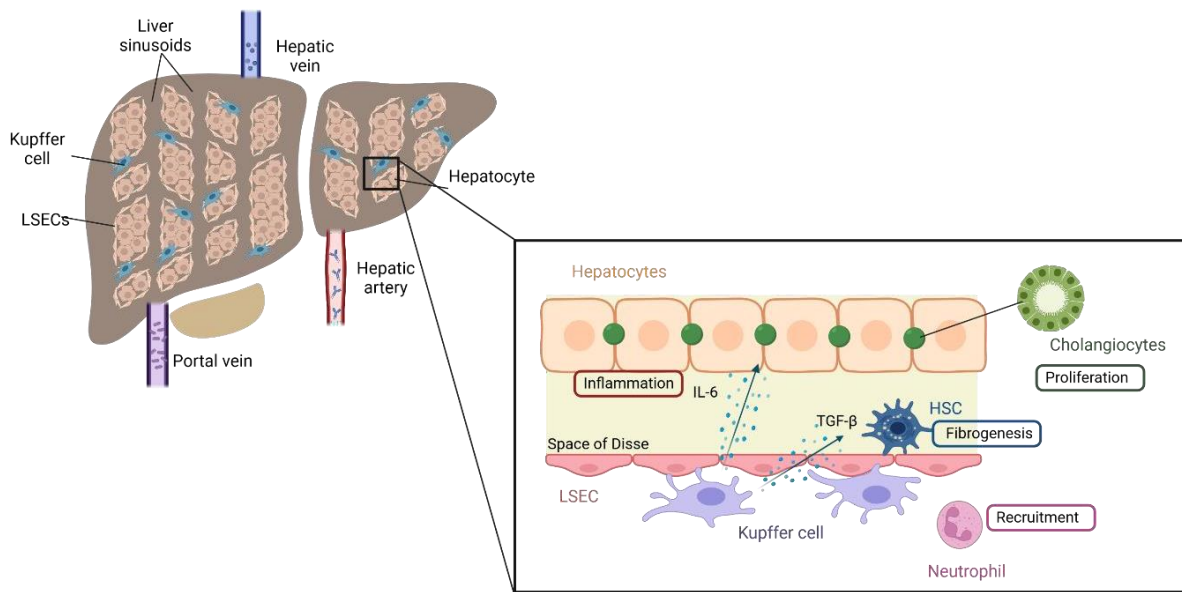


**Fig 2: The role of Kupffer cells during liver disease.**

KCs are localised in the hepatic sinusoid, in proximity of the space of Disse. KCs can interact with other immune cells via the secretion of various mediators, such as cytokines and chemokines, in order to stimulate other immune cells to initiate an inflammatory response (e.g. neutrophil recruitment). Specifically, transforming-growth-factor  $\beta$  (TGF- $\beta$ ) can be released to stimulate hepatic stellate cells (HSCs), leading to the initiation of fibrosis. Cytokines, such as IL-6, contribute to the inflammation and induce proliferation in hepatocytes and cholangiocytes. Figure adapted from Sato et al, 2016<sup>166</sup>. Figure created with Biorender.com. LSEC: liver sinusoidal endothelial cell.

## 1.5 Primary sclerosing cholangitis (PSC)

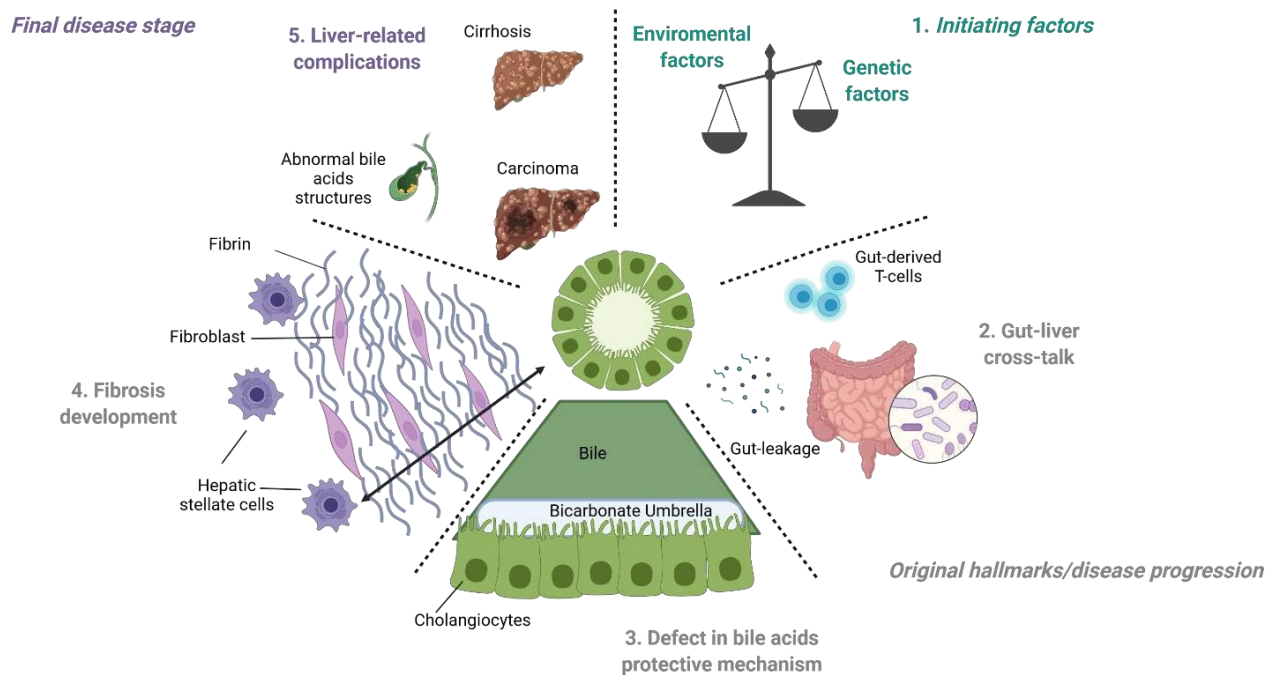


**Fig. 3: General overview of the pathophysiology of primary sclerosing cholangitis.**

The figure illustrates the main factors that characterise the development of PSC. The upper part on the right, in green, shows the initiating factors (1). It has been reported that the onset of the disease is characterised by both environmental and genetic factors, with the involvement of more than 20 susceptibility genes. Following a clockwise direction, the original hallmarks that characterise the disease progression are presented in grey. (2) Although the dynamic of the gut-liver cross-talk in PSC is not completely understood, it has been hypothesised that a leakage of bacteria-derived products (e.g LPS) contributes to the engagement of both the innate and adaptive immune response, resulting in T cell activation and migration to the liver and gut after clonal expansion. (3) Cholangiocytes are protected by the toxicity of bile acids by the formation of the bicarbonate umbrella. Defective mechanisms in the protection against bile acids have been shown to contribute to the disease progression. (4) The development of fibrosis is the result of the continuous cross-talk between cholangiocytes, hepatic stellate cells and portal myofibroblasts. Although the exact mechanism is still unknown, this undefined cross-talk leads to the formation of "onion skin" features. (6) The end-stage liver-related complications are mainly represented by cirrhosis, formation of abnormal bile acid structures and carcinoma. Figure adapted from Karlsen et al., 2017<sup>167</sup>. Figure created with Biorender.com.

Primary sclerosing cholangitis (PSC) is a rare disease, with a prevalence of 1 per 10,000 individuals and an incidence rate of between 0.4 and 2.0 per 100,000 per year in Northern Europe and the US <sup>168</sup>. PSC is a chronic cholestatic liver disease characterised by liver inflammation and fibrosis that leads to multifocal biliary structures. PSC is strongly associated with inflammatory bowel disease (IBD) and with an increased susceptibility for cholangiocarcinoma (CCA) <sup>169</sup> and colon neoplasia <sup>170</sup>. In the healthy liver, cholangiocytes are protected against bile acid (BA) toxicity by several mechanisms. These include the generation of an  $\text{HCO}_3^-$  layer ("umbrella") through involvement of the  $\text{Na}^+$ -independent  $\text{Cl}^-/\text{HCO}_3^-$  anion exchanger (AE2) and active Cl transporters <sup>171 172</sup>. In PSC, several defective mechanisms against the protection against BA toxicity have been shown to play a fundamental role in the disease progression

<sup>173 174 172</sup>. In the liver, hepatocyte apoptosis and bile duct deterioration increase the accumulation of BAs and induce oxidative stress and liver parenchyma damage <sup>175 176</sup>. However, the accumulation of BAs is not only liver-restricted, but has also been reported in the serum of PSC patients <sup>177</sup>.

Chronic bile duct injury is a common hallmark of PSC and is considered to be responsible for the concentric fibrosis, also called “onion skin-like” scars around the bile duct. During the course of PSC and other chronic cholestatic liver diseases, the bile ducts undergo an irregular proliferation, creating a portal-parenchymal interface. This atypical proliferation results in a distorted hepatic architecture due to a disorganised tubular structure that spreads into the hepatic lobules <sup>178</sup>.

Although the factors that initiate the pathogenic process are unknown, genome-wide association studies (GWAS) have identified 23 genome-wide significant loci involved in PSC progression and outcome <sup>179 180</sup>. There is a genetic risk for this disease that is associated with a wide number of genes, each of them with a minimum impact on the overall risk. Genetic studies associate the human leukocyte antigen (HLA) as the main risk loci for PSC. Indeed, HLA can present gut-derived antigens to the T-cell receptor (TCR) and in turn promote the activation and migration of T cells to both the liver and gut <sup>181</sup>. In addition, other non-HLA genes related to innate immunity (e.g. NFKB1, PSMG1) and bile acid homeostasis (e.g. TGR5 on chromosome 2) have been identified as genetic risk factors for PSC <sup>180 182</sup>. However, PSC is a multifactorial disease and other insults can play a role in its pathogenesis: recruitment of gut-derived T cells, disturbances in the gut microbiota or leakage of microbial components (e.g. LPS) into the portal circulation have been suggested <sup>183 184 185 186</sup>.

MDR2 knock-out mice (*Abcb4*, bile canalicular phospholipid flippase) lack the ability to secrete phospholipids from the liver to the bile and it is considered an animal model for the human MDR3 deficiency, which ranges from familiar intrahepatic cholestasis type 3 to adult liver cirrhosis <sup>187 188</sup>. The model reflects the main pathophysiological features of the human disease and is characterised by the disruption of tight junctions and bile leakage into the portal tract. As a consequence, the liver will undergo inflammation, cholestasis and periportal biliary fibrosis <sup>189</sup>. Interestingly, for a better comparison between the mouse model and the human disease, mice on BL/6 background should be used, as their disease progression is milder and more similar to the human patients than mice on a FVB/N background, which develop severe chronic hepatitis that rapidly progresses to hepatocellular carcinoma <sup>190</sup>.

The role of macrophages in the development of PSC has not yet been fully elucidated. Guicciardi et al. have shown the importance of macrophages in the regulation of the fibrogenic response and disease progression via multiple mechanisms in *Mdr2*<sup>-/-</sup> mice <sup>191</sup>. Moreover, an accumulation of monocyte-derived MOs expressing CD68 and CCR2 in the liver parenchyma and peribiliary areas of patients during the late stage of PSC has been reported <sup>191</sup>. In line with this, in *Mdr2*<sup>-/-</sup> mice, increased recruitment of CCR2<sup>+</sup> macrophages occurs while both pro-inflammatory (iNOS<sup>+</sup>) and anti-inflammatory (CD206<sup>+</sup>) macrophages are disseminated to the peribiliary areas of the liver. Furthermore, CCR2<sup>+</sup> macrophages have been shown to play a pivotal role in acute and chronic cholangitis in mice. *Ccr2*<sup>-/-</sup> mice have reduced liver injury and cholestasis and express lower levels of inflammation and fibrosis-related markers (e.g. Tgfβ, Coll1a1) compared to BV6-injected mice, an acute model of biliary injury <sup>191</sup>. Interestingly, monocyte-derived macrophages can also be recruited after damage occurs to cholangiocytes and other biliary epithelial cells, inducing cholestasis and fibrosis <sup>192</sup>. The recruitment of liver monocyte-derived macrophages occurs in the presence of IFN-γ. In a similar fashion, its absence in *Mdr2*<sup>-/-</sup> x *Irfng*<sup>-/-</sup> mice reduces the hepatic fibrosis and the cytotoxic profile of CD8<sup>+</sup> T cells and NK cells <sup>193</sup>. Furthermore, in PSC patients, IFN-γ was suggested as a hepatocyte/cholangiocyte cell-death enhancer in a TRAIL/TRAIL receptor 5-dependent manner <sup>193</sup>. It has also been shown that IL-17 plays a role in the disease progression. IL-17-producing cells can accumulate in the inflamed liver and the administration of anti-IL17A reduces liver injury and fibrosis in mice <sup>194 195</sup>.

Although the role of macrophages in the pathogenesis of the diseases has been addressed so far, little is known about how phagocytosis contributes to development or disease progression in PSC. However, impairment in phagocytosis has been observed in PBMCs isolated from patients suffering from autoimmune hepatitis (AIH) <sup>196</sup>, suggesting a possible involvement of the phagocytic machinery in liver autoimmune diseases.



## **Aim of the study**

Phagocytosis exerted by macrophages as a process to maintain the liver homeostasis and tolerance has been broadly investigated. Furthermore, functional impairment in the phagocytic capacity of apoptotic cells by macrophages has been reported in several autoimmune disease models. However, whether initiation or perpetuation of liver damage is the result of an inability of liver macrophages to eliminate immunoreactive material in autoimmune liver diseases such as PSC has not been tested so far. The aim of the study was to investigate whether the impaired phagocytosis of apoptotic cells by liver macrophages contributes to the development and/or progression of PSC. In particular, an impaired phagocytic capacity in liver-resident macrophages during their response to BAs was observed. These findings shed light on the role of macrophages in the disease progression and pave the way for a deeper understanding of the phagocytic process during cholestatic diseases.

## 2. Material

### 2.1 Laboratory equipment

**Table 1: Laboratory equipment and companies**

Name	Company
Agarose gel electrophoresis chamber	BioRAD, Munich, Germany
Benchtop centrifuge	Eppendorf, Hamburg, Germany
Cell sorter FACSaria III	Becton Dickinson, Heidelberg, Germany
Centrifuge	Eppendorf, Hamburg, Germany
ChemiDoc Touch Imaging System	BioRAD, Munich, Germany
Cytek Aurora	Cytek Biosciences, California, USA
Dissection instruments (forceps & scissors)	Neolab, Heidelberg, Germany
Freezer -20°C /-70°C	Liebherr, Biberach an der Riss, Germany
Fridge	Liebherr, Biberach an der Riss, Germany
LSR II	BD Biosciences, Heidelberg, Germany
MACS magnet	Miltenyi Biotec, Bergisch Gladbach, Germany
Microscope Keyence	Nikon GmbH, Düsseldorf, Germany
Multichannel pipettes	Eppendorf, Hamburg, Germany
NanoDrop 2000C	ThermoScientific, Waltham, USA
PCR machine (Pqstar 96x Universal Gradient)	Peqlab, Erlangen, Germany
Pipettboy Acujet pro	Brand, Wertheim Germany
Pipettes (10 µL, 20 µL, 200 µL, 1000 µL)	HTL, Wertheim, Germany
Thermomixer MM	B Braun, Melsungen, Germany
Vortexer Genie 2	Bender & Hobein AG, Zürich, Switzerland
Water bath	Haake, Karlsruhe, Germany

### 2.2 Chemical reagents

**Table 2: Chemical and molecular biology reagents**

Name	Company
Adenine	Sigma Aldrich, Darmstadt, Germany
Agarose	Biomol, Hamburg, Germany
Ampuwa, water	Fresenius, Graz, Austria
Collagenase IV	Stem Cell, Köln, Germany, Worthington, USA

## Material

---

DMEM	PAA Laboratories GmbH, Pasching, Austria
DMEM high Glucose GlutaMAX	Invitrogen, Gibco, Auckland, New Zealand
DNase I	Quaigen, Hilden, Germany, Roche, Germany
DPBS 10 x	Capricon, Ebsdorfergrund, Germany
Epinephrine	Sigma Aldrich, Darmstadt, Germany
Fetal calf serum (FCS)	Capricon, Ebsdorfergrund, Germany
Ficoll-Paque	Sigma Aldrich, Darmstadt, Germany
Generuler 100 bp DNA Ladder	ThermoFisherScientific, Waltham, USA
Gentamycin	Capricon, Ebsdorfergrund, Germany
HAM's F12 Nutrient mix	Invitrogen, Gibco, Auckland, New Zealand
Hydrocortisone	Sigma Aldrich, Darmstadt, Germany
Endothelial growth factor (hEGF)	Sigma Aldrich, Darmstadt, Germany
Insulin-transferrin-Selenium (ITS) 100X	Invitrogen, Gibco, Auckland, New Zealand
L-Glutamine	Capricon, Ebsdorfergrund, Germany
Normal human serum (NHS)	Sigma Aldrich, Darmstadt, Germany
Percoll	Sigma Aldrich, Darmstadt, Germany
RPMI 1640 without L-Glut	PAA Laboratories GmbH, Pasching, Austria
Trypan blue solution 0.4%	Invitrogen, Gibco, Auckland, New Zealand
Trypsin-EDTA (1x)	PAA Laboratories GmbH, Pasching, Austria
$\beta$ -Mercaptoethanol	Invitrogen, Gibco, Auckland, New Zealand
3,3, 5-Triiodo-L-thyronine	Sigma Aldrich, Darmstadt, Germany

---

All other, not listed chemicals or molecular biology reagents were purchase at Merck (now including Sigma-Aldrich) or Roth.

## 2.3 Glass and plastic consumables

**Table 3: Plastic and glass consumables**

<b>Name</b>	<b>Company</b>
Cell culture plate (6/24/96 U/R bottom)	Greiner bio-one, Frickenhausen, Germany
Cell strainer (100, 70, 40 $\mu$ m)	Pluriselect, Leipzig, Germany
Cryo tubes	Nunc, Wiesbaden, Germany
FACS tubes	Sarstedt, Nürmbrecht, Germany
Falcons (15, 50 mL)	Sarstedt, Nürmbrecht, Germany
Glass pipettes (2, 5, 10, 20 mL)	Brand GmbH, Wertheim, Germany

## Material

---

Glass bottles (50, 100, 200, 500, 1000 mL)	Schott AG, Mainz, Germany
LS-MACS columns	Miltenyi Biotec, Bergish Gladbach, Germany
Neubauer Chamber (0.1 x 0.0025 mm <sup>2</sup> )	Sigma Aldrich, Darmstadt, Germany
Pasteur pipettes glass	Fisher Scientific GmbH, Schwerte, Germany
Petri dish 15 cm	Sarstedt, Nürmbrecht, Germany
Pipette tips (10,20,200,1000 µL)	Sarstedt, Nürmbrecht, Germany
Plastic pipettes (5, 10, 25 mL)	Sarstedt, Nürmbrecht, Germany
Single-use hypodermic needles (Gr 1, 2, 16, 18)	B Braun Melsungen AG, Melsungen, Germany
Syringes (5 mL, 10 mL, 20 mL)	B Braun Melsungen AG, Melsungen, Germany
Tubes (0.5 mL, 1.5 mL, 2 mL)	Sarstedt, Nürmbrecht, Germany
Venofix A 21 G butterfly	B.Braun Melsungen AG, Melsungen, Germany

---

## 2.4 Media and buffer

**Table 4: Media and buffer**

<b>cDMEM:</b>	<b>cRPMI:</b>
+ 10 % FCS	+ 10 % FCS
+ 2.5 % L-Glutamine	+ 2.5 % L-Glutamine
+ 0.5 % Gentamycin	+ 0.5 % Gentamycin
<b>Digestion Buffer Liver 10 mL DMEM/ sample:</b>	<b>Macrophage Media (RPMI):</b>
+ 1mg /mL Collagenase IV	+ 20 % FCS
+ 100µL MgCl <sub>2</sub> (0.2M)	+20-30% L929 sup.
+ 40µL CaCl <sub>2</sub> (0.5 M)	+ 2.5 % L-Glutamine
+ 50µL DNase I (150 U/mL)	+ 0.5 % Gentamycin
<b>FACS Buffer:</b>	<b>MACS Buffer:</b>
PBS	PBS PH 7.2
+ 2 % FCS	+ 0.5 % BSA
	+ 2 mM EDTA
<b>cH69 medium:</b>	<b>Digestion Buffer (Biopsies):</b>
DMEM high glucose/HAM's F12 1:3	0.1 M Tris·Cl pH 8.0
+10% NHS	+ 0.005 M EDTA
+ ITS 1X	+ 0.2 M NaCl
+ Pen/Strep 100U/mL	+ 0.2% SDS
+Adenine 26µg/mL	

---

## Material

---

- + hEGF 10 ng/mL
- + Epinephrine 1 µg/mL
- + Hydrocortisone 400 ng/mL
- + 3,3', 5-Triiodo-L-thyronine 2nM
- + L-Glutamine 2mM

---

<b>Apoptotic neutrophil aging Buffer:</b>	<b>TBE Buffer (in H<sub>2</sub>O) for Agarose-gel:</b>
RPMI	+ 89 mM Tris base
+ 5 % FCS	+ 89 mM boric acid
+ 2.5 % L-Glutamine	+ 2mM EDTA
+ 0.5 % Gentamycin	

---

## 2.5 Commercially available kits

**Table 5: Kits**

<b>Name</b>	<b>Company</b>
DreamTaq	ThermoFisherScientific, Waltham, USA
FITC Annexin V Apoptosis Detection Kit with PI	BioLegend, San Diego, USA
Fixable blue dead staining	Invitrogen, Gibco, Auckland, New Zealand
Intracellular Fixation/Permeabilisation Buffer Set Foxp3	ThermoFisherScientific, Waltham, USA
iScript <sup>TM</sup> cDNA synthesis Kit	BioRAD, Munich, Germany
Maxima SYBR <sup>TM</sup> Green qPCR Master Mix	ThermoFisherScientific, Waltham, USA
QiaShredder	Quiagen, Hilden, Germany
RNeasy Mini Kit	Quiagen, Hilden, Germany

---

## 2.6 Software

**Table 6: Used software**

<b>Software Name</b>	<b>Purpose</b>
BD FACS DIVA 6.2	FlowJo data acquisition
Biorender	Illustrations creation
Flow Jo Version 10.01	Flow cytometry data processing
Graphpad Prism 8 for Windows	Graph creation and statistical analysis

---

Inkscape 0.92.3	Graph processing
Mendeley Desktop 1.16.3	Citations
Microsoft Office 2013	Word and graphic processing

---

## 2.7 Antibodies

**Table 7: Mouse antibodies specifications**

<b>Epitope</b>	<b>Fluorochrome</b>	<b>Clone</b>	<b>Dilution Factor</b>	<b>Company</b>
CX3CR1	BV785	SA011F11	1:300	Biologend
CD11c	PE-Cy5	N418	1:300	Biologend
CD64	BV711	X54-5/7.1	1:100	Biologend
Ly6G	BUV395	1A8	1:300	BD Biosciences
CCR2	BV650	SA203G11	1:400	Biologend
CD45	PeCy7	30-F11	1:1300	Biologend
CD11b	APC/Cy7	M1/70	1:400	Biologend
F4/80	AF700	BM8	1:400	Biologend
CLEC4F	APC	3E3F9	1:400	Biologend
Ly6C	BV570	HK1.4	1:300	Biologend
CD68	BV421	FA-11	1:500	Biologend
CD115	BUV737	AFS98	1:100	Biologend
MERTK	PE	2B10C42	1:300	Biologend

## Material

---

TIM4	PerCP-eFluor710	54 (RMT4-54)	1:500	Invitrogen
CD206	PE-Dazzle	C068C2	1:600	Biolegend
CD36	FITC	HM36	1:500	Biolegend
MHCII	BV510	M5/114.15.2	1:500	Biolegend

---

### 2.7.1 Antibodies

**Table 8: Human antibodies specifications**

<b>Epitope</b>	<b>Fluorochrome</b>	<b>Clone</b>	<b>µL/sample</b>	<b>Company</b>
CD86	PE-Cy5	IT2.2	1	Biolegend
CX3CR1	APC/Cy7	G025H7	3	Biolegend
MARCO	PE	PLK-1	1	eBiosciences
CD14	BUV737	M5E2	1	BD Biosciences
CD16	PerCP-Cy5.5	B73.1	1:400	Biolegend
CD64	AF700	10.1	3	Biolegend
MERTK	APC	125518	2.2	R&D
CD206	BV510	15-2	3	Biolegend
CD163	BV650	GHI/61	1	BD Biosciences
CD66b	PE/Fire640	6/40c	1	Biolegend

## Material

---

CD68	BV785	Y1/82A	3	Biolegend
CCR2	PE/Dazzle594	K036C2	1	Biolegend
CD36	BV421	5-271	3	Biolegend
TIM4	PE-Cy7	9F4	3	Biolegend
HLA-DR	BV711	L243	3	Biolegend
CD83	FITC	HB15e	3	Biolegend

---

## 2.8 Primer sequences for qPCR

**Table 9: Mouse primers**

<b>Name</b>	<b>Sequence 5' -&gt; 3'</b>
<i>Gapdh fw</i>	TCCCACTCTTCCACCTTCGA
<i>Gapdh rev</i>	AGTTGGGATAGGGCCTCTCTT
<i>Fxr fw</i>	GCACGCTGATCAGACAGCTA
<i>Fxr rev</i>	CAGGAGGGTCTGTTGGTCTG
<i>Tgr5 fw</i>	CCTGGCAAGCCTCATCGTC
<i>Tgr5 rev</i>	AGCAGCCCGGCTAGTAGTAG

---

All oligonucleotides were synthesised and purchased by Eurofins.

## 2.9 Cell lines

**Table 10: Eukaryotic cell lines**

<b>Name</b>	<b>Origin</b>
Hepa 1-6 (Hepatocytes cell line)	Hepatoma (mouse)
H69 (Cholangiocytes cell line)	Human biliary hepitelial cell
Jurkat (T-cells line)	Acute T cell leukemia (human)

---



## 2.10 Mice strains

Table 11: mice strains

Name	Origin
C57BL/6	BNITM, Hamburg, Germany
<i>Mdr2</i> <sup>-/-</sup>	Schwinge Lab, UKE, Hamburg, Germany
<i>Mdr2</i> <sup>+/+</sup>	Schwinge Lab, UKE, Hamburg, Germany
<i>Csf1R-Cre</i> <sup>+</sup> <i>Ax1</i> <sup>fl/fl</sup> <i>Mertk</i> <sup>fl/fl</sup>	Rothlin Lab Yale, USA, breeding at BNITM, Hamburg, Germany
<i>Csf1R-Cre</i> <sup>-</sup> <i>Ax1</i> <sup>fl/fl</sup> <i>Mertk</i> <sup>fl/fl</sup>	Rothlin Lab Yale, USA, breeding at BNITM, Hamburg, Germany
<i>Cd36</i> <sup>-/-</sup>	Worthmann Lab, UKE, Hamburg, Germany
<i>Cd36</i> <sup>+/+</sup>	Worthmann Lab, UKE, Hamburg, Germany

---

### 3. Methods

#### 3.1 Cell culture

Cell cultures and *in vitro* experiments were performed under sterile conditions. All cells were cultured in 37°C 5 % CO<sub>2</sub>, except the Hepa 1-6 cell culture. All cell lines were routinely tested for the presence of mycoplasma.

#### 3.2 Hepa 1-6 culture

The Hepa 1-6 cells were maintained at 37°C 9 % CO<sub>2</sub>. In order to maintain the cell culture, serial dilutions were performed. The cells were detached with trypsin for 5 min at 37°C and complete DMEM 5% FCS media was added to stop the reaction. In order to perform the experiments, the cells were washed with PBS and detached using a cell scraper. For the experiments with bile acids (TLCA), 30µM of TLCA were added to the culture in complete medium for 2 hours. The medium was then harvested and the Hepa 1-6 were washed with PBS. In the following chapters, this cell line will be referred to as hepatocytes.

#### 3.3 Jurkat cell culture

The Jurkat cell line was used as a source of T cells for the human phagocytosis assays. To maintain the cell culture, cells were split twice a week with RPMI containing 10% FCS, 1% L-Glutamin and 0.5% Penicillin/Streptomycin.

#### 3.4 H69 cell culture

The H69 were used as a source of human cholangiocytes for the human phagocytosis assays. To maintain the cell culture, serial dilutions were performed. The cells were detached with trypsin for 5 min at 37°C and complete media was added to stop the reaction. The media was composed of DMEM High glucose, 10% NHS, 1X Insulin-transferrin-Selenium (ITS) (Gibco), adenine 26µg/mL (Sigma-Aldrich), hEGF (endothelial growth factor) (Sigma-Aldrich) 10 ng/ml, epinephrine (Sigma-Aldrich) 1µg/ml, hydrocortisone (Sigma-Aldrich) 400 ng/ml, 3,3, 5-triiodo-L-thyronine (Sigma-Aldrich) 2nM, L-glutamin 2 nM, 100 U/ml penicillin

### 3. Methods

---

#### 3.5 Cell count

The cell count of a cell suspension was determined with a Neubauer chamber. The following formula was used to calculate the cell concentration:

$$\text{cell count} \div \text{big squares} \cdot \text{dilution factor} \cdot 10^4 = \text{cells/mL}$$

#### 3.6 Isolation of bone marrow-derived macrophages

Bone marrow-derived macrophages (BMDMs) were obtained from the femur and tibia of mice. The bones were removed and disinfected for 30 sec in 70 % Ethanol (EtOH) and cut open at one epiphysis. The bones were then placed into a perforated 0.5 mL tube and then placed into a 1.5 mL tube and centrifuged at 13000 rpm for 2 min. The bone marrow was then resuspended in 0.5 mL RPMI and filtered through a 40  $\mu\text{m}$  cell strainer. The cells were then seeded into a 15 cm petri dish in 10 mL RPMI containing 20 % FCS, 30 % L929-cell line supernatant, 2.5 % L-glutamine and 0.5 % gentamycin (macrophage media). In order to differentiate the macrophages from the bone marrow, the media was changed at day 3 via centrifugation at 300 xg for 5 min and the cells resuspended in 10 mL fresh new media. The cells were then split at day 5 into two new 15 cm dishes with 10 mL fresh media. At day 7, the cells were fully differentiated into macrophages and seeded into a concentration of  $0.33 \cdot 10^6$  cells/well into a 24-well plate to perform the experiments.

#### 3.7 Isolation of neutrophils

Neutrophils were isolated from the bone marrow of >11 weeks WT mice (as described above; see 3.6). A negative selection was performed via MACS-selection kit for neutrophils (Miltenyi) according to the manufacturer's protocol. Briefly, a streptavidin-labelled antibody cocktail was added to the cell suspension and incubated for 10 min at 4°C. After washing steps, to remove the unbound antibodies, cells were incubated with biotin-conjugated beads (15 min 4°C) and the neutrophils were obtained via the collection of the flow-through fluid from the magnetic column separation. Ly6G and CD11b staining was performed to verify the purity of the isolation.

#### 3.8 Induction of apoptosis

Apoptosis was induced in neutrophils (aN) by aging the cells for 24 h in cRPMI media containing a reduced amount of FCS (5 % FCS) at 37°C 5 % CO<sub>2</sub> in a 15 cm dish.

### 3. Methods

---

The thymus was isolated from WT mice and mashed over a 40 µm cell strainer. Apoptosis was induced in thymocytes/T cells (aT) by aging for 24 h at 37°C 5 % CO<sub>2</sub> in a 15 cm dish.

In hepatocytes (Hepa 1-6, aH) the apoptosis was induced by heating the cell suspension for 1 h at 43 °C in PBS with 0.5 % FCS while shaking.

#### **3.9 Apoptotic cell staining with Annexin V and PI**

For all the cell types, the apoptosis rate was measured via Annexin V and PI staining. The cells were stained directly in a FACS tube containing 100 µL of Annexin V binding buffer. 2µl of Annexin V was added in order to stain the PtdSer on the apoptotic cell surface. The cells were incubated for 15 min at room temperature (RT) in the dark. Afterwards, 200 µL Annexin V binding buffer was added to the cell suspension together with 1 µL PI staining solution and the samples were directly measured at the LSR II.

#### **3.10 Phagocytosis assay**

The cells were plated in two separate 24-well plates at a concentration of  $0.33 \times 10^6$  cells/well. One plate was kept at 4°C on ice 15 minutes before starting the assay. The two conditions, at 37°C and 4°C, were performed simultaneously, whereby at 37°C, the apoptotic cells can be bound and phagocytosed by MOs and at 4°C, the MOs are only able to bind to the apoptotic cells but are not able to uptake them. The apoptotic cells were pre-labelled with apoptotic cell dyes (as described below, see 3.11) and co-cultured with MOs for 45 minutes. Afterwards, free apoptotic cells were washed out 5 times with PBS and MOs were then stained and analysed at the LSR II. The ratio between MOs positive for the apoptotic cells at 37°C and 4°C was calculated and displayed as phagocytosing macrophages.

#### **3.11 Apoptotic cell dyes**

When just one single type of apoptotic cell was co-cultured with MOs, cells were pre-labelled with CFSE in a final concentration of  $10 \times 10^6$  cells/mL. To this end, apoptotic cells were washed twice with PBS to remove any serum and resuspended in PBS. A CFSE solution of 20µM was added to the apoptotic cell solution while vortexing. The cells were incubated for 10 min at 37°C in the dark. The labelling-process was stopped by adding 10 mL of cold cRPMI and incubating for 5 min on ice.

When more than one apoptotic cell type (e.g. aN, aT and aH) was used in combination for the phagocytosis assay, different cell dyes were used. CFSE was used as described above for the aT staining. eFluor450 cell dye was used for the staining of aH. To this end, aH were resuspended in PBS

### 3. Methods

---

( $1 \times 10^7$  cells/mL). The eFluor450 stock solution (10mM) was diluted in PBS to obtain 20 $\mu$ M/mL. The cell suspension and the diluted cell dye were then mixed 1:1 and incubated for 10 min at 37°C in the dark. In order to stop the reaction, 10mL cold complete RPMI medium was added and the cells were incubated on ice for 10 minutes. DRAQ5 was used for the staining of aN. Cells were resuspended in PBS in a concentration of  $4 \times 10^5$  cells/mL and 1 $\mu$ L/mL of the 5mM stock solution was added to the cell suspension. Cells were then vortexed and incubated for 30 minutes at RT in the dark. To remove the unbound dye from the cell suspension two washing steps in PBS were performed.

#### **3.12 Flow cytometry**

Flow cytometry is a technique that allows the morphological investigation of the cells via the granularity and size by sideward scatter (SSC) and forward scatter (FSC). The cells are squeezed through a capillary tube and separated into a single cell solution before passing the laser, allowing the analysis of expression levels of extra and intracellular proteins/molecules. The cells are labelled with fluorescence-conjugated antibodies excited by different wavelengths in order to perform analysis of multiple proteins at the same time. Cells derived from mice or cell lines were stained based on the following protocol. Cells were incubated with anti-CD16/CD32 (1:10000 in PBS/2 % FCS) for 15 min at 4°C in order to block unspecific binding of antibodies to the Fc-receptor. To remove unbound antibodies during surface staining, cells were washed 3 times with 200 $\mu$ L PBS/2 % FCS per well (96-well plate). During the surface staining, antibodies were diluted in 50 $\mu$ L of PBS/2 % FCS/well and incubated for 35 min at 4°C in the dark. When intracellular epitopes were analysed, a fixation with 100 $\mu$ L of 1 % paraformaldehyde (PFA) for at least 20 min at 4°C in the dark followed by a permeabilization with 100 $\mu$ L permeabilization buffer (BD Bioscience) for 15 min at RT was performed. The intracellular antibodies were diluted in permeabilization buffer and then incubated for 45 min at 4°C in the dark. When liver samples were analysed, cells were fixed and permeabilised using the Foxp3 staining Kit (eBioscience). Antibodies used for the cell staining are listed in Table 7 and 8. The samples were measured at the LSR II or at the Cytex Aurora.

#### **3.13 Fluorescence-activated cell sorting (FACS)**

Fluorescence-activated cell sorting (FACS) was used in order to obtain specific cell populations. Surface staining was performed as described above (see 3.12). Cells are enclosed in liquid droplets and labelled with an electric charge that allows the sorting of cells into different populations when they pass an electric

### 3. Methods

---

field. Cells were sorted with the use of a 70µm nozzle and collected in cold PBS/2 % FCS. A BD FACSAria was used.

#### **3.14 t-distributed stochastic neighbour embedding (tSNE)**

t-distributed stochastic neighbour (tSNE) is a statistical method that allows the visualization of high-dimensional data in a bidimensional map. The tSNE algorithm creates a probability distribution, in that similar data points are assigned a higher probability and they will be located close to each other in the bi-dimensional map. Flow Jo Version 10.01 was used in order to perform tSNE analysis.

#### **3.15 Competitive phagocytosis assay**

The competitive phagocytosis assays, in which different apoptotic cell types were co-cultured simultaneously with BMDMs and analysed via IF, was performed in collaboration with Irene Aranda-Pardos (Noelia-Gonzalez lab, Munich). The BMDMs were isolated and differentiated as described above (see 3.6). The apoptotic cells, generated as described above (see 3.8), were stained as follows: apoptotic thymocytes (aT) with 5µM CFDA SE Cell Tracer (Invitrogen) in PBS for 15 min at 37°C. Apoptotic neutrophils (aN) with 5µM Cell tracker Red CMTPIX (Invitrogen) in serum-free medium for 30min at 37°C. Apoptotic hepatocytes (aH) with 5µM CellTrace Violet Dye (Invitrogen) in PBS for 15 min at 37°C.

All apoptotic cell types were simultaneously co-cultured with the differentiated BMDMs in a 1:5 (aT, aNs; 2.5x10<sup>6</sup> cells/well) or 1:2 (aHs, 10<sup>6</sup> cells/wells) ratio for 5, 15, 30, 60 and 90 min, to study different stages of the phagocytic process in the presence of different apoptotic cells. Afterwards, cells were washed x3 times with 1x PBS to remove the remaining non-phagocytosed ACs and then fixed with 2% PFA in PBS for 5 min. Cover slips were then transferred to a wet chamber for staining of BMDMs, first with 2.5 µg/ml of rat anti-mouse F4/80 primary antibody (eBioscience™) at 4°C overnight and followed by incubation with 4 µg/ml of goat anti-rat Alexa Fluor 647 secondary antibody (Invitrogen) for 1 hour at room temperature, both in blocking solution (PBS 1% FCS). Cover slips were mounted on microscopy slides for imaging using Dako Fluorescence Mounting Medium.

#### **3.16 Imaging and quantification**

For quantification of phagocytic macrophages at different stages of phagocytosis, a Zeiss LSM800 confocal microscope was used to take images at 20x (quantification) and 40x magnification. 6-8 fields

### 3. Methods

---

per time point were manually counted for macrophages phagocytosing single aT, aN, aH, or the combination of aT+aN, aT+ aH, aN+aH or aT + aN + aH. Results are shown as the percentage of phagocytic macrophages for each condition from the total of macrophages per field and time point.

#### **3.17 RNA isolation and quantitative real-time PCR analysis**

In order to obtain RNA from liver-sorted cells, the Qiagen RNeasy mini Kit was used by following the manufacturer's instructions. Via the use of 350µL RLT buffer containing β-mercaptoethanol (10µL/1mL RLT) per sample, cells were lysed and spun down over the shredder column for 2 min. 350µL of 70 % EtOH were added to the suspension and the transferred to the RNeasy mini column and briefly centrifuged (15 s) at 13000 rpm. Afterwards, 350µL RW1 buffer was added to the column, spun down and a DNase I digestion was performed for 15 min at RT. The column was then washed again with RW1 buffer and two more washing steps were performed on the column with 500 µL RPE2 solution. The RNA from the liver-sorted cells was eluted with 32 µL RNase-free water and RT incubation for 5 min. The purity and the amount of RNA was measured via NanoDrop. cDNA synthesis was performed with the iScript™ cDNA synthesis Kit from BioRad (see cDNA cycles). To quantify the specific DNA-sequence in real time, a quantitative real-time polymerase chain reaction (qPCR) was performed using the Maxima™ SYBR™ Green qPCR Master Mix (2X), with separate ROX™ vial from Thermo Fischer. Via the use of a fluorescence dye (SYBR™ Green), that intercalates with the amplified PCR product during the reaction (see qPCR cycles below) the DNA sequence can be quantified and measured by the Rotor-gene 6000 machine. The reactions were performed in duplicates, with 40ng cDNA and a final volume of 12µL per reaction. The analysis was performed with Rotor-gene 6000 Series Software 1.7. *Gapdh* was used as reference gene. The primers are listed in Table 9.

#### **Reaction Mix for cDNA – iScript™ cDNA Synthesis Kit**

1 µL iScript Reverse Transcriptase

4µL 5x iScript Reaction Mix

X µL Nuclease-free water

X µl RNA template (200-400ng)

#### **cDNA cycles**

### 3. Methods

---

Priming 25°C for 5 min

Reverse transcription 46°C for 20 min

RT inactivation 95°C for 1 min

#### **Reaction Mix for qPCR – Maxima™ SYBR™ Green qPCR Master Mix**

6 µL Master Mix

0.15 µL per primer (forward and reverse)

4.7 µL Ampuwa water

1 µL RNA template (40 ng)

#### **qPCR cycles**

UDG pre-treatment 50°C for 2 min

Initial denaturation 95°C for 10 min

Denaturation 95°C for 15s (repeat 40 x)

Annealing 60°C for 30 s

Extension 72°C for 30 s

#### **3.18 Mice**

All experiments were approved by the office for consumer protection of the city of Hamburg (2021\_T\_001 and 0055\_2018). Mice were bred and kept in a SPF facility at the BNITM.

#### **3.19 Genotyping of *MDR2*<sup>-/-</sup> and *MDR2*<sup>+/+</sup> mice**

The ear tissue samples from mice were used to perform the genotyping. The tissue samples were lysated with 10µL proteinase K and 90µL digestion buffer per sample and then stored at 37°C at 200 rpm overnight. The day after, the reaction was stopped by adding 200µL Ampuwa water and incubating the samples for 10 min at 95°C. Samples were roughly vortexed in between the steps. The genomic DNA (gDNA) was amplified by PCR using the DreamTaq™ PCR Kit from Thermo Fisher. An agarose electrophoresis was performed in order to evaluate the specific amplification using 1.5 % agarose in TBE buffer. The expected band size as well as the PCR Primers and PCR cycles are depicted below.



### 3. Methods

---

#### **Primer sequence:**

*Mdr2* fwd: CCA CAG CCA CAC ACT CAC CT

*Mdr2* Mut rev: CCA GAC TGC CTT GGG AAA AG

*Mdr2* rev: CAT CAA ACC ACG TGC AGA AAA

*Mdr2*-mut: 169 bp

*Mdr2*-WT: 374 bp

#### **PCR cycles**

Denaturation: 94°C for 3 min

Denaturation 94°C for 30s (repeat 35 x)

Annealing 60°C for 30s

Elongation 72°C for 1 min

Final elongation 72°C for 10 min

#### **3.20 Cell isolation from different organs**

The mice were sacrificed with the use of CO<sub>2</sub>/O<sub>2</sub>. The cornea and foot reflexes were checked twice to ensure a proper anaesthesia and cervical dislocation was performed to ensure the complete death of the animal. The organs were harvested and collected in tubes containing PBS/2 % FCS before the processing for the analysis.

#### **3.21 Isolation of macrophages from the liver**

To isolate the macrophages from the liver, a perfusion was performed by inserting a Venofix 27 G butterfly needle into the vena cava and slowly removing the blood via injecting PBS. The liver was then collected and stored in in 2mL PBS/2 % FCS on ice. After removing the gallbladder, the liver was minced into pieces and digested with 10mL digestion buffer (DMEM, 1mg/mL Collagenase IV, 150U/mL DNaseI, 0.2M MgCl<sub>2</sub>, 0.5M CaCl<sub>2</sub>). The liver was then incubated in the digestion buffer for 45 min at 37°C while shaking. The digested cell suspension was passed through a 70µm cell strainer and then centrifuged at least twice at 300 xg for 5 min at 4°C and washed in PBS/2 % FCS. In order to obtain the non-

### 3. Methods

---

parenchymal fraction, the suspension was centrifuged at 50 xg for 4 min and the supernatant was transferred into a new falcon. The non-parenchymal cells were then resuspended in 6mL 37 % Percoll and centrifuged for 10 min at 400 xg (dec.1 acc.9). After a red blood cell lysis step and a further washing step in PBS/2 % FCS, the cells were used for RNA analysis, cell sorting at the FACSaria or phenotypical investigations at the LSR II or Cytex Aurora.

#### **3.22 Kupffer cell isolation**

To isolate the Kupffer cells (KCs) out of the total non-parenchymal cell population, the liver collection and digestion was performed as described above (see 3.21). The obtained liver cells were then counted and plated to a concentration of  $0.66 \cdot 10^6$  /cells in a 6-well plate in cDMEM (10 % FCS) for 2 hours at 37°C. The KCs were discriminated based on the method of selective adherence <sup>197</sup>, in which only the KCs attach to the plate. The non-adherent cell fraction was removed with gentle PBS washing steps. The functional (phagocytosis) assays were performed the day after the plating.

#### **3.23 Isolation of peritoneal macrophages**

To isolate the peritoneal macrophages, mice were sacrificed with CO<sub>2</sub>/O<sub>2</sub> following cervical dislocation and the fur was carefully removed. A solution composed of PBS/2 % FCS was injected into the intact peritoneum and the peritoneum was massaged for at least 30s to detach the macrophages. Carefully, to avoid puncturing the organs, the fluid was reobtained with a syringe. Afterwards, a red blood cell lysis was performed, the cells were plated for 2 hours and the phagocytosis assays were performed the same day.

#### **3.24 Isolation of macrophages from the spleen**

In order to isolate macrophages from the spleen, mice were sacrificed with CO<sub>2</sub>/O<sub>2</sub> following cervical dislocation and the spleen was removed and stored in PBS/2 % FCS. The spleen was then passed through a through a 70µm cell strainer and centrifuged at least twice at 300 xg for 5 min at 4°C and washed in PBS/2 % FCS. The whole spleen was then plated into a 15 cm dish in 10mL RPMI containing 20 % FCS, 30 % L929-cell line supernatant, 2.5 % L-glutamine and 0.5 % gentamycin. To differentiate macrophages from the spleen, half of the media was changed every 2 days via centrifugation at 300 xg for 5 min and the cells were resuspended in 10 mL fresh new media. At day 7, the macrophages are fully differentiated and seeded into a concentration of  $0.33 \cdot 10^6$  cells/well into a 24-well plate to perform the experiments.

### 3. Methods

---

#### **3.25 Bile acid measurement**

The measurement of bile acids was performed in collaboration with Sebastian Graute (Anna Worthmann lab, Hamburg). Bile acids were measured using high performance liquid chromatography (HPLC) coupled with electrospray ionization (ESI) tandem mass spectrometry <sup>198</sup>. Briefly, samples were prepared using a simple methanol liquid-liquid extraction. Quantitative measurement of bile acids was performed using a LC-ESI-QqQ system run in multiple reaction monitoring (MRM) mode. HPLC analysis was performed using NEXERA X2 LC-30AD HPLC PUMP (Shimadzu, Tokyo, Japan) equipped with a Kinetex C18 column (100 Å, 150 mm × 2.1 mm i.d., Phenomenex, Torrance, CA, USA). For HPLC, a mobile phase A consisting of water and a mobile phase B consisting of acetonitrile methanol (3/1 v/v) were used. Both mobile phases were enriched with 0.1% formic acid and 20 mM ammonium acetate. The column was coupled to a QqQ: Q trap 5500 System (SCIEX, Darmstadt, Germany). Peaks were identified and quantified by comparing retention times, MRM transitions and peak areas, respectively, to particular corresponding standard chromatograms.

#### **3.26 Isolation of peripheral blood mononuclear cells (PBMCs) using Ficoll density gradient.**

The collection of the blood from healthy donors and PSC patients was performed in collaboration with Jonas Bahn, AG Schwinge. The blood withdrawal was approved by the Ethics Committee of Hamburg, and written informed consent was obtained from all patients and healthy controls (PV4081). In order to obtain the PBMC fraction, the blood, collected in heparin tubes, was diluted 1:2 in PBS. 35mL of the diluted blood was then carefully layered on 15mL Ficoll-Paque in 50mL canonical tubes. A centrifugation step at 400 xg for 30 min (acc. 2 brake 0) was performed and the upper layer was removed leaving the interphase (containing the mononuclear cells) undisturbed. The interphase was transferred into a new tube and two washing steps with PBS 2% FCS were performed. The cells were then stained for phenotypical investigations at the Cytex Aurora. The antibodies used for the staining are listed in Table 8.

#### **3.27 Purification of CD14<sup>+</sup> cells from PBMCs**

To obtain CD14<sup>+</sup> monocytes from the total PBMC fraction, CD14 magnetic particles (BD Biosciences) were used by following the manufacturer's instructions. Briefly, total PBMCs were counted and 50µl anti-human CD14 magnetic particles were added for every 10<sup>7</sup> cells. The cell suspension was then incubated

### 3. Methods

---

for 30 min at RT in a FACS tube. The tube was then placed into a cell separation magnet for 8 min. With the tube still attached to the magnet, the supernatant was carefully removed. The remaining cell fraction was then resuspended in 1 ml MACS buffer and the tube was placed back into the magnet for 4 min. This step was repeated 2 times. The cells were then resuspended in RPMI containing 10 % FCS, 1 % L-glutamine and 0.5 % penicillin/streptomycin and plated at  $0.4 \times 10^6$ /well in a 24-well plate for 2 hours before performing the phagocytosis assay (as described above, see 3.10).

#### **3.28 Statistics**

Detailed information on the statistical analyses is supplied in the figure legends. Briefly, all data were analysed for normal distribution before running statistical tests. All of the provided data did not reach normal distribution. All the statistical tests, based on the comparison between two groups, were performed via Mann-Whitney U test. Statistical significance is indicated for  $p \leq 0.05$ . All data are shown as mean  $\pm$  SEM; each data point indicates one independent sample/mouse.

## 4. Results

Apoptotic cell clearance exerted by macrophages is essential for the maintenance and re-establishment of homeostasis in steady state and during pathological conditions. The phagocytic machinery prevents autoreactive processes operated by immune cells and, in the liver, plays a key role for self-tolerance. The impairment of this process has been reported for several autoimmune diseases, such as systemic lupus erythematosus and rheumatoid arthritis. The aim of this work is to dissect the role of macrophages in the phagocytosis of the apoptotic cells, both via the investigation of macrophage behaviour towards an apoptotic cell with a specific identity in *in vitro* experimental settings and in a mouse model of liver disease (primary sclerosing cholangitis).

### 4.1 Phagocytic receptor expression is downregulated in liver MOs from *Mdr2*<sup>-/-</sup> mice and correlates with an impaired ability to phagocytose apoptotic cells.

When apoptotic cells are not phagocytosed, they accumulate in the tissues, promoting inflammation and acting as a source of self-antigens. This leads to a sustained immune response, exacerbating the outcome of autoimmune diseases <sup>125 126 127 128</sup>. To investigate the process of apoptotic cell clearance exerted by liver macrophages (MOs) during the course of primary sclerosing cholangitis (PSC), mice at 8 (in green), 12 (in orange) and 25 (in blue) weeks of age, representing the early, intermediate and late stage of the disease, respectively, were analysed for phagocytic receptor expression in two different MOs populations. In detail, cells from the liver of *Mdr2*<sup>-/-</sup> and *Mdr2*<sup>+/+</sup> mice (control) at the above ages were characterised based on the expression of their surface markers via flow cytometry. Within the CD45<sup>+</sup> cell fraction, neutrophils (Ly6G<sup>+</sup>) and dendritic cells (CD11c<sup>+</sup>) were excluded from the analysis (Fig. 1A). Further characterization was performed based on the expression of the classical MO markers CD11b and F4/80. Next, in order to distinguish between the two main subsets of liver MOs (resident vs infiltrating), cells were distinguished by their expression of Ly6C, a classical marker of infiltrating cells. Cells were subsequently distinguished by their expression of CLEC4F and CX3CR1 and the frequency of resident and infiltrating MOs analysed (Fig. 1). No differences were found regarding the frequency of resident MOs in the *Mdr2*<sup>-/-</sup> compared to the controls at different stages of the disease (Fig. 1B). However, an increased frequency in the infiltrating Ly6C<sup>+</sup>CLEC4F<sup>+</sup>CX3CR1<sup>+</sup> MO population was observed in 12-week-old *Mdr2*<sup>-/-</sup> mice (Fig. 1C).

## Results

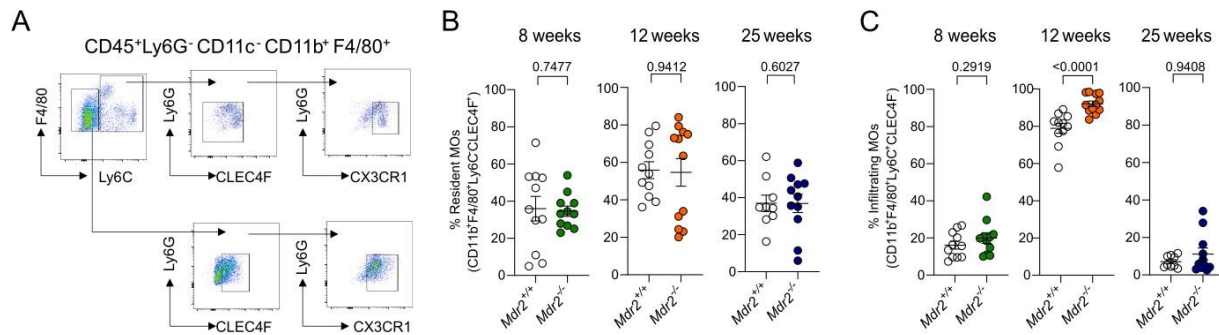


**Fig. 1: The frequencies of resident and infiltrating macrophages is comparable between *Mdr2*<sup>-/-</sup> and *Mdr2*<sup>+/+</sup> mice.**

(A) Flow cytograms representing the gating strategy adopted for the liver macrophage analysis. Dead and single cells were excluded. Starting from CD45<sup>+</sup> cells, neutrophils and dendritic cells were excluded via Ly6G and CD11c staining, respectively. Resident and infiltrating MOs were selected by their expression of Ly6C and then further distinguished using CLEC4F and CX3CR1 staining. After the first general discrimination of MOs, resident cells will be defined as Ly6G<sup>-</sup>CLEC4F<sup>+</sup>CX3CR1<sup>+</sup>, whereas infiltrating macrophages are Ly6G<sup>+</sup>CLEC4F<sup>-</sup>CX3CR1<sup>+</sup>. (B, C) Graphs representing the frequencies of resident (B) and infiltrating (C) MOs in *Mdr2*<sup>-/-</sup> and *Mdr2*<sup>+/+</sup> at 8 (in green), 12 (in orange) and 25 (in blue) weeks of age. An increased frequency of infiltrating MOs at 12 weeks of age was observed. Each data point indicates one independent sample. Mean ± SEM, Mann-Whitney U test was performed.

To provide a more detailed phenotypical characterization of the two MO subsets, the frequencies of the mannose receptor CD206 and the macrophage colony-stimulating factor receptor CD115 were also evaluated. In the resident MO population present in 8-week-old mice, a significant downregulation of MERTK and CD206 in *Mdr2*<sup>-/-</sup> mice compared to the controls was observed (Fig. 2A). In the infiltrating MO subset, CD206 and TIM4 expression was downregulated in *Mdr2*<sup>-/-</sup> mice compared to controls, while only a non-significant decrease in the expression of MERTK was observed (Fig. 2B).

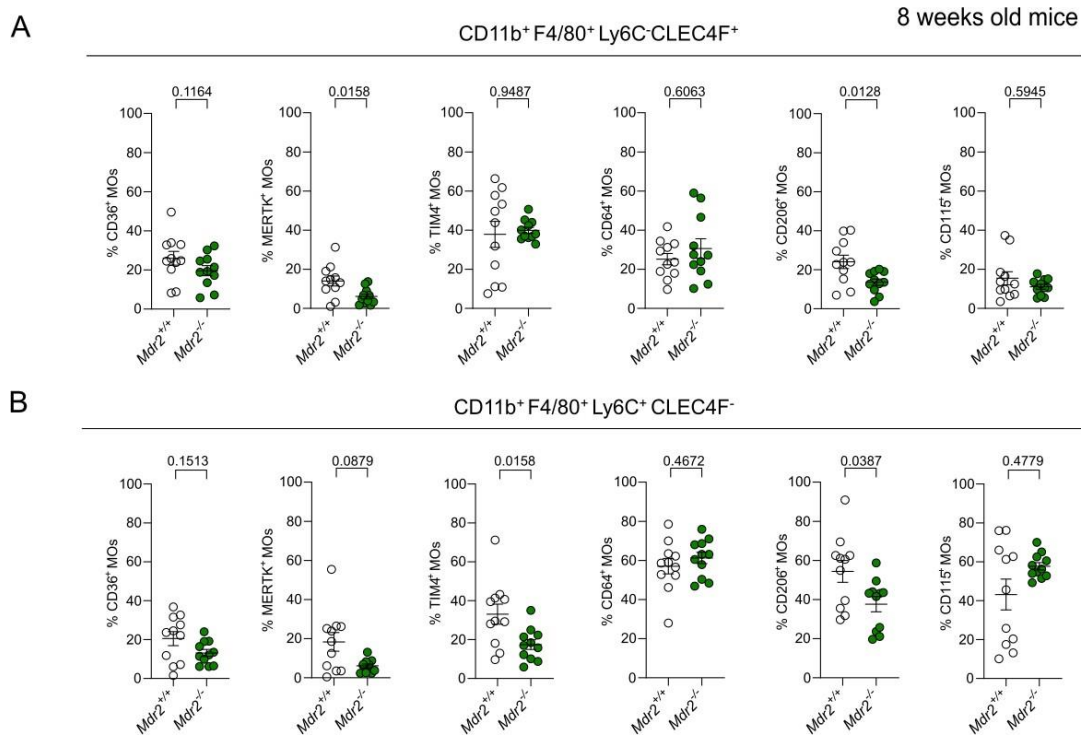


**Fig. 2: Phenotypical characterization of resident and infiltrating liver MOs in 8-weeks old *Mdr2*<sup>-/-</sup> mice compared to the controls (*Mdr2*<sup>+/+</sup>)**

Graphs representing the frequencies of different surface markers in the resident (A) and infiltrating (B) MO population in 8-week-old mice. (A) Frequencies of CD36, MERTK, TIM4, CD64, CD206 and CD115 receptors in *Mdr2*<sup>-/-</sup> and *Mdr2*<sup>+/+</sup> mice in the resident population (Ly6C<sup>+</sup> CLEC4F<sup>+</sup>) of liver MOs. A significant downregulation of MERTK and CD206 was observed. (B) Frequencies of the same markers in the infiltrating (Ly6C<sup>+</sup> CLEC4F<sup>-</sup>) MO population. TIM4 and CD206 were observed to be significantly downregulated. No significant changes in the other markers were noticed. Each data point represents one independent sample. Mean ± SEM. Mann-Whitney U test was performed.

Similar results were found at the intermediate and at late stage of the disease. On one hand, at 12 weeks, the resident population of MOs showed a significant downregulation of CD36 and MERTK expression (Fig. 3A). On the other hand, in the infiltrating MOs, a strong downregulation was observed for CD36, MERTK, TIM4 and CD206, suggesting an exacerbation of the disease (Fig. 3 B). Interestingly, an increased frequency in the key MO marker CD115, an essential marker for MO growth, survival and differentiation, and CD64 (Fc-γ receptor I), which plays a central role in MOs antibody-dependent cellular cytotoxicity and the clearance of immune complexes<sup>199</sup>, was observed.

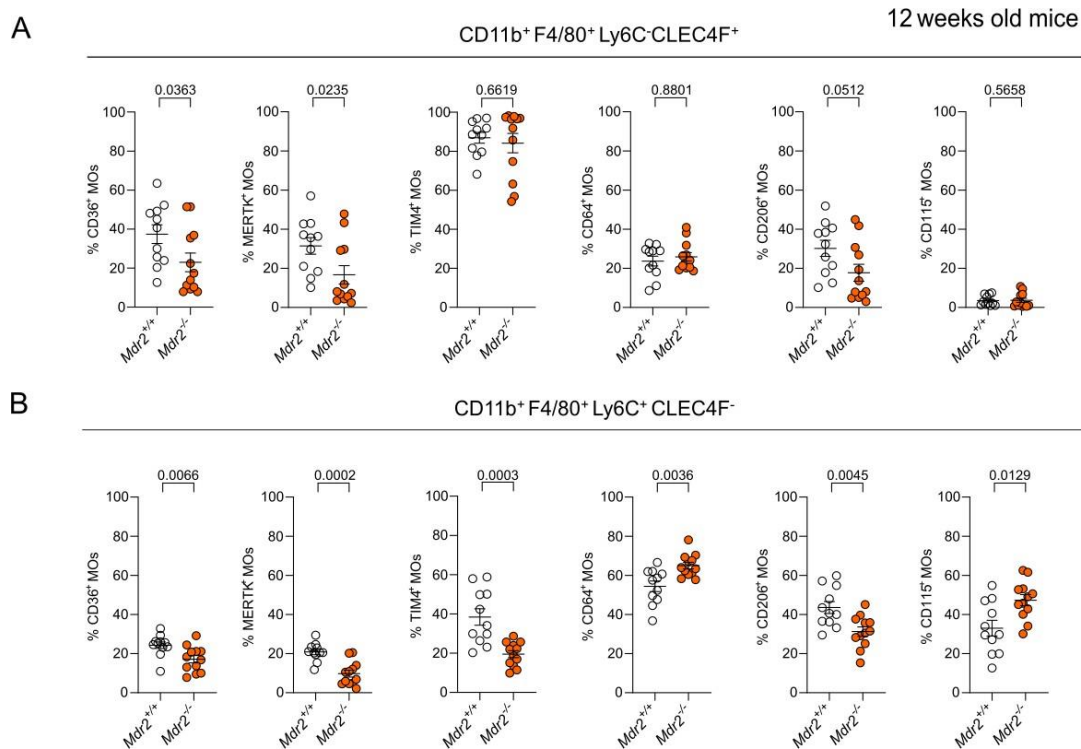


**Fig. 3: Phenotypical characterization of resident and infiltrating liver MOs in 12-week-old *Mdr2*<sup>-/-</sup> mice compared to the controls (*Mdr2*<sup>+/+</sup>)**

Graphs representing the frequencies of different surface markers in the resident (A) and infiltrating (B) MO population in 12-week-old mice. (A) Frequencies of CD36, MERTK, TIM4, CD64, CD206 and CD115 in the liver resident MO population (Ly6C<sup>-</sup> CLEC4F<sup>+</sup>). CD36, MERTK and CD206 were significantly downregulated. (B) Frequencies of the same markers in the infiltrating (Ly6C<sup>+</sup> CLEC4F<sup>-</sup>) liver MO population. CD36, MERTK, TIM4 and CD206 were significantly downregulated, whereas an increased frequency of CD115 and CD64-positive cells was observed. Each data point represents one independent sample. Mean ± SEM. Mann-Whitney U test was performed.

In the late stage of the disease (25 weeks), *Mdr2*<sup>-/-</sup> mice show a milder downregulation of the markers analysed, similar to the early stage of the disease (8 weeks). Indeed, the resident liver MOs show downregulation of MERTK and CD206 (Fig. 4A), whereas in the infiltrating MOs MERTK, TIM4, CD206 and CD115 expression was strongly downregulated (Fig. 4B).



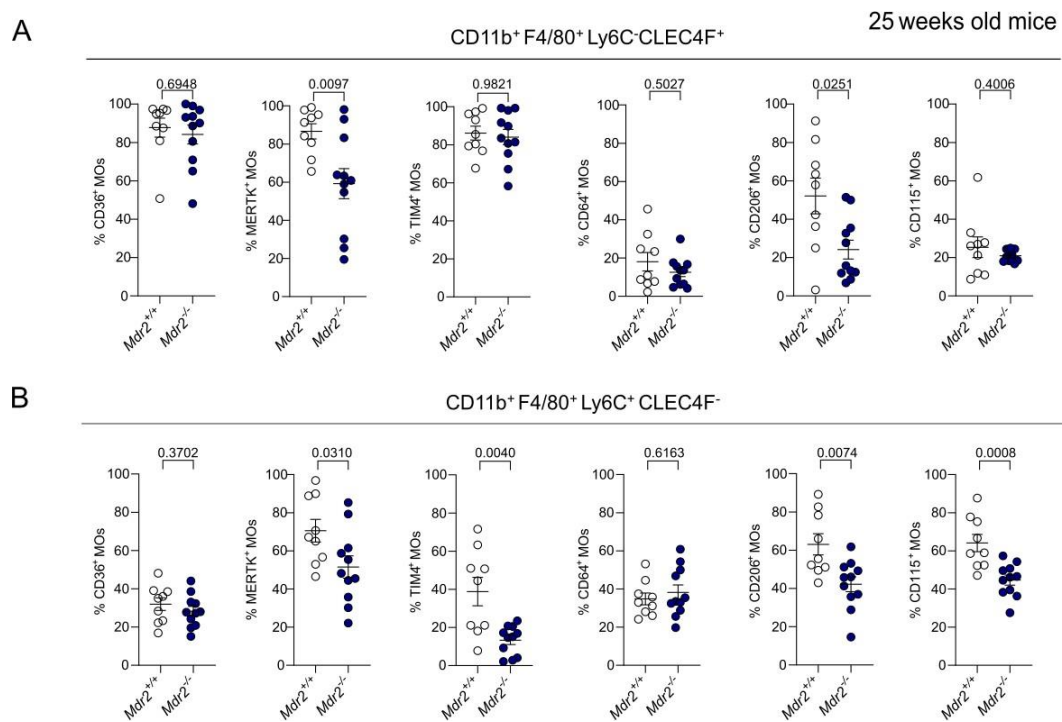


**Fig. 4: Phenotypical characterization of resident and infiltrating liver MOs in 25-week-old *Mdr2*<sup>-/-</sup> mice compared to the controls (*Mdr2*<sup>+/+</sup>)**

Graphs representing the frequencies of different surface markers in the resident (A) and infiltrating (B) MO population in 25-week-old mice. (A) Frequency of CD36, MERTK, TIM4, CD64, CD206 and CD115 in the resident (Ly6C-CLEC4F<sup>+</sup>) population of liver MOs. A significant downregulation of MERTK and CD206 was observed compared to the *Mdr2*<sup>+/+</sup> mice (controls). (B) Frequencies of the same receptors in the infiltrating (Ly6C<sup>+</sup>CLC4F<sup>-</sup>) MO population in the liver. In this cell subset, downregulation occurs in MERTK, TIM4, CD206 and CD115. Each data point represents one independent sample. Mean ± SEM, Mann-Whitney U test was performed.

The results demonstrate that the phagocytic machinery is altered during the course of cholangitis in a mouse model of the disease. The downregulation of several phagocytic receptors occurs at different disease stages, indicating a potential impairment in the capacity of MOs to recognise and/or uptake dying cells during disease progression.

Considering that the impairment of recognition and uptake of dying cells by MOs often results in their accumulation in the damaged tissue, we next evaluated the amounts of apoptotic cells present in the liver of 8, 12 and 35-week-old *Mdr2*<sup>-/-</sup> mice. The apoptotic cells are defined based on the expression of phosphatidylserine (PtdSer), which can be detected via Annexin-V (Ann-V) staining. The apoptotic cells, identified as Ann-V<sup>+</sup>, were then characterised for their specific cellular identity via cell-specific antibody staining. CD45<sup>+</sup> cells were distinguished into neutrophils (Ly6G<sup>+</sup>) and T cells (CD3<sup>+</sup>), while CD45<sup>-</sup> cells included all non-parenchymal cells, mainly represented by the hepatocytes (Fig. 5). In line with previous findings, apoptotic cells with different identities can be found in the liver of *Mdr2*<sup>-/-</sup> mice independently of

## Results

their age, suggesting that there is a link between the downregulation of phagocytic receptors on MOs and the accumulation of apoptotic cells.

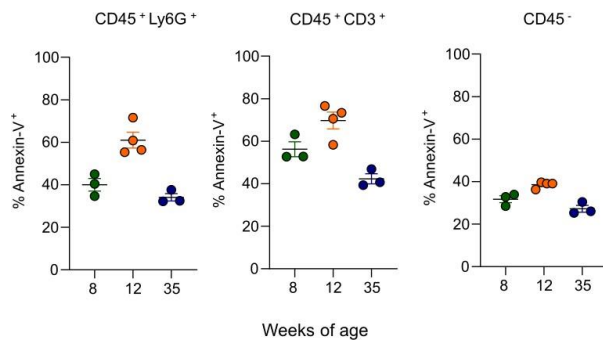


**Fig. 5: Apoptotic cells are present in the liver of *Mdr2*<sup>-/-</sup> mice during the course of the disease.**

Percentages of Annexin V<sup>+</sup> liver cells in *Mdr2*<sup>-/-</sup> mice at 8 (in green), 12 (in orange) and 35 (in blue) weeks of age, resembling the early, intermediate and late disease stage. From the left, Annexin V<sup>+</sup> neutrophils (CD45<sup>+</sup>Ly6G<sup>+</sup>), T cells (CD45<sup>+</sup>CD3<sup>+</sup>) and non-parenchymal cells (CD45<sup>-</sup>) are displayed. Each data point represents one independent sample. Mean ± SEM.

Given the reduced expression of several phagocytic receptors (Fig. 2, 3, 4) and the subsequent accumulation of apoptotic cells (Fig. 5) in the liver of *Mdr2*<sup>-/-</sup> mice, the phagocytic capacity of MOs isolated from different organs was then analysed *in vitro*. MOs were isolated from the liver<sup>197</sup>, peritoneum, bone marrow and spleen of 12-week-old *Mdr2*<sup>-/-</sup> and *Mdr2*<sup>+/+</sup> mice and their capacity to phagocyte cells with two different identities, apoptotic T cells (aT) and apoptotic hepatocytes (aH), was evaluated. To this end, apoptotic cells were stained with a cell tracker (CFSE) and the MOs were distinguished via the classical MO markers CD11b and F4/80. Next, their phagocytic capacity was assessed via flow cytometry. Detection of the apoptotic cell dye (CFSE) within the MO population (CD11b<sup>+</sup>F4/80<sup>+</sup>) allows the discrimination of the phagocytic MOs (CD11b<sup>+</sup>, F4/80<sup>+</sup> and CFSE<sup>+</sup>) from the non-phagocytic ones (CD11b<sup>+</sup>F4/80<sup>+</sup> and CFSE<sup>-</sup>). The phagocytosis assay is then performed under two conditions (representative dot plots, Fig. 6B): at 37°C, a circumstance in which MOs can bind and uptake the apoptotic cells, and at 4°C, in which cytoskeletal rearrangement is inhibited and MOs can bind, but not uptake the apoptotic cells. By subtracting the percentages of MOs (CD11b<sup>+</sup>F4/80<sup>+</sup> CFSE<sup>+</sup>) that bind and uptake the apoptotic cells (37°C) and the MOs that only bind the apoptotic cells (4°C), the frequency of phagocytic MOs can be determined. Notably, MOs isolated from the liver of *Mdr2*<sup>-/-</sup> showed an impaired capacity to phagocytose apoptotic T cells, but not apoptotic hepatocytes, compared to the *Mdr2*<sup>+/+</sup> MO counterparts. Interestingly, the MOs isolated from the spleen of *Mdr2*<sup>-/-</sup> also showed a decreased phagocytic rate. In this context, spleen MOs phagocytose apoptotic T cells normally, but show impaired engulfment of apoptotic hepatocytes (Fig. 6C).

## Results

Taken together, these results suggest that in the cholestatic liver of *Mdr2*<sup>-/-</sup> mice, MOs have a reduced phagocytic capability which potentially leads to an accumulation of apoptotic cells, thus sustaining the inflammation and the disease progression.

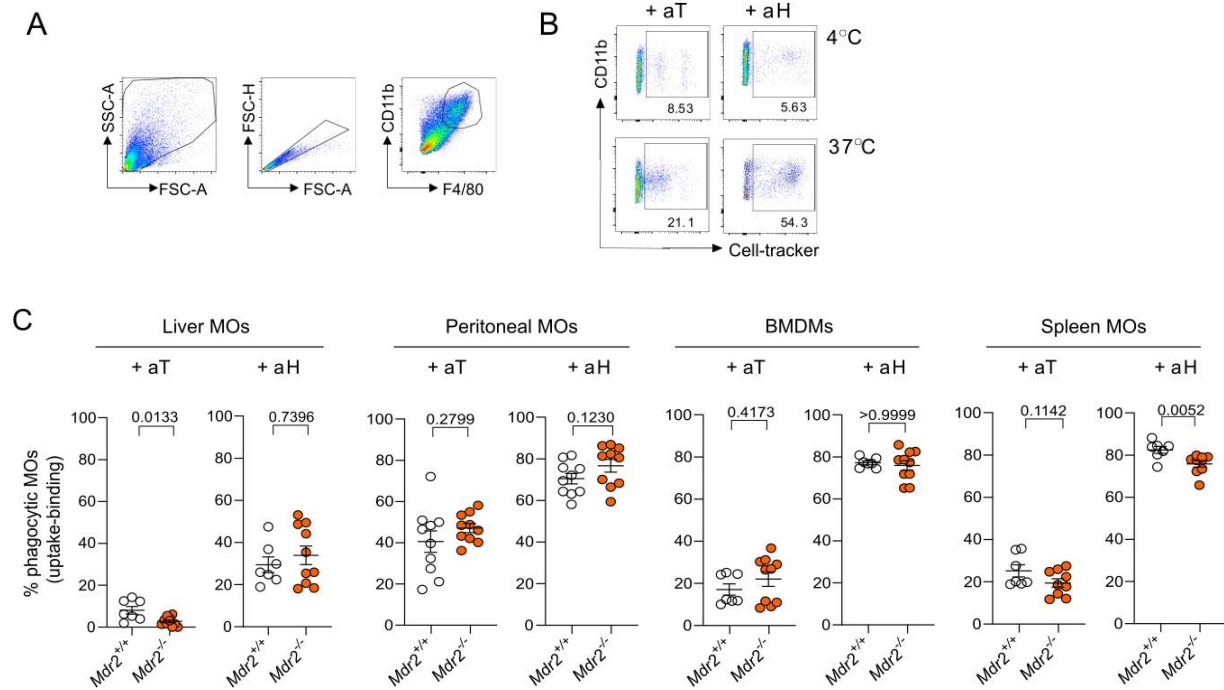


**Fig. 6: MOs isolated from the liver of *Mdr2*<sup>-/-</sup> have a reduced capacity to phagocytose apoptotic T cells *in vitro***

(A) Gating strategy. Flow cytograms representing the gating strategy adopted for the phagocytosis assay. Dead and single cells were excluded. MOs were identified by the expression of CD11b and F4/80. (B) Representative flow cytograms displaying liver MOs phagocytosing apoptotic T cells (aT) and apoptotic hepatocytes (aH), identified as positive for the cell tracker CSFE. The phagocytic MOs are defined as the difference of cells positive for the apoptotic cell tracker at 37°C (binding + uptake) and at 4°C (only binding). (C) Graphs representing the percentages of phagocytic MOs isolated from liver, peritoneum, bone marrow (BMDMs) and spleen in *Mdr2*<sup>-/-</sup> and *Mdr2*<sup>+/+</sup> mice at 12 weeks of age. A significant downregulation of the MOs' ability to phagocytose was noticed in MOs isolated from the liver and the spleen. Each data point represents one independent sample. Mean ± SEM, Mann-Whitney U test was performed.

### **4.2 The uptake of apoptotic cells with different identities is mediated by distinct phagocytic receptors**

PtdSer is the best characterised “eat me” signal on the apoptotic cell surface<sup>71 72</sup>. Although PtdSer has been extensively studied and identified as one of the main signals that can activate the phagocytic process in MOs, nothing is known about its role in the recognition of apoptotic cells with different identities. Therefore, in order to dissect the role of PtdSer in the sensing and uptake of different apoptotic cells, BMDMs were exposed to apoptotic T cells (aT) or apoptotic hepatocytes (aH) in the presence of Ann-V, a protein that binds negatively charged phospholipids on the cell surface and with a higher affinity for PtdSer compared to other phospholipids. The Ann-V binds the PtdSer exposed on the apoptotic cell surface, preventing the binding and recognition of the apoptotic cells by PtdSer phagocytic receptors expressed on MOs. Here, the Ann-V treatment significantly reduced the uptake of aT and aH (Fig. 7A), suggesting that PtdSer receptors are involved in the recognition of both cell types. To go deeper into the recognition of apoptotic cells by phagocytic receptors, BMDMs isolated from *Csf1r-Cre-Axl<sup>fl/fl</sup>Mertk<sup>fl/fl</sup>* mice, transgenic mice with a conditional knockout for the PtdSer receptors *Axl* and *Mertk* in MOs, and *Cd36<sup>-/-</sup>* mice were challenged with aT, aH and apoptotic neutrophils (aN) (Fig. 7B). Interestingly, the decrease in the phagocytic capacity of aN and aT in the absence of *Axl* and *Mertk* suggest these are critical receptors for the phagocytosis of neutrophils and T cells (although with less efficiency, p value 0,0026), but not involved in the phagocytosis of hepatocytes (Fig. 7B, on the left). In contrast, the knockout of *Cd36* does not affect the phagocytic capability of MOs, suggesting a dispensable role of this receptor in the uptake of all the cell types analysed (Fig. 7B, on the right). The data suggests that not all the phagocytic receptors are involved in the uptake of apoptotic cells with different identities with the same efficiency. Indeed, the potential specificity between the phagocytic receptors expressed on MOs and the identity of the apoptotic cell phagocytosed indicate a possible role of these receptors in the uptake of selected cell types during the course of PSC, and lays the foundation for a deeper and more specific analysis of the impact of phagocytosis in this context.

## Results

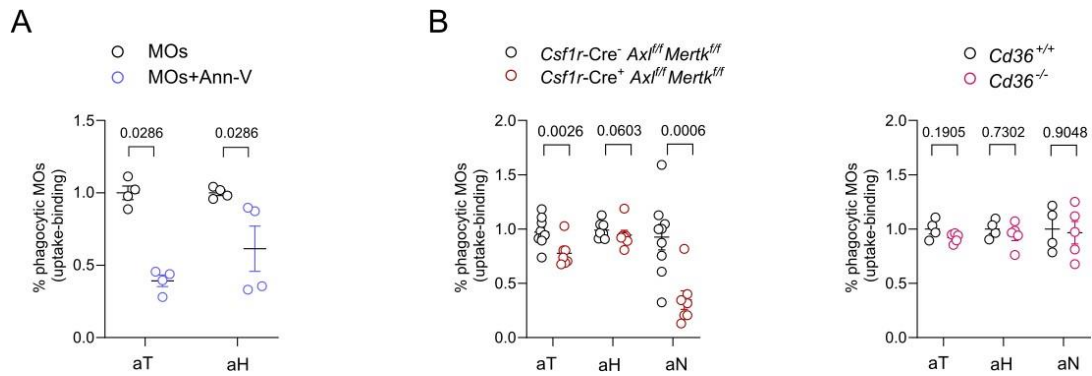


**Fig. 7: The phagocytosis of apoptotic cells is mediated by different phagocytic receptors *in vitro***

(A) BMDMs were exposed to aT and aH in the presence (in blue) or absence (in black, control) of Ann-V. Ann-V blocks the sensing of the PtdSer on the apoptotic cells' surface, thereby impairing the uptake of apoptotic cells that are recognised in a PtdSer-dependent fashion. Here, blocking PtdSer sensing significantly reduces the phagocytic rate for both aT and aH. (B) BMDMs isolated from *Cd36* (in pink) and *Axl* and *Mertk* knockout mice (in red) showed a different specificity for the uptake of the apoptotic cells. *Axl* and *Mertk* were found to be essential for the phagocytosis of both T cells and neutrophils, whereas *Cd36* was dispensable for the phagocytosis of all three cell types. In this experimental setting, the phagocytic MOs are defined as the difference between the percentage of MOs positive for the apoptotic cell tracker at 37°C (when binding and uptake occurs) and at 4°C (when only binding occurs). Each data point represents one independent sample. Mean  $\pm$  SEM, Mann-Whitney U test was exclusively performed between indicated samples.

Since the previous results showed a specificity between the phagocytic receptor engaged in MOs and the apoptotic cell identity, a deeper investigation on the prototypical behaviour of MOs when they encounter different apoptotic cells was needed. In detail, MOs were analysed for their capability to phagocytose one or multiple apoptotic cells at the same time, since the possibility that MOs can engage different phagocytic receptors in order to simultaneously phagocytose apoptotic cells with different identities cannot be excluded. To this end, MOs were exposed to aT, aH and aN singularly or concomitantly (Fig. 8A). The apoptotic cells were stained with different cell dyes and the phagocytic rate was measured via flow cytometry. tSNE (t-distributed stochastic neighbour embedding) analysis, a statistical method where a nonlinear dimensionality reduction technique is applied to embed high-dimensional data and visualise them in two dimensions, was used to represent the phagocytic MOs (Fig. 8A). tSNE plots show the MOs (CD11b<sup>+</sup>F4/80<sup>+</sup>) that have been uptaken – aH (in blue), aT (in light blue) and aN (in pink) – whereas the non-phagocytic MOs in each condition are shown in black. The gate present in all the three plots represents MOs that phagocytosed all three cell types. The data show that MOs preferentially phagocytose a single type of apoptotic cell at one time and just a small percentage of MOs was able to phagocytose all three apoptotic cell types concomitantly at each of the time point analysed (2,34%  $\pm$  SEM). To confirm the results obtained via flow cytometry, in collaboration with Irene Aranda Pardos (N. Gonzalez lab, Munich), a time lapse analysis was performed on BMDMs exposed to the multiple apoptotic cells concomitantly (aH, aT and aN) (Fig. 8B). The phagocytic rate of MOs was

## Results

recorded over time (5, 15, 30, 60 and 90 min) and analysis performed via immunofluorescence (IF). The obtained data corroborate the flow cytometry analysis and indicate that each single MO is not only more predisposed toward the phagocytosis of an apoptotic cell with a single identity, but also that a concomitant phagocytosis of apoptotic cells with different identities occurs only at later time points during MO-apoptotic cell interactions (90 min). These results suggest that the sensing and subsequent uptake of apoptotic cells by MOs is mainly restricted to one cell type at a time, and that MOs can phagocytose multiple cell types only at later time points during apoptotic cell-MO cell contact.

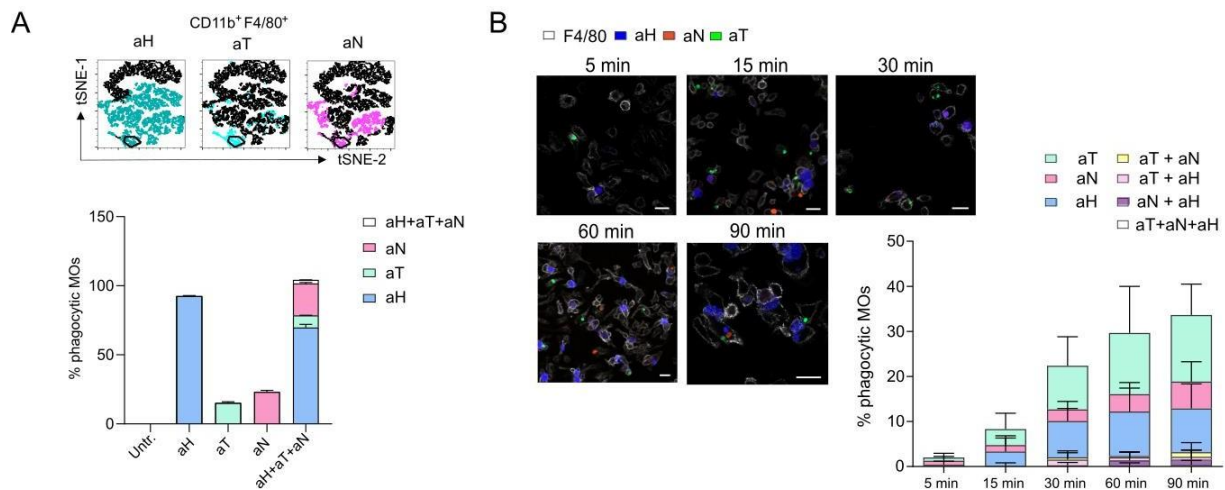


**Fig. 8: When exposed concomitantly to apoptotic cells with different identities, MOs preferentially phagocytose one type of apoptotic cell at the time**

(A) BMDMs were exposed to aH, aT, aN or all three cell types. Apoptotic cells were stained with different cell dyes and the phagocytic capacity of MOs was tracked via FACS. tSNE plots represent the MOs that have been exposed to aH (in blue), aT (in light blue) or aN (in pink). Non-phagocytic MOs are represented in black in each tSNEplot. The gate (black circle) in each plot shows the MOs that have been phagocytosed aH, aT and aN simultaneously. The graph below shows the percentage of phagocytic MOs at 37°C for aH, aT, aN or all the three cell types. (B) IF was performed on MOs (here stained for F4/80, in white) during the phagocytosis of aH (in blue), aT (in green) and aN (in red). The phagocytic rate was recorded 5 min after adding the apoptotic cells and further analysed at min 15, 30, 60 and 90. The left side shows representative images of the phagocytic MOs. On the right, the graph shows the quantification of the phagocytic rate. IF analysis performed in collaboration with Irene Aranda Pardos, AG Alonso-Gonzalez (Uni Münster). Each data point represents one independent sample. Mean  $\pm$  SEM, Mann-Whitney U test was performed.

### **4.3 Bile acids can modulate the phagocytic receptor expression and the phagocytosis capacity in liver MOs**

In order to investigate the mechanism that regulates the phagocytic function of liver MOs and whether this can affect the uptake of different immune cells, leading to an alteration of the immune response, the impact of bile acid on MOs was tested. In cholestatic liver diseases an accumulation of bile acids occurs in the liver and in system circulation <sup>177</sup>. This accumulation can result in oxidative stress and mitochondrial damage that triggers the inflammatory response and the recruitment of neutrophils and other immune cells, which in turn contribute to the disease development <sup>176</sup>. In order to test whether bile acids can alter the MO phagocytic machinery and thus affect MO phagocytic capacity, we first isolated MOs from the liver of WT mice <sup>197</sup>. Cells were then stimulated *in vitro* with a secondary BA, tauro lithocholic acid (TLCA), a strong TGR5 agonist. The cytotoxic effect of both primary and secondary bile acids on hepatocytes has been described as occurring through the induction of mitochondrial permeability transition (MPT)<sup>200</sup> and the activation of death receptors Fas and TRAILR-2 <sup>201</sup>, thereby leading to hepatocyte apoptosis, whereas in human MOs, TLCA treatment strongly affects their transcriptomic signature <sup>202</sup>. Here, liver-isolated MOs were pre-treated for 2 hours with 30 $\mu$ M of TLCA, a concentration which is lower than what is found in cholestatic patients, where the total bile acid concentration has been reported to be up to 200 $\mu$ M <sup>203</sup>. Treatment of MOs with TLCA led to a significant downregulation of the expression of MERTK and CD64 compared to the controls (MOs treated with DMSO alone), while CD36 expression was not affected (Fig. 9 A). To evaluate the effect of TLCA on the cell viability of MOs in our experimental setting, analysis of PtdSer exposure via Ann-V staining as well as propidium iodide (PI) staining, a dye that enters the nucleus when the cell membrane disintegrates and that helps to distinguish between late apoptotic (Ann-V<sup>+</sup>PI<sup>+</sup>) and necrotic (Ann-V<sup>+</sup>PI<sup>+</sup>) cells, was performed and analysed by FACS. The percentage of alive cells between the samples was comparable, thus indicating that the TLCA treatment, at the concentration used, did not influence the viability of the cells (Fig. 9B).



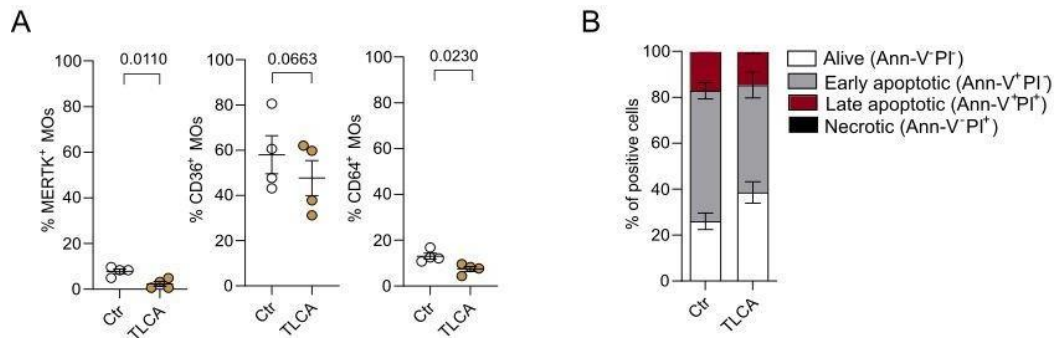


**Fig. 9: TLCA treatment downregulates the phagocytic receptor expression without affecting their viability *in vitro***

(A) MOs were isolated from the liver of WT mice and stained for the MO markers CD11b and F4/80 (data not shown). Liver MOs were then treated with 30µM of TLCA or with the vehicle (DMSO alone, control) for 2 hours. The expression of the phagocytic receptors MERTK, CD36 and CD64 was checked via FACS. The graphs show a significant reduction of MERTK and CD64 when treatment with TLCA occurs. The frequency of CD36<sup>+</sup> liver MOs was not altered. Each data point represents one independent sample. Mean ± SEM, Mann-Whitney U test was performed. (B) The viability of MOs was tested via FACS via AnnV/PI staining. The graph shows the percentages of cells positive for Ann-V and PI in TLCA-treated MOs (30µM) compared to the control (DMSO only). Alive cells (in white) are defined as negative for both Ann-V and PI. Early apoptotic cells (in grey) expose PtdSer and are therefore positive for Ann-V, but negative for PI. Late apoptotic cells (in red) are positive for both Ann-V and PI, whereas necrotic cells (in black) are positive for PI, but negative for Ann-V staining. Mean ± SEM.

To verify whether the downregulation in the expression of the phagocytic receptors could be associated with a reduced phagocytic capacity, liver MOs were then exposed to two apoptotic cell types, hepatocytes and T cells (Fig. 10) and their phagocytic ability was assessed after TLCA treatment (2h, 30µM). The phagocytic rate of TLCA-treated liver MOs was drastically reduced for the phagocytosis of both cell types, indicating a detrimental role of bile acids not only in the expression of phagocytic receptors, but also in the phagocytic function of MOs in the liver.

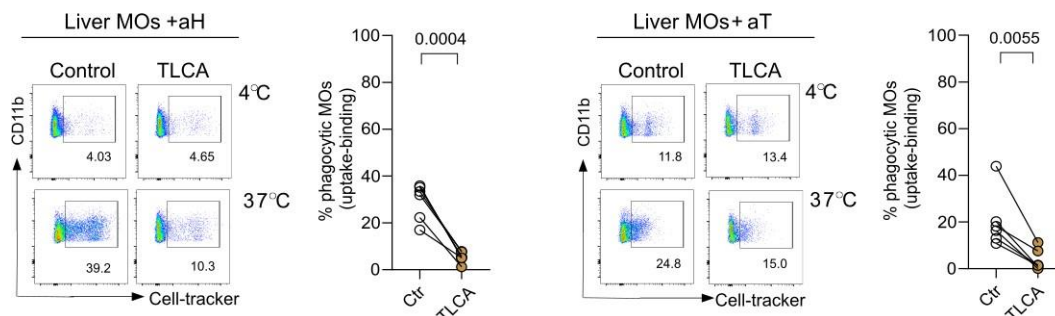


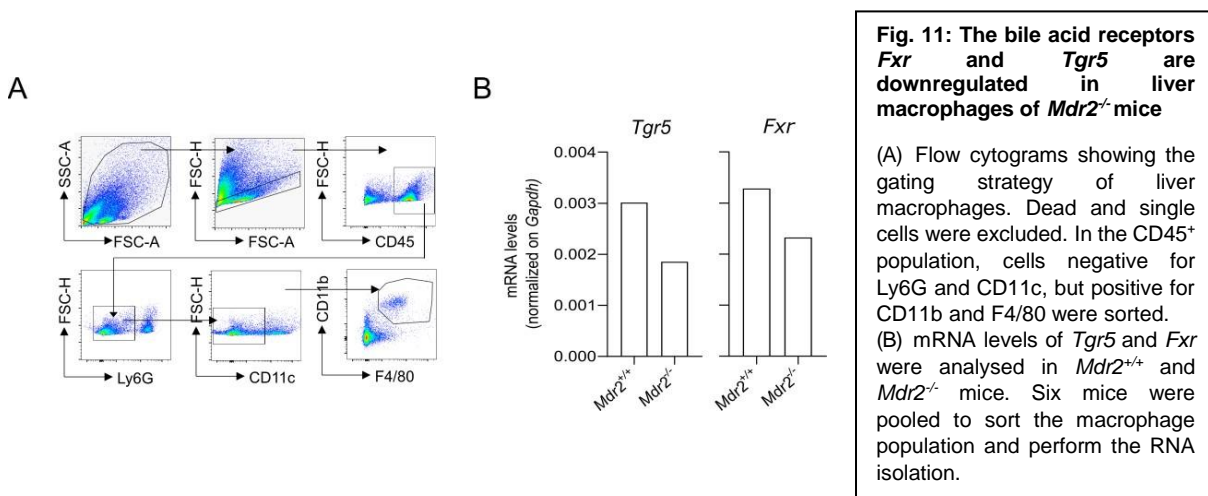
**Fig. 10: Liver MOs show a reduced phagocytic capacity after TLCA treatment *in vitro***

Liver-isolated MOs from WT mice show an impaired phagocytic capability after being exposed to apoptotic hepatocytes (on the left) or apoptotic T cells (on the right). Representative flow cytograms displaying liver MOs phagocytosing apoptotic T cells (aT) and apoptotic hepatocytes (aH), identified as positive for the cell tracker (CSFE). The phagocytic MOs are defined as the difference of cells positive for the apoptotic cell tracker at 37°C (binding + uptake) and at 4°C (only binding). Graphs representing the percentages of phagocytic MOs isolated from the liver of WT mice and treated with TLCA (30µM, in brown) or with DMSO alone (control, in white) Each data point represents one independent sample. Mann-Whitney U test was performed.



#### 4.4 Bile acids accumulate in liver MOs and impair their ability to phagocytose apoptotic cells.

Bile acids can act as signalling molecules, exerting pleiotropic activities via the activation of evolutionarily conserved bile acid-activated receptors (BARs)<sup>204</sup>. FXR and TGR5 are the best characterised bile acid receptors both in mouse and human and are highly expressed in several immune cells, including MOs<sup>205</sup>. FXR and TGR5 are known for their role in the maintenance of the tolerogenic phenotype of MOs, as shown in *Tgr5*<sup>-/-</sup> and *Fxr*<sup>-/-</sup> mice<sup>206 207</sup>. These mice are more prone to developing immune dysfunction and are characterised by increased bile acid levels. To further investigate the role of bile acids during PSC, liver MOs from 8-week-old *Mdr2*<sup>-/-</sup> mice and littermate control mice were cell-sorted as CD45<sup>+</sup>Ly6G<sup>-</sup>CD11c<sup>-</sup>CD11b<sup>+</sup>F4/80<sup>+</sup> cells, after exclusion of dead and doublets (Fig. 11A). The expression of the bile acid receptors *Tgr5* and *Fxr* was then assessed via qPCR. The results indicate a slight decrease of both *Fxr* and *Tgr5* in *Mdr2*<sup>-/-</sup> MOs compared to controls, thus potentially suggesting a potential dysregulation in the damaged liver of *Mdr2*<sup>-/-</sup> (Fig. 11B).



In order to be secreted into the bile ducts, the two primary bile acids CA and CDCA, products of the conversion of cholesterol in the liver, are conjugated with glycine or taurine at the C-24 carboxyl group. In the human liver, primary bile acids are conjugated with glycine and taurine at a 3:1 ratio. In contrast, in the mouse liver, 95% of the bile acids are tauro-conjugated. The conjugated bile acids then undergo further metabolic processing by the intestinal microbiota in the distal Ileum to generate secondary bile acids, before circulating back to the liver via the entero-hepatic circulation<sup>205</sup>. To better dissect the role of bile acids related to their ability to shape MO phagocytosis and phenotype, liver MOs from 8-week-old *Mdr2*<sup>-/-</sup> mice were FACS-sorted based on their expression of the phagocytic receptors CD36 and

## Results

MERTK. To this end, dead cells, single cells, CD45<sup>-</sup>, neutrophils (Ly6G<sup>+</sup>) and dendritic cells (CD11c<sup>+</sup>) were excluded. MOs were then defined based on the markers CD11b and F4/80 and FACS-sorted based on the expression of the phagocytic receptors MERTK and CD36 as MERTK<sup>+</sup>CD36<sup>+</sup> and MERTK<sup>-</sup>CD36<sup>-</sup> MOs (Fig. 12A). The two subsets of MOs, one negative for the above-mentioned phagocytic receptors (or phagocytic receptor-deficient MOs) and the other one positive for both MERTK and CD36 (or phagocytic receptor-enriched MOs), were analysed via lipidomic analysis (Fig. 12B) performed in collaboration with Sebastian Graute (Jorg Heeren lab, Hamburg). Bile acids were measured using high performance liquid chromatography (HPLC) coupled with electrospray ionization (ESI) tandem mass spectrometry<sup>198</sup>. Quantitative measurement of bile acids was performed using a LC-ESI-QqQ system run in multiple reaction monitoring (MRM) mode. Peaks were identified and quantified by comparing retention times, MRM transitions and peak areas, respectively, to particular corresponding standard chromatograms. Lipidomic analysis provides not only the identification, but also the quantification of the bile acids that are present within the two different MO subsets. The results, expressed in  $\mu\text{M}/1$  million cells, revealed an increased accumulation of bile acids, both conjugated (CBA) and unconjugated (UBA), in the phagocytic receptor-enriched MO population.

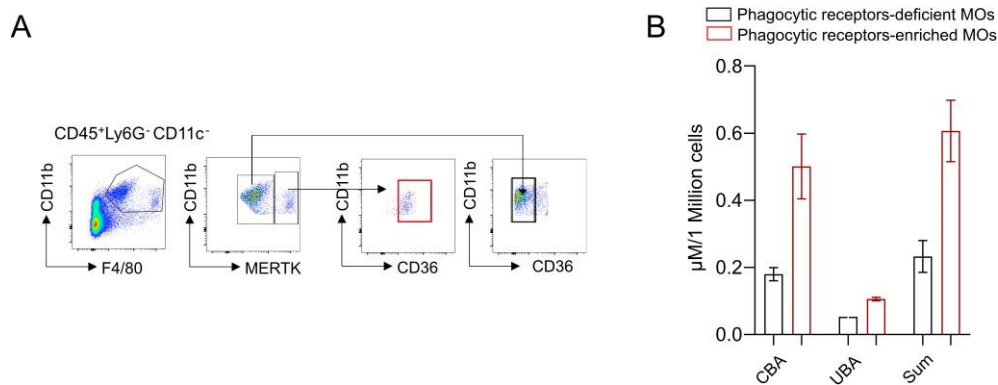


**Fig. 12: Bile acids accumulate in phagocytic receptor-enriched *Mdr2*<sup>-/-</sup> mice liver MOs.**

(A) Flow cytograms representing the gating strategy adopted for the lipidomic analysis. The MO populations were identified by their expression of CD45, CD11b and F4/80, excluding dead cells, single cells, Ly6G and CD11c-positive cells. The MO populations were then divided by their expression of the phagocytic receptor MERTK and CD36 and sorted accordingly. The phagocytic receptor-enriched MOs are defined as MERTK<sup>+</sup>CD36<sup>+</sup>, whereas the phagocytic receptor-deficient MOs are MERTK<sup>-</sup>CD36<sup>-</sup>. (B) Graph representing the quantification of conjugated bile acids (CBA) and unconjugated bile acids (UBA) between the two sorted MO subsets. The black bars represent the phagocytic receptor-deficient MOs, whereas the red bars represent the phagocytic receptor-enriched MOs. Mean  $\pm$  SEM. Two independent experiments were performed. Six pooled mice were used in each experiment.

## Results

To then go deeper into the bile acid content in the two MOs subsets, bile acids were divided into conjugated and unconjugated, and further distinguished based on their identity (Fig. 13). The results show the amount of bile acid, expressed in  $\mu\text{M}/1$  million cells, in the phagocytic receptor-enriched MOs (in red) compared to the phagocytic receptor-deficient MOs (in black) in the liver of *Mdr2*<sup>-/-</sup> mice. For almost all the bile acids identified, the concentration was higher in the MOs enriched for MERTK and CD36. Specifically, a high concentration of taurocholic acid (TCA) was found in this MO subset. The data demonstrated that an accumulation of bile acids mainly occurs in MOs expressing the phagocytic receptors, rather than in MOs in which expression of MERTK and CD36 is downregulated. This result, although not anticipated, since our data in Fig. 9 and 10 showed that *in vitro* treatment with BAs triggers an impairment in phagocytic receptor expression and consequent impairment in phagocytosis, indicate that other mechanisms of bile acid sensing by MOs or bile acid accumulation occur within MOs without affecting their phagocytic receptor expression. Therefore, the reason for the bile acid accumulation inside the phagocytic receptor-enriched MOs was further investigated.

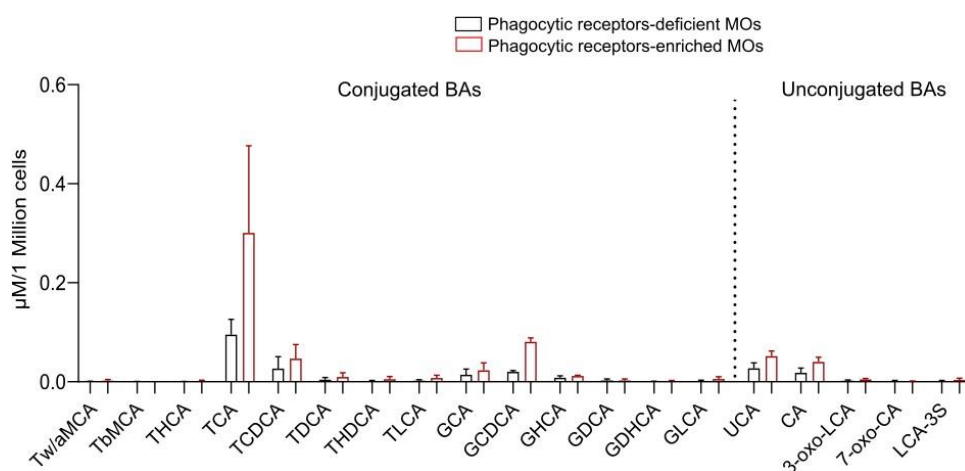


**Fig. 13: Characterization of the bile acid profile in phagocytic receptor-enriched and -deficient *Mdr2*<sup>-/-</sup> mice liver MOs.**

Graph representing the bile acids found in  $\mu\text{M}/1$  million cells in two subsets of liver MOs (phagocytic receptor-enriched MOs in red and phagocytic receptor-deficient MOs in black) isolated from 8-week-old *Mdr2*<sup>-/-</sup> mice. The left part shows the conjugated BAs, the right part the unconjugated ones. Bile acids were identified via HPLC combined with ESI tandem mass spectrometry. The bile acids that were below the detection levels were excluded from the analysis. Mean  $\pm$  SEM. Two independent experiments were performed.

## Results

---

In the liver of cholestatic patients, bile acids accumulate inside the hepatocytes, leading to their apoptosis<sup>208</sup>, and a high concentration of free bile acids can be found in the serum<sup>203</sup>. In addition, an impaired phagocytic capacity was observed in liver MOs isolated from *Mdr2*<sup>-/-</sup> compared to the controls (Fig. 6). In line with this, alternative paths by which bile acids are internalised inside the MOs was hypothesised and investigated by measuring bile acid accumulation in MOs following the engulfment of bile acid-loaded hepatocytes. To this end, MOs were exposed to either untreated hepatocytes or BA-treated hepatocytes (Fig. 14A). The *in vitro* experiment was conducted as described below: first, hepatocytes were treated with the vehicle control (DMSO) or with the secondary bile acid TLCA at a concentration of 30µM (TLCA-treated hepatocytes) for 2 hours. Then, hepatocyte apoptosis was induced by heating them for 45 min at 43 °C. Next, the apoptotic hepatocytes, labelled with a cell tracker dye (CFSE), were cocultured with BMDMs and a phagocytosis assay was performed, with co-culture taking place for 1 hour at 37°C (at which uptake and binding occur) or at 4°C (where only binding occurs, see above) (Fig. 14B). The phagocytic rate for both conditions was detected via flow cytometry and the percentages of phagocytic MOs were evaluated as the difference of cells positive for the apoptotic cell tracker at 37°C and at 4°C (Fig. 14B, right). No differences were found in the phagocytic ability of BMDMs to internalise either untreated hepatocytes or TLCA-treated hepatocytes. Next, lipidomic analysis on BMDMs in both conditions was performed via HPLC and ESI tandem mass spectrometry and the TLCA presence inside the MOs was analysed (Fig. 14C). The graph shows the amount of TLCA detected in MOs that have internalised TLCA-treated apoptotic hepatocytes, thereby indicating that bile acids can accumulate inside the MOs via phagocytosis of bile acid-loaded hepatocytes. All together, these data suggest that phagocytosis is an alternative path by which bile acids can accumulate and thus affect MO function in the cholestatic liver.

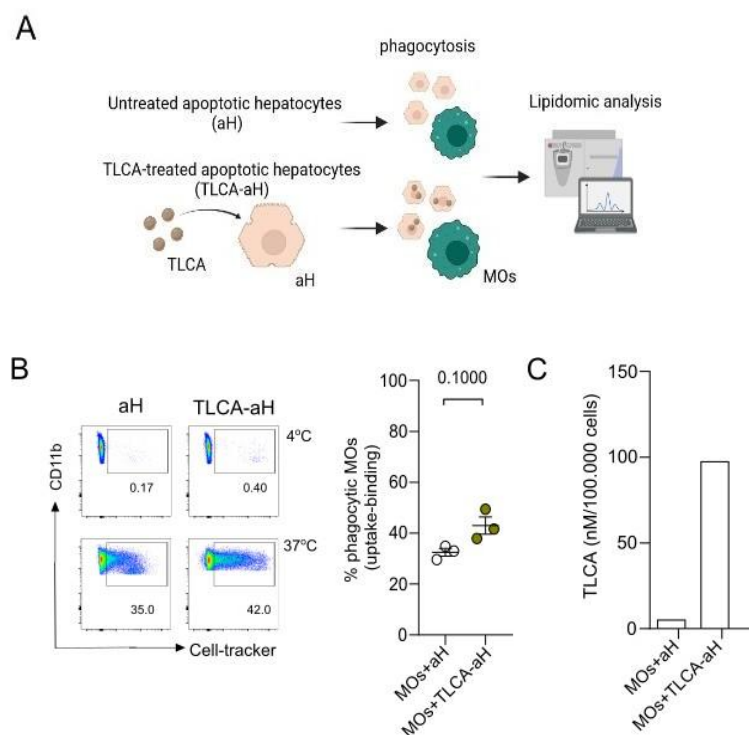


**Fig. 14: Bile acids can accumulate inside MOs that have been phagocytosed bile acid-treated-aH**

(A) Experimental scheme. Hepatocytes were treated with the vehicle (DMSO) or with 30 $\mu$ M of the secondary BA TLCA for 2 hours. Next, BMDMs were cocultured with hepatocytes from both conditions and the level of TLCA inside the MOs was analysed via lipidomic analysis. Figure created with Biorender (B) On the left, representative flow cytograms displaying BMDMs after the phagocytosis of the hepatocytes either treated or untreated, identified as positive for the cell tracker (CSFE). On the right, phagocytic MOs are defined as the difference of cells positive for the apoptotic cell tracker at 37°C (binding + uptake) and at 4°C (only binding) in MOs that phagocytosed untreated aH (white dots) or TLCA-treated aH (brown dots). Each data point represents one independent sample. Mean  $\pm$  SEM. Mann-Whitney U was performed. (C) Lipidomic analysis. Graph representing the amount of TLCA (nM/100.000 cells) detected inside the MOs phagocytosing TLCA-treated or untreated apoptotic hepatocytes via HPLC and ESI tandem mass spectrometry.

To better investigate whether internalised bile acids can alter the phagocytic capacity of MOs, the ability of MOs to phagocyte apoptotic T cells was tested after MOs were co-cultured with bile acid-treated hepatocytes. In detail, hepatocytes were treated with 30 $\mu$ M of TLCA for 2 hours or with DMSO (control) as previously described (Fig. 14A, left panel). Next, BMDMs were exposed to control (DMSO alone) or TLCA-treated aH for 1 hour at 37°C and 4°C (as shown in Fig.14B). Then, hepatocytes that had not been phagocytosed were removed via multiple washing steps with PBS and the percentages of phagocytic MOs were analysed. As shown in the previous results via lipidomic analysis, MOs that phagocytosed TLCA-treated hepatocytes can internalise the bile acid (as reported in Fig. 14C). In order to further test whether the accumulation of BA within the MO can further affect their functions, MOs were rested for 1 hour and another phagocytosis assay with apoptotic T cells was performed. Similarly to the previously described assays, phagocytosis of apoptotic T cells was also performed for 1 hour at 37°C and 4°C in order to discriminate between binding and actual uptake of apoptotic cells. The results (Fig. 15 C) show that MOs that were challenged with TLCA-treated aH have a significant impairment in the further phagocytosis of other apoptotic cells (aT) compared to MOs which did not accumulate BAs during the first round of phagocytosis (due to being exposed to control-treated hepatocytes). These data suggest that bile acids can not only act as signal molecules and impact MO function in an exogenous

## Results

manner (Fig. 10), but they can be carried within MOs via the uptake of apoptotic hepatocytes that have previously internalised bile acids. These data are particularly relevant in the context of cholestatic diseases, in which a strong accumulation of bile acids inside the hepatocytes has been reported<sup>208</sup>. The detrimental effect of bile acids on the phagocytic capability of liver MOs could help to explain the accumulation of apoptotic cells and the sustained inflammation that aggravates PSC progression. Moreover, in this experimental set-up, additional technical controls were added: untreated MOs and MOs challenged with 30  $\mu$ M of TLCA for 2 hours were exposed to apoptotic T cells and the phagocytic rate was recorded (data not shown). The significant phagocytosis impairment after TLCA treatment was confirmed, as previously shown in Fig. 10. Furthermore, the percentage of phagocytic MOs after their exposure to untreated aH and TLCA-treated aH was analysed and no differences were reported (data not shown). In summary, bile acids, and in particular TLCA, as tested in our experimental setting, can affect the phagocytic capability of MOs both when they are present in the surrounding environment as a free molecule (as reported in Fig. 10) and via the uptake of apoptotic hepatocytes loaded with bile acids (Fig. 15).

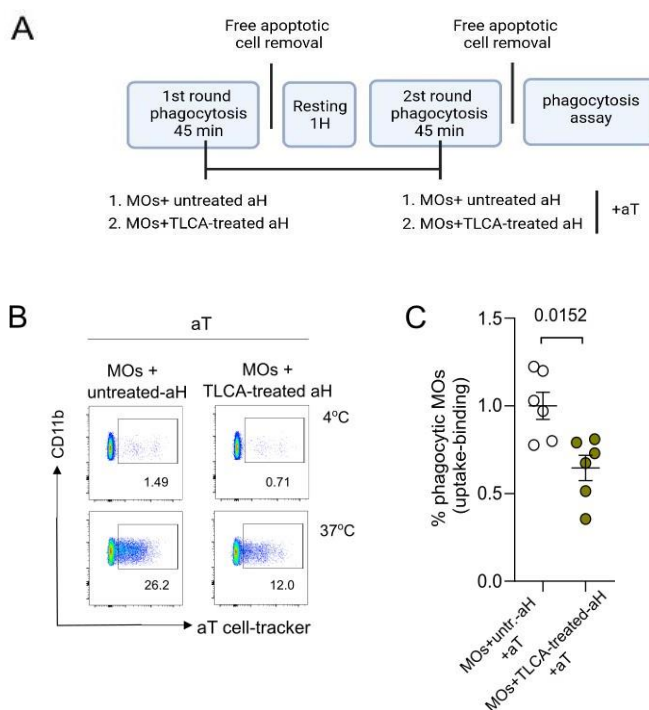


**Fig. 15: MOs exposed to TLCA-treated hepatocytes are shown to have a decreased phagocytic rate.**

(A) Experimental scheme. MOs were fed with untreated aH (control) or with TLCA-treated aH for 45 minutes. After the removal of the apoptotic cells that were not internalised, MOs were rested for one hour before being exposed to aT for a second round of phagocytosis. Free aT were removed from the medium and the phagocytic rate was analysed via FACS. Figure created with Biorender (B) Representative dot plots showing the phagocytosis of aT of MOs that phagocytosed untreated aH (control) or TLCA-treated aH at 37°C and at 4°C (C). Graph reporting the percentage of MOs that phagocytosed aT. The phagocytosing BMDMs are identified as positive for the cell tracker (CSFE). The phagocytic MO rate is defined as the difference of cells positive for the apoptotic cell tracker at 37°C (binding + uptake) and at 4°C (only binding). Each data point represents one independent sample. Mean  $\pm$  SEM. Mann-Whitney U test was performed. Three independent experiments were performed.

In order to investigate the phagocytic receptor expression and subsequent phagocytic capability of MOs in cholestatic patients, blood samples from PSC patients were collected and further investigations were performed.

### **4.5 Characterization of phagocytic receptor expression on human monocytes during primary sclerosing cholangitis**

The relevance of phagocytosis during primary sclerosing cholangitis (PSC) in patients has not been fully elucidated so far. Therefore, in order to investigate whether the difference observed in the phagocytic machinery of murine liver MOs isolated from the liver of the *Mdr2*<sup>-/-</sup> can be translated to the human setting, the phagocytic receptor expression and the subsequent phagocytic capability of blood-derived monocytes from cholestatic patients was investigated.

Here, monocytes isolated from blood samples from a cohort of patients affected by PSC were analysed for the expression of phagocytic receptors and compared to age and sex-matched healthy donors (HD). The cohort used for this study included 8 PSC patients (4 females and 4 males), with ages between 20 and 57 years old. Samples were collected in Hamburg. The alanine transaminase (ALT) levels in the serum, a common indicator of liver damage, were at a range between 9 and 47 (Normal range: <35). 6 out of 8 patients were also affected by PSC-associated colitis, and none of them presented cholangiocarcinoma.

The analysis for the expression of phagocytic receptors was performed on two different monocyte subsets, classical and non-classical monocytes, defined as CD14<sup>+</sup>CD16<sup>-</sup> and CD14<sup>-</sup>CD16<sup>+</sup>, respectively (Fig. 16). Classical monocytes are mainly associated with their innate immune response, migration and phagocytic capacity, whereas non-classical monocytes are involved in adhesion, complement and Fc- $\gamma$ -mediated phagocytosis<sup>209,210</sup>. A further discrimination of both populations by expression of chemokine receptor CCR2, which defines the ability of monocytes to migrate to the inflamed tissues<sup>210</sup>, was performed. No differences were found regarding the frequency of classical and non-classical monocytes in PSC patients compared to the controls.



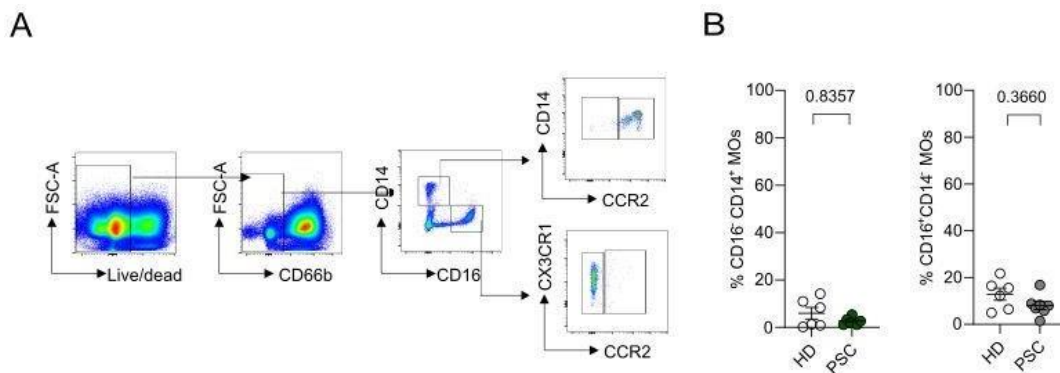


**Fig. 16: Frequencies of classical and non-classical monocytes in PBMCs isolated from PSC patients and healthy donors.**

(A) Flow cytograms representing the gating strategy adopted for the monocyte analysis from patient and HD PBMCs. Dead cells, single cells and CD66b-positive cells (neutrophils) were excluded. Both populations of monocytes were further distinguished for their expression of the chemokine receptor CCR2. (B) Graphs representing the frequencies of classical (on the left, in green) and non-classical (on the right, in grey) monocytes of PSC patients compared to healthy donor (HD) sex and age-matched controls. Each data point represents one independent sample. Mean  $\pm$  SEM. Mann-Whitney U test was performed.

To investigate whether phagocytic receptors could be differentially expressed in the PSC patients compared to the HDs, three different phagocytic receptors in the two main monocyte populations were analysed. In both classical and non-classical monocytes, no differences were found related to the expression of the phagocytic receptors CD36, MERTK and TIM4 (Fig.17). A slight tendency toward decreased expression of TIM4 in the classical monocyte subset and CD36 expression in the non-classical monocyte subpopulation was observed, though not to a significant extent.

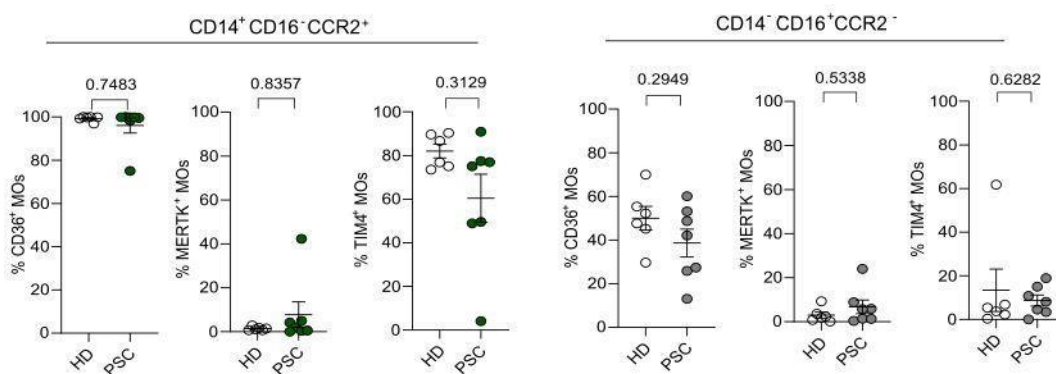


**Fig. 17: Phagocytic receptor expression in classical and non-classical monocytes in PSC patients and HDs**

Graphs representing the frequency of the expression of the phagocytic receptors CD36, MERTK and TIM4 in PSC patients and HD controls in the classical (on the left, in green) and non-classical (on the right, in grey) monocyte population. Classical monocytes are defined as CD14<sup>+</sup>CD16<sup>-</sup> cells, whereas non-classical monocytes are defined as CD16<sup>+</sup>CD14<sup>-</sup>. In the analysis dead cells, single cells and neutrophils (CD66b) were excluded. All the patients and healthy donor controls were age and sex-matched. Each data point represents one independent sample. Mean  $\pm$  SEM. Mann-Whitney U test was performed.



## Results

To further verify whether peripheral monocytes from PSC patients show an impaired phagocytic capability compared to the corresponding monocyte population from HDs, CD14<sup>+</sup> monocytes were isolated from the total PBMC fraction. The monocytes were then plated and a phagocytosis assay was performed with a human cholangiocyte cell line (H69) and a human T-cell cell line (Jurkat) (Fig.18B). In detail, CD14<sup>+</sup> cells were isolated from sex and age-matched PSC patients and HD controls. Apoptosis was induced in the H69 cell line by heating cells to 43°C for 45 min, while apoptosis was induced in Jurkat T-cells by aging them for 24 hours in RPMI media containing a reduced percentage of FCS (1% FCS). The assay was performed at 37°C and 4°C in order to discriminate between binding and actual uptake of the apoptotic cells. The phagocytic monocytes are defined as the cells positive for the cell tracker (CSFE, data not shown). No differences were observed in the phagocytic rate of the CD14<sup>+</sup> cells isolated from PSC patients compared to the control counterpart population isolated from the HDs.

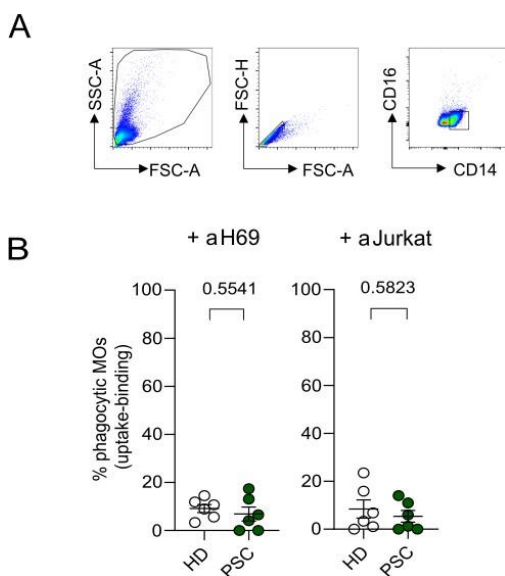


**Fig. 18: The phagocytic capability of peripheral monocytes is not impaired in PSC patients**

(A) Flow cytograms representing the gating strategy adopted for the phagocytosis assay. Dead and single cells were excluded. The analysis was exclusively performed on CD14<sup>+</sup> monocytes. The phagocytosing monocytes are defined as positive for the cell tracker CSFE. The phagocytic monocyte rate is defined as the difference between cells positive for the apoptotic cell tracker at 37°C (binding + uptake) and at 4°C (only binding). (B) Graphs representing the percentage of CD14<sup>+</sup> cells that phagocytosed apoptotic cholangiocytes (aH69) or apoptotic T-cells (aJurkat) in PSC (in green) patients compared to sex and age-matched HDs (in white). Each data point represents one independent sample. Mean  $\pm$  SEM. Mann-Whitney U test was performed.

These data show that circulating blood monocytes from PSC patients do not show an impairment in phagocytic capacity compared to their counterparts in HD, and suggest that, similar to what was observed in the bone marrow and liver MOs of *Mdr2*<sup>-/-</sup> mice (Fig. 6), a liver-specific dysregulation of MO phagocytic capacity could occur. Therefore, further studies are required in order to provide a more detailed analysis on the variety of phagocytic receptors and phagocytic downstream signalling events engaged in human CD14<sup>+</sup> cells in the context of PSC. Additionally, considering the data generated in mice regarding the downregulation of several phagocytic receptors during the course of the disease (Fig. 2, 3 and 4), the decreased phagocytic rate occurring selectively in liver-isolated MOs (Fig. 6) and

## Results

---

the proposed bile acid-dependent mechanism of impairment in phagocytosis (Fig. 15), a deeper and expanded investigation into the phagocytic receptor expression and the related phagocytosis of apoptotic cells in the liver of PSC patients is needed.

The presented results demonstrate that an alteration in the MO phagocytic machinery occurs during the course of cholangitis in a mouse model of the disease (*Mdr2*<sup>-/-</sup> mice). A downregulation of phagocytic receptor expression in KCs and accumulation of apoptotic cells in the liver of *Mdr2*<sup>-/-</sup> mice was observed. In addition, KCs exposed to the secondary bile acid TLCA *in vitro* show reduction in their phagocytic capacity and the bile acid lipidomic profile of liver-isolated MOs was analysed. Finally, the phagocytic receptor expression and phagocytic capacity of peripheral monocytes from PSC patients and healthy donors was evaluated.

## 5. Discussion

Macrophages play an essential role in the maintenance of homeostasis not only via trophic and regulatory functions, but also via the phagocytosis of apoptotic cells. Macrophages have the potential to acquire either a pro-inflammatory or an anti-inflammatory function, a characteristic which makes them a heterogeneous cell population in different tissue environments. Phagocytosis can be considered an anti-inflammatory process in which macrophages contribute to the preservation of self-tolerance via the engulfment of apoptotic cells, generated under physiological or pathological conditions. In this study, the phagocytic function of macrophages was investigated in a model of liver autoimmune disease similar to PSC.

Defects in apoptotic cell clearance have been associated with several autoimmune diseases. However, the role of macrophages during the course of PSC has not been addressed so far. The presented results show that, in the context of liver injury, the phagocytic function of macrophages is impaired, thereby inducing apoptotic cell accumulation and influencing the disease progression. A bile acid-dependent mechanism was proposed to drive the impairment in the phagocytic receptor expression in macrophages and their subsequent capacity to phagocytose dying cells within the damaged liver. Finally, the phagocytosis-related phenotype and function of circulating monocytes in PSC patients and sex/age-matched healthy donor controls were analysed. No significant differences were observed in the blood, suggesting a liver-specific immune dysregulation.

### 5.1 The downregulation of phagocytic receptors leads to an accumulation of apoptotic cells

The liver is considered an immunologically privileged organ, capable of inducing a local and systemic immune response while promoting self-tolerance. The peculiarity of this organ can be attributed to a distinct population of specialised antigen-presenting-cells, such as KCs or LSECs, that in turn promote a hepatic tolerogenic environment via the clearance of gut-derived particles, the induction of T cell anergy and the contribution to the formation of regulatory cell subsets. These tolerogenic mechanisms allow the maintenance of the liver under homeostatic conditions, despite being continuously exposed to food and microbial-derived antigens from the gut. However, disturbances in the tolerogenic function of the liver can lead to an overactivation state and the development of autoimmune diseases. Specifically, impairment in the apoptotic cell clearance, mainly mediated by macrophages, has been associated with

autoimmune disease development and progression<sup>211 212 213</sup>. In line with this, several mouse lineages with deficiencies in the engulfment of apoptotic cells, such as *Mfge8*-, *Bai1*-, *Tim4*-, or *Mertk*-deficient mice, have been used as models for autoimmune diseases since they develop similar pathological features<sup>214 215 105 216</sup>. The hepatic niche is characterised by heterogenous populations of MOs that exhibit distinct phenotypes and functions depending on their ontogeny and the signalling pathways triggered by surrounding stimuli. KCs, the liver resident MOs, are localised in the hepatic sinusoid, in proximity of the space of Disse, where they can interact with several immune cells. KCs exert different functions depending on their localization in the liver lobule<sup>217 218</sup> and, besides their contribution to adaptive immunity and their responsiveness to inflammatory triggers<sup>145</sup>, they are characterised by high phagocytic capacity<sup>219</sup>. However, following liver inflammation or injury, monocytes can be recruited from the circulation and acquire a similar transcriptomic profile, thereby replenishing the resident populations of liver MOs<sup>148</sup>. Indeed, during the course of PSC, the recruitment of monocyte-derived MOs, following cholangiocyte insult, in a CCR2-dependent fashion, has been reported<sup>220</sup>. These results point to a role of macrophages in PSC pathogenesis. Nevertheless, the phagocytic function and contribution of MOs in the context of PSC has not been addressed so far. Here, liver MOs have been distinguished based on expression of resident/infiltration surface markers and further characterised by their expression of phagocytic receptors. MOs in the liver were identified by the expression of the classical MO markers CD11b and F4/80 and, in order to distinguish between resident and infiltrating MOs, the populations were divided based on the expression of Ly6C. Indeed, it has been reported that Ly6C<sup>+</sup> MOs derive from the peripheral circulation and mainly have pro-inflammatory capacities<sup>221</sup>, whereas Ly6C<sup>-</sup> MOs are generally referred to as tissue-resident MOs<sup>222</sup>. To further distinguish between these two main populations of MOs in the liver, the expression of the unique KC marker CLEC4F<sup>223</sup> was analysed. Next, in both MO populations, the resident Ly6C<sup>-</sup>CLEC4F<sup>+</sup> KCs and the infiltrating Ly6C<sup>+</sup>CLEC4F<sup>-</sup> cells were characterised by their expression of the chemokine receptor fractalkine CX3CR1, expressed in multiple cells of the MO lineage<sup>16</sup>. It has been shown that efferocytic MOs can express CX3CR1 in order to migrate toward an apoptotic cell<sup>224</sup>. Furthermore, CX3CR1 is also involved in the colonisation of macrophages at the embryonic stage, leading to differentiation of KCs<sup>225</sup>. The resident and infiltrating populations of MOs were then analysed in *Mdr2*<sup>-/-</sup> and congenic controls at 8, 12 and 25 weeks of age, resembling the early, intermediate and late disease stage, respectively (Fig. 1). The increased frequency of infiltrating MOs at 12 weeks of age suggest that circulating monocytes were recruited *in situ* in

response to liver injury, while the percentages of resident cells remained unchanged. In line with the observation that in an acute and chronic mouse model of PSC, infiltrating monocyte-derived MOs were significantly increased in the liver, thus not affecting the frequency of resident MOs, this result suggests that this MO subset contributes to the pathology<sup>220</sup>. Next, the potential phagocytic capability of the two MO subsets was investigated based on the expression of their phagocytic receptors. Several phagocytic receptors that bind PtdSer either directly or indirectly were found to be downregulated in all disease stages. Surprisingly, of all the receptors, only MERTK expression was downregulated in both resident and infiltrating MOs and in all the three disease phases (Fig. 2-4). The importance of MERTK on macrophages is mirrored by its abundant expression in the liver under homeostatic conditions<sup>226</sup> and the complete depletion of this receptor is associated with apoptotic cell accumulation and the development of a lupus-like autoimmune syndrome<sup>227</sup>. In line with the literature, the key role of MERTK in the phagocytosis of apoptotic cells has already been described<sup>228</sup> and the relevance of both AXL and MERTK in the engulfment of both apoptotic neutrophils and T cells was also observed in the present thesis (Fig. 7B). This suggests a strong connection between the decreased frequency of MERTK-expressing MOs and the apoptotic cell accumulation in the *Mdr2*<sup>-/-</sup> mouse liver (Fig. 5) that, in turn, could contribute to the inflammation and alteration of homeostasis. With regard to the other markers analysed, the class B scavenger receptor CD36 was downregulated specifically at 12 weeks of age in both resident and infiltrating MOs (Fig. 3) and its expression was found to be dispensable for the phagocytosis of all three apoptotic cell types analysed (later discussed in Fig. 7B). However, it has been reported that the phagocytic capability of human CD36-deficient MOs is significantly impaired in women affected by endometriosis, a disease characterised by chronic peritoneal inflammation. Its ectopic restoration *in vitro* is able to rescue the MOs' phagocytic capacity<sup>229</sup>, which suggests that other phagocytosis-related mechanisms may be involved in the CD36-mediated phagocytosis of apoptotic cells. Therefore, the decreased frequency of CD36<sup>+</sup> MOs, although not directly linked to the apoptotic cell accumulation, could play a key role in affecting the MOs' phagocytic capacity *in vivo* and underline the importance of a proper expression of this marker in the MOs subsets for an effective clearance of the apoptotic bodies. Moreover, the expression of other phagocytic receptors was found to be downregulated during the course of the disease. Among these, the expression of TIM4 was downregulated during all the three stages of the disease analysed here, but only in the infiltrating MOs, whereas its expression in the resident subsets of MOs remained unchanged (Fig. 2-4). TIM4 is a PtdSer receptor that is able to induce

the phagocytosis of both apoptotic cells and exogenous particles<sup>230</sup>. Although TIM4 can directly recognise PtdSer on the apoptotic cell surface, the transduction signals that occur during the efferocytic process are mainly mediated through the involvement and combined action of fibronectin and integrins<sup>231</sup>. Besides its role as a phagocytic receptor, TIM4 can also interact with TIM1 to induce T cell proliferation<sup>232</sup> and, in combination with CLEC4F, can be considered a marker for the identification of KCs in the liver<sup>233</sup>. Furthermore, in line with the observed accumulation of apoptotic cells in the liver (Fig. 5), the absence of TIM4 in MOs results in an impairment in apoptotic cell engulfment, leading to dysregulated lymphocyte activation and the general hallmarks of systemic autoimmunity<sup>216</sup>. Following KC depletion, BMDMs can replace the resident niche of liver MOs via the acquisition of a resident-like transcriptomic profile<sup>148</sup>. Indeed, the expression of TIM4 after the colonisation of the liver from circulating monocyte-derived MOs can be gradually acquired over the time<sup>148</sup>. Therefore, the specific downregulation of TIM4 in the infiltrating liver MOs suggests that during the course of PSC, infiltrating MOs can lose their ability to partially acquire resident-like features, maintaining their pro-inflammatory profile.

It has been reported that, during PSC, both pro-inflammatory (iNOS<sup>+</sup>) and anti-inflammatory (CD206<sup>+</sup>) infiltrating MOs can accumulate in the liver biliary microenvironment of both patients and mice<sup>220 234 235</sup>. In this study, a decreased frequency of total liver CD206<sup>+</sup> MOs was noticed in both resident and infiltrating populations (Fig. 2-4). In contrast, it has been shown that in the human liver, a population of CD68<sup>+</sup>CD206<sup>+</sup> MOs was predominant in PSC patients compared to other liver diseases<sup>234</sup>. However, the prevalence of accumulating MOs in PSC was related to the sinusoidal and perisinusoidal area of the liver<sup>235</sup>. Similarly, in *Mdr2*<sup>-/-</sup> mice, the accumulation of CD206<sup>+</sup> MOs was observed in the biliary epithelium or associated with its luminal side<sup>220</sup>. Despite a decreased frequency in total CD206<sup>+</sup> MOs observed in the present thesis, no further distinction in the localisation of these cell types was made, so an accumulation of CD206<sup>+</sup> MOs in specific areas of the liver cannot be excluded, nor that specific subsets of MOs can colonise different areas of the liver during pathological conditions.

In contrast to the remarkable downregulation of the receptors described above, the FcγRI CD64 was upregulated in *Mdr2*<sup>-/-</sup> mice at 12 weeks of age, whereas its expression on resident MOs was not altered. As mentioned above, at 12 weeks, *Mdr2*<sup>-/-</sup> mice showed a significant increase in the frequency of infiltrating MOs (Fig. 1). Indeed, the expression of CD64 is associated with a pro-inflammatory MO profile and the depletion of CD64-expressing MOs from the skin results in the local resolution of chronic

inflammation<sup>236</sup>. Furthermore, the role of CD64 in autoimmune diseases such as RA has been further demonstrated by its elevated presence in the inflammatory synovial fluid (SF)<sup>237</sup> and its contribution to joint damage<sup>238</sup>. This result suggests that during the course of PSC and in different stages of liver damage (here at 12 weeks), CD64<sup>+</sup> MOs can be recruited to the liver and thereby contribute to the progression of inflammation.

Following liver injury or partial hepatectomy, MO recruitment is required in order to promote rapid liver regrowth<sup>239 240</sup>. Notably, hepatic MOs can control the CSF1 levels in circulation via the CSF1R (CD115)<sup>241</sup>, thereby promoting the migration of MOs and liver regeneration. Interestingly, here CD115 was upregulated at 12 weeks, whereas it was significantly downregulated at 25 weeks in *Mdr2*<sup>-/-</sup> mice, both in the infiltrating MO populations. This, in line with the significant increase of infiltrating MOs at 12 weeks (Fig. 1), suggests that in *Mdr2*<sup>-/-</sup> mice, liver MOs can express CD115 in response to liver injury and inflammation in order to recruit MOs from the blood. The recruited MOs then infiltrate the liver and contribute to the fibro-inflammatory cholangiopathy, favouring the clinical evidence of the disease progression<sup>220</sup>.

Autoimmune disorders are characterised by a sustained inflammation and breakdown of the natural tissue or systemic homeostasis. An impaired phagocytic capability in MOs can lead to the formation of a necrotic core that, in turn, contribute to the maintenance of the pro-inflammatory state. A strong relationship between improper MO efferocytosis and autoimmune diseases has been described so far<sup>215 242 243 244</sup>. Of note, PBMCs isolated from AIH-patients have shown reduced capacity to uptake *Escherichia coli* compared to patients with other liver disorders<sup>196</sup>. Interestingly, the accumulation of several apoptotic cells has also been observed in models of local chronic inflammation, such as asthma, cystic fibrosis or chronic obstructive pulmonary disease (COPD)<sup>245</sup>, though without clear evidence of a link between impaired phagocytosis and the presence of apoptotic cells in the lungs. Nevertheless, the presence of apoptotic cells has not only been described in autoimmune diseases, but also neurodegenerative diseases, such as Parkinson's, Alzheimer's and Huntington's<sup>246</sup>. Here, apoptotic cells contribute to a worsening disease progression and escape phagocytic engulfment via the loss of fractalkine signalling, an apoptotic cell "find me" signal<sup>247</sup>. In the present study, apoptotic cells with different identities were found in the liver of *Mdr2*<sup>-/-</sup> mice (Fig. 5). In detail, Annexin V<sup>+</sup> neutrophils (Ly6G<sup>+</sup>), T cells (CD3<sup>+</sup>) and stromal cells were identified at 8, 12 and 35 weeks of age, linking the

downregulation of phagocytic receptors to the inability of MOs to phagocytose, thus resulting in an accumulation of apoptotic cells and suggesting that an impaired efferocytosis process contributes to liver inflammation.

In line with the previous results (Fig. 2-5), a diminished phagocytosis was observed in the liver MOs of *Mdr2*<sup>-/-</sup> mice (Fig. 6). Interestingly, the phagocytic capacity was only altered towards apoptotic T cells, whereas no differences were noticed with regard to apoptotic hepatocytes. This suggests that specific phagocytic receptors are engaged in the efferocytosis process of apoptotic cells with different identities (although not anticipated before Fig. 7). To further verify whether the phagocytosis impairment in *Mdr2*<sup>-/-</sup> mice occurs specifically in the liver or whether it could be extended to other organs, the phagocytic capacity of MOs was also analysed in bone marrow-derived, spleen and peritoneal MOs. Notably, an impairment in the capability to phagocytose apoptotic hepatocytes was observed in MOs isolated from the spleen, whereas no differences were noticed in the other organs (Fig. 6). Indeed, the spleen is a secondary lymphoid organ anatomically linked to the liver via the portal vein system. Liver fibrosis and cirrhosis, two of the main features of PSC, are clinically associated with spleen complications like splenomegaly or hypersplenism via the congestion of the portal system<sup>248 249 250</sup>. During liver fibrosis, HSCs and KCs contribute to the collagen formation and deposition via the pro-fibrogenic cytokine transforming growth factor beta 1 (TGF- $\beta$ 1)<sup>251</sup>. However, splenic red pulp MOs can be considered another source of TGF- $\beta$ 1 and splenectomy can reduce the serum levels of TGF- $\beta$ 1 and improve the clinical evidence of liver fibrosis<sup>250</sup>. During liver cirrhosis, splenic MOs can exhibit a hyperactivated phenotype and release pro-inflammatory and pro-fibrogenic factors such as IL-1 $\beta$ , IFN- $\gamma$  and TNF- $\alpha$ <sup>252</sup>. This highly activated state in MOs, due to the elevated NF- $\kappa$ B signalling, was found to be responsible for an enhanced phagocytic capability in MOs isolated from the spleen of patients affected by hypersplenism and cirrhosis<sup>253 254</sup>. Notably, the phagocytic capability in both studies was assessed using *E. coli*-customised phagocytosis assays and no further investigations into the engulfment of apoptotic cells were performed. In this study, a reduction in the capacity of splenic MOs in *Mdr2*<sup>-/-</sup> mice to uptake aH but not aT was observed, suggesting that the identity of the apoptotic cell can shape the phagocytic capacity of splenic MOs *in vitro*. However, many factors can be involved in shaping the ability of MOs to phagocytose and, in contrast to the spleen, *Mdr2*<sup>-/-</sup> mice liver MOs showed an impaired capacity to uptake aT. This might be explained by the complexity of the surrounding environment during



pathological conditions that can affect the expression of specific markers, thereby affecting the MO function in different ways, depending on the stimuli involved.

### **5.2. The engagement of phagocytic receptors is mediated by the identity of the apoptotic cell**

To further verify whether the phagocytic receptors engaged by MOs during phagocytosis might drive the uptake of an apoptotic cell with a certain identity, the specificity between the apoptotic cell phagocytosed and its recognition by the phagocytic receptors on MOs was investigated. In detail, the sensing of PtdSer on the apoptotic cell surface was blocked via Annexin V in two apoptotic cell types, T cells and hepatocytes. The significant downregulation of the phagocytosis of both cell types revealed that their uptake is mediated by PtdSer-dependent phagocytic receptors (Fig. 7A). Multiple phagocytic receptors can be expressed by MOs in order to phagocyte an apoptotic cell. Furthermore, evidence that phagocytic receptors can act in concert (e.g. TIM4 and  $\beta$ 1 integrin or Stabilin-2 and  $\alpha$ v $\beta$ 5)<sup>255 256</sup>, suggest that they can physically interact via a “signalling synapse” or be engaged individually and converge in the downstream cytoplasmic signalling cascade to exert an efficient phagocytosis. However, no studies regarding the connection between a phagocytic receptor and a specific apoptotic cell type has been reported to the literature so far. After the confirmation that the phagocytosis of both T cells and hepatocytes was partially mediated by PtdSer-dependent receptors, a more detailed analysis via the use of BMDMs from transgenic mice lacking two well-established PtdSer-dependent phagocytic receptors, *Axl* and *Mertk*, was performed (Fig. 7B, on the left). Interestingly, the lack of *Axl* and *Mertk* strongly impairs the phagocytosis of neutrophils and, to a lesser extent, T cells, which suggests that the downregulation of these receptors can strongly influence apoptotic cell accumulation in the tissue and, in turn, promote inflammation and the disease progression. However, the phagocytosis of apoptotic hepatocytes was not affected by the lack of these receptors, suggesting that other receptors are involved in the uptake of this cell type. To this end, the engagement of another phagocytic receptor, CD36, was investigated (Fig. 7B). It has been reported that CD36 is able to mediate the uptake of apoptotic cells via oxidised low density lipoprotein (oxLDL) and to play a role in several cells' processes as a fatty acid transporter, suppressing angiogenesis and inflammation<sup>257 258</sup>. Indeed, CD36 has been described to be a cofactor in the apoptotic cell engulfment by PtdSer-recognising MOs<sup>259</sup>. In this study, BMDMs isolated from *Cd36*<sup>-/-</sup> mice did not show any significant impairment in the phagocytosis of neutrophils, thymocytes and hepatocytes (Fig. 7B, on the right), indicating a dispensable role of this receptor in the phagocytosis

of these cell types. Interestingly, an early study identified a direct role of CD36 during apoptotic cell clearance in an oxidised PtdSer (ox-PtdSer)-dependent manner <sup>260</sup>. In detail, the binding and phagocytosis mediated by CD36-transfected cells was observed in ox-PtdSer-coated liposomes, but not in non-oxidised-PtdSer (PtdSer) liposomes. Of note, many methodologies for the preparation of PtdSer-liposomes induce oxidation (e.g. sonication or dialysis) and are used as source of PtdSer to test phagocytosis in MOs <sup>259 261 262</sup>. However, although the oxidation of PtdSer occurs before its externalisation during apoptosis <sup>263</sup>, phagocytic cells are able to uptake apoptotic cells even when the PtdSer oxidation is blocked, albeit to a lesser extent <sup>264</sup>. In the present study, the apoptosis in thymocytes and neutrophils was induced via aging in a reduced amount of serum, and in hepatocytes via heating the cell suspension (as described in the materials and methods section) and the induction of apoptosis was then confirmed via Annexin-V staining. Nevertheless, no further distinctions on the oxidation level of PtdSer were performed. Furthermore, taking into consideration the complexity of the MOs-apoptotic cell interaction, a mechanism in which other phagocytic receptors can compensate for the lack of CD36 can not be excluded. Of note, the surrounding environment can influence the oxidation of phospholipids on the apoptotic cell. Indeed, the liver contains large amounts of polyunsaturated fatty acid species that are susceptible to oxidation, which suggests that proper CD36 expression in the liver environment is important for an efficient phagocytosis. Therefore, although in the present study the expression of CD36 was not directly correlated with the uptake of the apoptotic cell types analysed, its phagocytosis-dependent role in the maintenance of liver tolerance and homeostasis cannot be excluded.

In order to better investigate the MOs' behaviour towards apoptotic cells, the ability to MOs to engulf apoptotic cells with different identities concomitantly was assessed (Fig. 8). MOs were then exposed to thymocytes, neutrophils and hepatocytes and the percentage of MOs that phagocytosed all the three cell types was confirmed both via flow cytometry and IF. Interestingly, only a small percentage of MOs were able to engulf all three apoptotic cell types concomitantly and only at later time points (60-90 min), suggesting that MOs preferentially apply their phagocytic capabilities to apoptotic cells with a specific identity. Although the MOs' capacity to phagocyte has already been investigated based on the shape <sup>265 266</sup>, the size <sup>267 268</sup>, the surface properties of the target <sup>269</sup> and several other mechanical aspects <sup>270</sup>, the possible link between MOs and the apoptotic cell identity has not yet been unveiled. These results suggest that after the engagement of specific phagocytic receptors, MOs are able to uptake apoptotic cells with a specific identity. However, it is possible that, in order to perform a subsequent phagocytosis

on other apoptotic cell types, different phagocytic receptors need to be involved, while others, which are not necessary any more, need to be downregulated. This might explain the MO behaviour observed in this study when a MO encounters apoptotic cells with many different origins (mainly resembling the physiological conditions in the liver and, in general, in an organ/tissue). Here, for the first time, correspondence between the phagocytic receptors engaged and the apoptotic cell target was hypothesised. Nevertheless, further studies are needed in order to provide a better understanding on the MOs-apoptotic cell interaction.

### **5.3 Bile acids can alter the phagocytic ability of macrophages**

Cholestatic liver diseases are characterised by an accumulation of BAs in the liver and in systemic circulation. BAs exert hormone-like functions and control glucose and lipid metabolism, cellular proliferation and modulate the immune system <sup>271 272 273</sup>. However, under pathological conditions, bile acids can disrupt the integrity of the biliary epithelium by affecting cholangiocyte proliferation and survival, initiating inflammatory processes and thereby leading to liver injury <sup>274</sup>. When bile acids accumulate in a concentration that overcomes the physiological levels, clinical hepatotoxicity is reported. In healthy individuals, the bile acid concentration in the serum is around 3  $\mu\text{M}$  <sup>203</sup>, while bile acid salts at a concentration of 15-25 $\mu\text{M}$  can act as signalling molecules and concentrations higher than 50 $\mu\text{M}$  cause apoptosis <sup>275 276 277</sup>. However, in cholestatic patients the bile acid concentration was found to be up to 200 $\mu\text{M}$  <sup>203</sup>. In the present study, the capability of BAs to modulate the phagocytic receptor expression and phagocytosis of MOs was analysed. In order to evaluate the effect of BAs, MOs were treated with the BA TLCA, a secondary bile acid, at a higher concentration (30 $\mu\text{M}$ ) compared to the physiological levels, but not sufficient to induce apoptosis in the treated cells. In human MOs, a total of 202 genes were shown to be modulated by treatment with TLCA <sup>202</sup>. Specifically, genes with key roles in the viral response (e.g. IL-6, TNF), cell activation (IRF1, CD80), migration (e.g. CCL5, IL-18), phagocytosis and autophagy (IRF8, LDLR, NAMPT) were downregulated by the effect of TLCA <sup>202</sup>. In this study, TLCA treatment affected the expression of the phagocytic receptors MERTK and CD64 in murine MOs, while not influencing their viability (Fig. 9). Furthermore, the downregulation of MERTK and CD64 was correlated with an impaired phagocytic capability, independent of the cellular identity of the apoptotic target (Fig. 10). In line with this, an early study shows that human KCs show defective particle clearance in patients affected by obstructive jaundice, a cholestatic disease in which the normal bile flow from the bloodstream to the intestine is impaired <sup>278</sup>. Interestingly, it has been reported that the phagocytic

capacity of liver endothelial cells is also significantly impaired in patients with alcohol-related liver cirrhosis<sup>279</sup>. These results shed light on the potential direct effect of BAs during cholestatic liver diseases and suggest a possible role of BAs in apoptotic cell accumulation and the consequent sustained liver inflammation.

The effect of BAs on the immune induction by activating the bile acid receptors TGR5 and FXR, expressed both in mice and humans, has been demonstrated in MOs and KCs. In KCs, TGR5 is localised in both the plasma membrane and the intracellular compartments and TLCA has been found to be one of the strongest TGR5 agonists<sup>280</sup>. The activation of both receptors effectively reduces the pro-inflammatory activity of MOs, and it has been reported that FXR confers a protective role against liver fibrosis via the inhibition of HSCs in a model of cholestasis<sup>281</sup>. Of note, the activation of these bile acid receptors via administration of INT-767, a dual TGR5/FXR agonist, reduces the BAs' toxicity and restores the BA pool, thus preventing BA-induced hepatocellular carcinoma (HCC) in *Mdr2*<sup>-/-</sup> mice<sup>282</sup>. However, no studies on altered mRNA expression of both receptors in *Mdr2*<sup>-/-</sup> mice/ liver MOs of PSC patients have been reported in the literature so far. In the present study, a slight downregulation in the expression of both TGR5 and FXR in MOs isolated from the liver of *Mdr2*<sup>-/-</sup> mice was noted (Fig. 11). It is tempting to hypothesise that a decreased level of bile acid receptors in MOs can increase the liver damage and contribute to the course of the disease. In line with this, mice with a knock-out for *Tgr5* display intestinal microbiota dysbiosis and higher levels of pro-inflammatory liver cytokines, chemokines and an activated MO profile overall<sup>283</sup>. In addition, the double knock-out of *Tgr5/Fxr* in mice is associated with alterations in the BA pool and correlates with liver fibrosis and inflammation<sup>284</sup>, consistent with the liver pathological hallmarks of *Mdr2*<sup>-/-</sup> mice. However, in order to evaluate the BA profile in MOs and their ability to shape their phagocytic capacity, lipidomic analysis was performed in phagocytic receptor-enriched and deficient MOs (Fig. 12 and 13). In contrast to the human liver, in which the majority of BAs are glycine conjugated, in mice, 97.7% of bile acids are taurine-conjugated, whereas 2.2% are unconjugated and only 0.1% are glycine-conjugated<sup>285</sup>. As reported in the literature, LC-ESI-QqQ analysis showed that the most prevalent bile acid in the liver is taurocholic acid (TCA), followed by taurochenodeoxycholic acid (TCDCA), taurodeoxycholic acid (TDCA) and tauroolithocholic acid (TLCA) as tauro-conjugated BAs, with glycolic acid (GCA) and glycochenodeoxycholic acid (GCDCA) as glycine-conjugated and cholic acid (CA) as unconjugated BAs. In contrast, hydrophilic muricholic acid (MCA) is normally strongly present in the mouse liver<sup>285</sup>, whereas in the present study only a small

concentration was detected in *Mdr2*<sup>-/-</sup> mice (Fig. 13). Indeed, lipidomic LC-ESI-QqQ analysis was performed exclusively on liver MOs from *Mdr2*<sup>-/-</sup> mice and an accumulation of several bile acids was noticed in the phagocytic receptor-enriched MOs subpopulation. These results, for the first time, not only report that bile acids can accumulate inside the MOs, but also that liver MOs from *Mdr2*<sup>-/-</sup> mice which express specific phagocytic receptors are more prone to accumulate BAs compared to macrophages isolated from the same livers which express low levels of phagocytic receptors. Interestingly, a study investigating the use of Colesevelam, a candidate for the treatment of PSC, on *Mdr2*<sup>-/-</sup> mice showed a reduction in TCA content in the hepatic biliary pool, consistent with reduced numbers of MOs in the liver<sup>286</sup>. In addition, the treatment was able to shift the BA profile into a more hydrophilic composition, with a predominance of tauro-conjugated MCA, barely detected in the liver MOs of this study (Fig. 13). In line with this, the MOs analysed in the present thesis showed a high TCA content, indicating that MOs could serve as reservoir for BAs in a pathological setting, thereby strongly contributing to the BA alterations that characterise the PSC progression and indicating a connection between the accumulation of BAs in MOs and the dysregulated BAs profile in the livers of *Mdr2*<sup>-/-</sup> mice.

As mentioned above, although the role of MOs in the contribution of cholestatic diseases has been investigated in several studies<sup>220 234 287 288</sup>, no accumulation of BA inside the MOs has been reported so far. Here, a phagocytosis-dependent mechanism of BA accumulation inside the MOs has been proposed (Fig. 14). It has been reported that in cholestatic liver diseases, an accumulation of BAs in the hepatocytes occurs<sup>275</sup>, leading to immune-mediated injury and periductal inflammation. In the present study, the BA TLCA inside the MOs that phagocytosed TLCA-treated hepatocytes was identified via lipidomic analysis (Fig. 14). This result hints towards the fact that BAs can be internalised by MOs in a BA receptor-independent fashion. Here, it has been demonstrated that the accumulation of BAs inside MOs significantly decreases their phagocytic capacity to further uptake apoptotic cells with different identities (Fig. 15), contributing to the presence of unremoved apoptotic cells in the liver and sustaining inflammation. In accordance with this hypothesis, liver MOs in *Mdr2*<sup>-/-</sup> mice show a downregulation of several phagocytic receptors (Fig. 2-4) and an impaired phagocytic capability (Fig. 6). These observations could be explained by the dysregulation of the BA homeostasis that characterises this cholestatic disease, and by the progressive accumulation of BAs inside the MOs in a hepatocyte phagocytosis-dependent manner which leads to the alteration of their phagocytic ability (as shown in Fig. 15). This proposed BA-mediated impairment of a proper MO phagocytic function could then lead to

a defective clearance of liver apoptotic cells (Fig. 5) and sustain the pathological hallmarks of PSC. In line with this, in a study in which obesity was linked to non-alcoholic fatty liver disease (NAFLD), the hepatic bile acid homeostasis was altered and liver-recruited BMDMs showed a decreased phagocytic capacity towards *Listeria monocytogenes*, consistent with reduced bacteria clearance and inflammation<sup>289</sup>. This suggests that, independent of the etiopathogenesis of the liver disease, a dysregulation in the BA pool can induce an alteration in MO function, that in turn contributes to inflammation and the loss of tolerogenic liver properties.

### 5.4 The relevance of proper phagocytosis in the liver of PSC patients

Although the *Mdr2*<sup>-/-</sup> mouse animal model effectively represents the pathogenesis of PSC in humans<sup>290</sup>, the characteristics of mouse and human MOs are only partially comparable. Furthermore, the bile acid composition is substantially different between the two species. Under basal conditions, in contrast to humans, 6-hydroxylated MCAs are contained in about half of the mouse BA pool<sup>291</sup>. The presence and physiological role of these hydrophilic bile acids is still unclear. However, they could be involved in quenching the responses of hydrophobic BAs, such as CA and CDCA, largely present in humans<sup>291</sup>. Another relevant difference between mice and humans is due to the effect of cholestasis on the BA production. After bile duct ligation (BDL), an increase of BA synthesis in mice and rats has been reported<sup>292</sup><sup>293</sup>, whereas in humans this is associated with reduced BA synthesis<sup>294</sup><sup>295</sup>. This response could be mainly derived from the incapability of the FXR-driven secretion of fibroblast growth factor FGF15 (human ortholog, FGF19)<sup>296</sup> and a negative gut-mediated feedback of BA synthesis. In contrast, in humans the *Fgf19* gene is widely expressed and leads to a sustained BA release in circulation<sup>294</sup>. Indeed, although the animal models feature many hallmarks of the liver pathology, many differences in the effect of cholestasis between mice and humans are still present. Therefore, the observations noticed in mouse must also be investigated in the human context.

In this study, no differences in the frequencies of classical and non-classical circulating MO subsets were identified in the PBMCs isolated from PSC patients compared to age and sex-matched HDs (Fig. 16). Accordingly, several studies identified an increased frequency of non-classical monocytes specifically in the liver, but no differences in cell frequency in the peripheral blood<sup>297</sup><sup>234</sup>. In addition, hepatic infiltration of monocyte-derived CD14<sup>+</sup>CD16<sup>+</sup> MOs has been described in chronic liver diseases, and accumulation in the peribiliary parenchyma of monocyte-derived MOs in PSC patients has been reported<sup>220</sup><sup>234</sup><sup>298</sup><sup>299</sup>. However, no further differences in the frequency of phagocytic receptors on

classical and non-classical monocytes were noted (Fig. 17). Consequently, the normal expression of phagocytic receptors correlates with a functional phagocytic capability in circulation (Fig. 18). These results suggest that the altered phenotype and function of MOs in PSC might be specifically related to the liver and that monocyte-derived MOs acquire the pathological impairment of phagocytosis after their migration to the liver niche. Notably, compared to mice, humans have high amounts of BAs in circulation<sup>294</sup>, which could lead to an dysfunctional phenotype in the blood. However, all the patients analysed were under ursodeoxycholic acid (UCDA) treatment, a hydrophilic BA, naturally present (<5%) in the human bile and used for the treatment of several cholestatic conditions<sup>300</sup>. Although the treatment shows beneficial effects on the liver biochemistry, it has been reported to modify the BA composition in the serum of patients, with a strong increase of LCA and UDCA after treatment<sup>301</sup>. This BA alteration in the peripheral circulation can affect the function of several immune cells, not reflecting the original properties of the disease. Nevertheless, a liver-related, BA-mediated impairment in the phagocytic capability of MOs during the course of PSC has been proposed. Furthermore, it has been shown that a decreased phagocytosis in the liver leads to accumulation of apoptotic cells, thus contributing to the inflammation and progression of the disease. Therefore, noneffective phagocytosis in the liver of PSC patients could lead to a sustained immune response and a breakdown of the liver tolerance. However, further investigations are needed to verify this hypothesis.

## 6. Future perspectives

The present thesis showed that an alteration of the phagocytic machinery in MOs occurs during the course of cholangitis. In particular, our results suggest that BAs can accumulate inside the MOs bypassing the canonical bile acid receptors. The BA accumulation within the macrophages is associated to a reduction in their phagocytic capacity, hence accumulation of apoptotic cells in the tissue and most likely to the progression of the liver disease. Considering these data, a deeper analysis of the BA-dependent regulation of phagocytosis should be performed in the future in order to strength the results. To this end, RNA bulk-sequencing analysis on KCs that have been phagocytosed BA-enriched hepatocytes or not would give an overview of the overall effect of BA on the transcriptomic signature of efferocytic macrophages, and in particular on the phagocytic receptor signature of these macrophages (e.g. expression of genes related to the phagocytic receptor cleavage (e.g. ADAM17<sup>302</sup>).

In addition, a key aspect which need to be deeper investigated in the future is the specificity between the apoptotic cell identity and the phagocytic receptors engaged by MOs, as hypothesized. In particular, additional experiments which will allow to dissect the phagocytic mechanism engaged for the uptake of aH are needed. The data suggest that a mechanism of PtdSer-dependent recognition and engulfment of aH occurs. However, this is not depending by the engagement of phagocytic receptors such as *Axl*, *Mertk* and *Cd36*. Therefore, macrophages isolated from mice deficient for other PtdSer-dependent phagocytic receptors (e.g. *Stab1*<sup>-/-</sup>, *Tim4*<sup>-/-</sup> mice) should be tested to dissect the mechanism involved in the engulfment of aH.

Interestingly, the experiments conducted on PBMCs from patients revealed that the phagocytic capacity of peripheral monocytes is unaltered in PSC patients compared to HDs. These data are in line with the results obtained in a mouse model of PSC (*Mdr2*<sup>-/-</sup> mice) which suggest that the impairment in the phagocytosis capacity of macrophages is liver-specific. Therefore, the expression of the phagocytic receptors in liver sections of PSC patients and HDs should be evaluated. Additionally, in order to deeper characterize the hepatic human MO core signature during the course of PSC, their phagocytic-associated transcriptomic profile should be investigated. To this end, single-cell RNA sequencing (sc-RNAseq) on total CD45<sup>+</sup> cells in liver explants of PSC patients, followed by an analysis based on the MOs “phagocytic signature” (e.g. expression of phagocytic receptors, bridging molecules or nuclear factors engaged after phagocytosis) should be performed. The analysis on the transcriptomic profile



would be able to shed light on the possible alterations that occur in MOs with a “reduced phagocytic signature” (e.g. increased pro-inflammatory profile).

Furthermore, the accumulation of specific subsets of MOs in proximity of different liver areas has been demonstrated <sup>191 234</sup>. In this regard, based on the phagocytic signature profile identified by sc-RNAseq, the localization of phagocytic and non-phagocytic MOs in sections derived from liver explants from PSC patient should be determined. For this purpose, the use of spatial transcriptomic analysis, in order to visualise and analyse cell to cell interaction of tissue sections should be performed to identify a selective MO signature in relation to its liver location.

---

## References

1. Buchmann K. Evolution of innate immunity: Clues from invertebrates via fish to mammals. *Front Immunol.* 2014;5(SEP):1-8. doi:10.3389/fimmu.2014.00459
2. Wen-Yuan S, Guo-Liang W, Li-Li C, et al. A receptor kinase-like protein encoded by the rice disease resistance gene, Xa21. *Science (80- ).* 1995;270(5243):1804-1806.
3. Janeway CA. Pillars article: approaching the asymptote? Evolution and revolution in immunology. Cold spring harb symp quant biol. 1989. 54: 1-13. *J Immunol.* 2013;191(9):4475-4487.
4. Medzhitov R, Preston-Hurlburt P, Janeway CA. A human homologue of the Drosophila toll protein signals activation of adaptive immunity. *Nature.* 1997;388(6640):394-397. doi:10.1038/41131
5. Stephen J Galli NB and TAW. Phenotypic and functional plasticity of cells of innate immunity: macrophages, mast cells and neutrophils. *Nat Immunol.* 2012;12(11):52-53. doi:doi:10.1038/ni.2109
6. Peter Stern, Magnus Gidlund AO& HW. Natural killer cells mediate lysis of embryonal carcinoma cells lacking MHC. *Nature.* 1980;285(May):5-24.
7. Tauber AI. Metchnikoff and the phagocytosis theory. *Nat Rev Mol Cell Biol.* 2003;4(11):897-901. doi:10.1038/nrm1244
8. Hochreiter-Hufford A, Ravichandran KS. Clearing the dead: Apoptotic cell sensing, recognition, engulfment, and digestion. *Cold Spring Harb Perspect Biol.* 2013;5(1):1-19. doi:10.1101/cshperspect.a008748
9. Abbas, A. K.; Lichtman, A. H.; Pillai, S.; Baker D. *Cellular and Molecular Immunology.*; 2017. doi:https://doi.org/10.1016/B978-1-4160-3123-9.50020-6.
10. Henson PM, Hume DA. Apoptotic cell removal in development and tissue homeostasis. *Trends Immunol.* 2006;27(5):244-250. doi:10.1016/j.it.2006.03.005
11. van de Laar L, Saelens W, De Prijck S, et al. Yolk Sac Macrophages, Fetal Liver, and Adult Monocytes Can Colonize an Empty Niche and Develop into Functional Tissue-Resident Macrophages. *Immunity.* 2016;44(4):755-768. doi:10.1016/j.immuni.2016.02.017
12. Hashimoto D, Chow A, Noizat C, et al. Tissue resident macrophages self-maintain locally. *Immunity.* 2013;38(4):792-804. doi:10.1016/j.immuni.2013.04.004.Tissue
13. Lavin Y, Winter D, Blecher-Gonen R, et al. Tissue-resident macrophage enhancer landscapes are shaped by the local microenvironment. *Cell.* 2014;159(6):1312-1326. doi:10.1016/j.cell.2014.11.018
14. Bain CC, Bravo-blas A, Scott CL, Perdiguero EG. Constant replenishment from circulating monocytes maintains the macrophage pool in adult intestine. *Eur PMC Funders.* 2015;15(10):929-937. doi:10.1038/ni.2967.Constant
15. Platt AM, Bain CC, Bordon Y, Sester DP, Mowat AM. An Independent Subset of TLR Expressing CCR2-Dependent Macrophages Promotes Colonic Inflammation. *J Immunol.* 2010;184(12):6843-6854. doi:10.4049/jimmunol.0903987
16. Yona S, Kim KW, Wolf Y, et al. Fate Mapping Reveals Origins and Dynamics of Monocytes and Tissue Macrophages under Homeostasis. *Immunity.* 2013;38(1):79-91. doi:10.1016/j.immuni.2012.12.001
17. Perdiguero EG, Klapproth K, Schulz C, et al. Tissue-resident macrophages originate from yolk sac-derived erythro-myeloid progenitors. *Exp Hematol.* 2015;43(9):S64. doi:10.1016/j.exphem.2015.06.130

## References

---

18. Gordon S, Plüddemann A, Martinez Estrada F. Macrophage heterogeneity in tissues: Phenotypic diversity and functions. *Immunol Rev.* 2014;262(1):36-55. doi:10.1111/imr.12223
19. A-Gonzalez N, Castrillo A. Origin and specialization of splenic macrophages. *Cell Immunol.* 2018;330(May):151-158. doi:10.1016/j.cellimm.2018.05.005
20. Chow A, Huggins M, Ahmed J, et al. CD169+ macrophages provide a niche promoting erythropoiesis under homeostasis, myeloablation and in JAK2V617F-induced polycythemia vera. *Nat Med.* 2013;19(4):429-436. doi:10.1038/nm.3057.CD169
21. Den Haan JMM, Kraal G. Innate immune functions of macrophage subpopulations in the spleen. *J Innate Immun.* 2012;4(5-6):437-445. doi:10.1159/000335216
22. Swirski FK, Nahrendorf M, Etzrodt M, et al. Identification of splenic reservoir monocytes and their deployment to inflammatory sites. *Science (80- ).* 2009;325(5940):612-616. doi:10.1126/science.1175202
23. Gabanyi I., Paul A Muller, Linda Feighery, Thiago Y Oliveira, Frederico A Costa- Pinto and DM. Neuro-immune interactions drive tissue programming in intestinal macrophages. *Cell.* 2016;164(3):378-391. doi:10.1016/j.cell.2015.12.023.Neuro-immune
24. Zigmond E, Bernshtein B, Friedlander G, et al. Macrophage-restricted interleukin-10 receptor deficiency, but not IL-10 deficiency, causes severe spontaneous colitis. *Immunity.* 2014;40(5):720-733. doi:10.1016/j.immuni.2014.03.012
25. Asano K, Takahashi N, Ushiki M, et al. Intestinal CD169 + macrophages initiate mucosal inflammation by secreting CCL8 that recruits inflammatory monocytes. *Nat Commun.* 2015;6(44):1-14. doi:10.1038/ncomms8802
26. De Schepper S, Verheijden S, Aguilera-Lizarraga J, et al. Self-Maintaining Gut Macrophages Are Essential for Intestinal Homeostasis. *Cell.* 2018;175(2):400-415.e13. doi:10.1016/j.cell.2018.07.048
27. Bou Ghosn EE, Cassado AA, Govoni GR, et al. Two physically, functionally, and developmentally distinct peritoneal macrophage subsets. *Proc Natl Acad Sci U S A.* 2010;107(6):2568-2573. doi:10.1073/pnas.0915000107
28. Okabe Y, Medzhitov R. Tissue-specific signals control reversible program of localization and functional polarization of macrophages. *Cell.* 2014;157(4):832-844. doi:10.1016/j.cell.2014.04.016
29. Jenkins SJ, Ruckerl D, Cook PC, et al. Local macrophage proliferation, rather than recruitment from the blood, is a signature of T H2 inflammation. *Science (80- ).* 2011;332(6035):1284-1288. doi:10.1126/science.1204351
30. Rosas M, Davies LC, Giles PJ, et al. The transcription factor Gata6 links tissue macrophage phenotype and proliferative renewal. *Science (80- ).* 2014;344(6184):645-648. doi:10.1126/science.1251414
31. Wang J, Kubes P. A Reservoir of Mature Cavity Macrophages that Can Rapidly Invade Visceral Organs to Affect Tissue Repair. *Cell.* 2016;165(3):668-678. doi:10.1016/j.cell.2016.03.009
32. Palecanda A, Paulauskis J, Al-Mutairi E, et al. Role of the scavenger receptor MARCO in alveolar macrophage binding of unopsonized environmental particles. *J Exp Med.* 1999;189(9):1497-1506. doi:10.1084/jem.189.9.1497
33. Gibbings SL, Thomas SM, Atif SM, et al. Three unique interstitial macrophages in the murine lung at steady state. *Am J Respir Cell Mol Biol.* 2017;57(1):66-76. doi:10.1165/rcmb.2016-0361OC
34. Guilliams M, Lambrecht BN, Hammad H. Division of labor between lung dendritic cells and macrophages in the defense against pulmonary infections. *Mucosal Immunol.* 2013;6(3):464-473. doi:10.1038/mi.2013.14
35. Yu X, Buttgerit A, Lelios I, et al. The Cytokine TGF- $\beta$  Promotes the Development and

## References

---

- Homeostasis of Alveolar Macrophages. *Immunity*. 2017;47(5):903-912.e4. doi:10.1016/j.immuni.2017.10.007
36. Schneider C, Nobs SP, Kurrer M, Rehrauer H, Thiele C, Kopf M. Induction of the nuclear receptor PPAR- $\gamma$  3 by the cytokine GM-CSF is critical for the differentiation of fetal monocytes into alveolar macrophages. *Nat Immunol*. 2014;15(11):1026-1037. doi:10.1038/ni.3005
37. Westphalen K, Gusarova GA, Islam MN, et al. Sessile alveolar macrophages communicate with alveolar epithelium to modulate immunity. *Nature*. 2014;506(7489):503-506. doi:10.1038/nature12902
38. Murray PJ, Allen JE, Fisher EA, Lawrence T. Macrophage activation and polarization: nomenclature and experimental guidelines. *Immunity*. 2014;41(1):14-20. doi:10.1016/j.immuni.2014.06.008.Macrophage
39. Mills CD, Kincaid K, Alt JM, Heilman MJ, Hill AM. M-1/M-2 Macrophages and the Th1/Th2 Paradigm. *J Immunol*. 2000;164(12):6166-6173. doi:10.4049/jimmunol.164.12.6166
40. Mills CD. Macrophage arginine metabolism to ornithine/urea or nitric oxide/citrulline: A life or death issue. *Crit Rev Immunol*. 2001;21(5):399-425. doi:10.1615/critrevimmunol.v21.i5.10
41. Mills CD, Shearer J, Evans R, et al. Macrophage arginine metabolism and the inhibition or stimulation of cancer. *Journal Immunol*. 1992;149:2709-2714.
42. Morris SM. Recent advances in arginine metabolism: Roles and regulation of the arginases. *Br J Pharmacol*. 2009;157(6):922-930. doi:10.1111/j.1476-5381.2009.00278.x
43. Mattila JT, Ojo OO, Kepka-Lenhart D, et al. Microenvironments in Tuberculous Granulomas Are Delineated by Distinct Populations of Macrophage Subsets and Expression of Nitric Oxide Synthase and Arginase Isoforms. *J Immunol*. 2013;191(2):773-784. doi:10.4049/jimmunol.1300113
44. Nathan C., Philip Liu JSA and RLM. Role of iNOS in Human Host Defense. *Science (80- )*. 2006;312(5782):1874-1875. doi:10.4135/9781412963954.n6
45. Hu X, Ivashkiv LB. Cross-regulation of Signaling and Immune Responses by IFN- $\gamma$  and STAT1. *Immunity*. 2009;31(4):539-550. doi:10.1016/j.immuni.2009.09.002.Cross-regulation
46. Kayagaki N, Wong MT, Stowe IB, et al. Noncanonical Inflammasome Activation by Intracellular LPS Independent of TLR4. *Science (80- )*. 2013;341(13):1246-1249. doi:10.5061/dryad.bt51g
47. Lilly MB, Zemskova M, Frankel AE, Salo J, Kraft AS. Distinct domains of the human granulocyte-macrophage colony-stimulating factor receptor  $\alpha$  subunit mediate activation of Jak/Stat signaling and differentiation. *Blood*. 2001;97(6):1662-1670. doi:10.1182/blood.V97.6.1662
48. Doherty TM, Kastelein R, Menon S, Andrade S, Coffman RL. Modulation of murine macrophage function by IL-13. *J Immunol*. 1993;151(12):7151-7160.
49. Loke P, Nair MG, Parkinson J, Guiliano D, Blaxter M, Allen JE. IL-4 dependent alternatively-activated macrophages have a distinctive in vivo gene expression phenotype. *BMC Immunol*. 2002;3:1-11. doi:10.1186/1471-2172-3-7
50. Stein BM, Keshav S, Harris N, Gordon S. Interleukin 4 Potently Enhances Murine Macrophage Mannose Receptor Activity: A Marker of Alternative Immunologic Macrophage Activation By Michael Stein, Satish Keshav, Neil Harris,\* and Siamon Gordon. *J Exp Med*. 1992;176(July):287-292.
51. Martinez FO, Helming L, Milde R, et al. Genetic programs expressed in resting and IL-4 alternatively activated mouse and human macrophages: Similarities and differences. *Blood*. 2013;121(9):57-69. doi:10.1182/blood-2012-06-436212
52. Khurana Hershey GK. IL-13 receptors and signaling pathways: An evolving web. *J Allergy Clin Immunol*. 2003;111(4):677-690. doi:10.1067/mai.2003.1333
53. Martinez FO, Gordon S. The M1 and M2 paradigm of macrophage activation: Time for

## References

---

- reassessment. *F1000Prime Rep.* 2014;6(March):1-13. doi:10.12703/P6-13
54. Sellon RK, Tonkonogy S, Schultz M, et al. Resident enteric bacteria are necessary for development of spontaneous colitis and immune system activation in interleukin-10-deficient mice. *Infect Immun.* 1998;66(11):5224-5231. doi:10.1128/iai.66.11.5224-5231.1998
  55. Xue J, Schmidt S V., Sander J, et al. Transcriptome-Based Network Analysis Reveals a Spectrum Model of Human Macrophage Activation. *Immunity.* 2014;40(2):274-288. doi:10.1016/j.immuni.2014.01.006
  56. Jenkins SJ, Ruckerl D, Thomas GD, et al. IL-4 directly signals tissue-resident macrophages to proliferate beyond homeostatic levels controlled by CSF-1. *J Exp Med.* 2013;210(11):2477-2491. doi:10.1084/jem.20121999
  57. Ueda Y, Kayama H, Jeon SG, et al. Commensal microbiota induce LPS hyporesponsiveness in colonic macrophages via the production of IL-10. *Int Immunol.* 2010;22(12):953-962. doi:10.1093/intimm/dxq449
  58. Bilyk N, Holt PG. Inhibition of the immunosuppressive activity of resident pulmonary alveolar macrophages by granulocyte/macrophage colony-stimulating factor. *J Exp Med.* 1993;177(6):1773-1777. doi:10.1084/jem.177.6.1773
  59. Monks J, Rosner D, Geske FJ, et al. Epithelial cells as phagocytes: Apoptotic epithelial cells are engulfed by mammary alveolar epithelial cells and repress inflammatory mediator release. *Cell Death Differ.* 2005;12(2):107-114. doi:10.1038/sj.cdd.4401517
  60. Martinez J. Prix Fixe: Efferocytosis as a Four-Course Meal. *Curr Top Microbiol Immunol.* 2017;37(October):403. doi:10.1007/82\_2015\_467.
  61. Green DR, Oguin TH, Martinez J. The clearance of dying cells: Table for two. *Cell Death Differ.* 2016;23(6):915-926. doi:10.1038/cdd.2015.172
  62. Lauber K, Bohn E, Kröber SM, et al. Apoptotic cells induce migration of phagocytes via caspase-3-mediated release of a lipid attraction signal. *Cell.* 2003;113(6):717-730. doi:10.1016/S0092-8674(03)00422-7
  63. Gude DR, Alvarez SE, Paugh SW, et al. Apoptosis induces expression of sphingosine kinase 1 to release sphingosine-1-phosphate as a “come-and-get-me” signal. *FASEB J.* 2008;22(8):2629-2638. doi:10.1096/fj.08-107169
  64. Truman LA, Ford CA, Pasikowska M, et al. CX3CL1/fractalkine is released from apoptotic lymphocytes to stimulate macrophage chemotaxis. *Blood.* 2008;112(13):5026-5036. doi:10.1182/blood-2008-06-162404
  65. Elliott MR, Cheken FB, Trampont PC, et al. Nucleotides released by apoptotic cells act as a find-me signal for phagocytic clearance. *Nature.* 2009;461(7261):282-286. doi:10.1038/nature08296.Nucleotides
  66. Rosen H, Goetzl EJ. Sphingosine 1-phosphate and its receptors: An autocrine and paracrine network. *Nat Rev Immunol.* 2005;5(7):560-570. doi:10.1038/nri1650
  67. Peter C, Waibel M, Radu CG, et al. Migration to apoptotic “find-me” signals is mediated via the phagocyte receptor G2A. *J Biol Chem.* 2008;283(9):5296-5305. doi:10.1074/jbc.M706586200
  68. Yamaguchi H, Maruyama T, Urade Y, Nagata S. Immunosuppression via adenosine receptor activation by adenosine monophosphate released from apoptotic cells. *Elife.* 2014;2014(3):1-15. doi:10.7554/eLife.02172
  69. Köröskényi K, Duró E, Pallai A, et al. Involvement of Adenosine A<sub>2A</sub> Receptors in Engulfment-Dependent Apoptotic Cell Suppression of Inflammation. *J Immunol.* 2011;186(12):7144-7155. doi:10.4049/jimmunol.1002284
  70. Murphy PS, Wang J, Bhagwat SP, et al. CD73 regulates anti-inflammatory signaling between apoptotic cells and endotoxin-conditioned tissue macrophages. *Cell Death Differ.* 2017;24(3):559-570. doi:10.1038/cdd.2016.159

## References

---

71. Fadok VA, Voelker DR, Campbell PA, Cohen JJ, Bratton DL, Henson PM. Exposure of phosphatidylserine on the surface of apoptotic lymphocytes triggers specific recognition and removal by macrophages. *J Immunol.* 1992;148(7):2207-2216.
72. Fadok V. A., Donna L. Bratton, S. Courtney Frasch MLW and PMH. The role of phosphatidylserine in recognition of apoptotic cells by phagocytes. *Cell Death Differ.* 1998;5(7):551-562. doi:10.1038/sj.cdd.4400404
73. Nagata S RH and KK. Autoimmunity and the Clearance of Dead Cells. *Cell.* 2010;140(5):619-630. doi:10.1016/j.cell.2010.02.014
74. Borisenko GG, Matura T, Liu SX, et al. Macrophage recognition of externalized phosphatidylserine and phagocytosis of apoptotic Jurkat cells - Existence of a threshold. *Arch Biochem Biophys.* 2003;413(1):41-52. doi:10.1016/S0003-9861(03)00083-3
75. Arur S, Uche UE, Rezaul K, et al. Annexin I is an endogenous ligand that mediates apoptotic cell engulfment. *Dev Cell.* 2003;4(4):587-598. doi:10.1016/S1534-5807(03)00090-X
76. Gardai SJ, McPhillips KA, Frasch SC, et al. Cell-surface calreticulin initiates clearance of viable or apoptotic cells through trans-activation of LRP on the phagocyte. *Cell.* 2005;123(2):321-334. doi:10.1016/j.cell.2005.08.032
77. Fadok V.A., Donna L. Bratton, S. Courtney Frasch MLW and PMH. The role of phosphatidylserine in recognition of apoptotic cells by phagocytes. *Cell Death Differ.* 1998;5(7):551-562. doi:10.1038/sj.cdd.4400404
78. Devitt A, Moffatt OD, Raykundalia C, Capra JD, Simmons DL, Gregory CD. Human CD14 mediates recognition and phagocytosis of apoptotic cells. *Nature.* 1998;392(6675):505-509. doi:10.1038/33169
79. Kinchen JM, Ravichandran KS. Journey to the grave: Signaling events regulating removal of apoptotic cells. *J Cell Sci.* 2007;120(13):2143-2149. doi:10.1242/jcs.03463
80. Fadok VA, Bratton DL, Konowal A, Freed PW, Westcott JY, Henson PM. Macrophages that have ingested apoptotic cells in vitro inhibit proinflammatory cytokine production through autocrine/paracrine mechanisms involving TGF- $\beta$ , PGE2, and PAF. *J Clin Invest.* 1998;101(4):890-898. doi:10.1172/JCI1112
81. Chung EY, Liu J, Homma Y, et al. Interleukin-10 expression in macrophages during phagocytosis of apoptotic cells mediated by the TALE homeoproteins Pbx-1 and Prep-1. *NIH Public Access.* 2008;27(6):952-964.
82. Kim S, Elkon KB, Ma X. Transcriptional suppression of interleukin-12 gene expression following phagocytosis of apoptotic cells. *Immunity.* 2004;21(5):643-653. doi:10.1016/j.immuni.2004.09.009
83. Huynh MLN, Fadok VA, Henson PM. Phosphatidylserine-dependent ingestion of apoptotic cells promotes TGF- $\beta$ 1 secretion and the resolution of inflammation. *J Clin Invest.* 2002;109(1):41-50. doi:10.1172/JCI0211638
84. Wahl SM. Transforming growth factor beta (TGF- $\beta$ ) in inflammation: A cause and a cure. *J Clin Immunol.* 1992;12(2):61-74. doi:10.1007/BF00918135
85. Freire-de-Lima CG, Yi QX, Gardai SJ, Bratton DL, Schiemann WP, Henson PM. Apoptotic cells, through transforming growth factor- $\beta$ , coordinately induce anti-inflammatory and suppress pro-inflammatory eicosanoid and NO synthesis in murine macrophages. *J Biol Chem.* 2006;281(50):38376-38384. doi:10.1074/jbc.M605146200
86. Shull MM, Ormsby I, Kier AB, et al. Targeted disruption of the mouse transforming growth factor- $\beta$ 1 gene results in multifocal inflammatory disease. *Nature.* 1992;359(6397):693-699. doi:10.1038/359693a0
87. Park SY, Jung MY, Kim HJ, et al. Rapid cell corpse clearance by stabilin-2, a membrane phosphatidylserine receptor. *Cell Death Differ.* 2008;15(1):192-201. doi:10.1038/sj.cdd.4402242

## References

---

88. Tibrewal N, Wu Y, D'Mello V, et al. Autophosphorylation docking site Tyr-867 in Mer receptor tyrosine kinase allows for dissociation of multiple signaling pathways for phagocytosis of apoptotic cells and down-modulation of lipopolysaccharide-inducible NF- $\kappa$ B transcriptional activation. *J Biol Chem.* 2008;283(6):3618-3627. doi:10.1074/jbc.M706906200
89. Oldenborg PA, Zheleznyak A, Fang YF, Lagenaur CF, Gresham HD, Lindberg FP. Role of CD47 as a marker of self on red blood cells. *Science (80- ).* 2000;288(5473):2051-2054. doi:10.1126/science.288.5473.2051
90. Oldenborg PA, Gresham HD, Lindberg FP. CD47-signal regulatory protein  $\alpha$  (SIRP $\alpha$ ) regulates Fc $\gamma$  and complement receptor-mediated phagocytosis. *J Exp Med.* 2001;193(7):855-861. doi:10.1084/jem.193.7.855
91. Kojima Y, Volkmer JP, McKenna K, et al. CD47-blocking antibodies restore phagocytosis and prevent atherosclerosis. *Nature.* 2016;536(7614):86-90. doi:10.1038/nature18935
92. Lew ED, Oh J, Burrola PG, et al. Differential TAM receptor-ligand-phospholipid interactions delimit differential TAM bioactivities. *Elife.* 2014;3:1-23. doi:10.7554/eLife.03385
93. Zagórska PG, Lew ED, Dransfield I, Lemke G. Diversification of TAM receptor function. *Nat Immunol.* 2014;15(10):920-928. doi:10.1038/ni.2986.Diversification
94. Grabiec AM, Goenka A, Fife ME, Fujimori T, Hussell T. Axl and MerTK receptor tyrosine kinases maintain human macrophage efferocytic capacity in the presence of viral triggers. *Eur J Immunol.* 2018;48(5):855-860. doi:10.1002/eji.201747283
95. Bosurgi, L.; Cao, Y. G.; Cabeza-Cabrerizo, M.; Tucci, A.; Hughes, L. D.; Kong, Y.; Weinstein, J. S.; Licona-Limon, P.; Schmid, E. T.; Pelorosso, F.; Gagliani, N.; Craft, J. E.; Flavell, R. A.; Ghosh S., Rothlin C V. Macrophage function in tissue repair and remodeling requires IL-4 or IL-13 with apoptotic cells. *Science (80- ).* 2017;8132(May):1-9. doi:https://doi.org/10.1126/science.aai8132.
96. Lu Q, Gore M, Zhang Q, et al. Tyro-3 family receptors are essential regulators of mammalian spermatogenesis. *Nature.* 1999;398(6729):723-728. doi:10.1038/19554
97. Tang H, Wang SCH, Wu H, Lu Q, Han D. TAM receptors and the regulation of erythropoiesis in mice. *Haematologica.* 2009;94(3):326-334. doi:10.3324/haematol.13635
98. Zheng Y, Wang Q, Xiao B, Lu Q, Wang Y, Wang X. Involvement of receptor tyrosine kinase Tyro3 in amyloidogenic APP processing and  $\beta$ -amyloid deposition in Alzheimer's disease models. *PLoS One.* 2012;7(6). doi:10.1371/journal.pone.0039035
99. Qi N, Liu P, Zhang Y, Wu H, Chen Y, Han D. Development of a Spontaneous Liver Disease Resembling Autoimmune Hepatitis in Mice Lacking Tyro3, Axl and Mer Receptor Tyrosine Kinases. *PLoS One.* 2013;8(6):1-11. doi:10.1371/journal.pone.0066604
100. Triantafyllou E, Pop OT, Possamai LA, et al. MerTK expressing hepatic macrophages promote the resolution of inflammation in acute liver failure. *Gut.* 2018;67(2):333-347. doi:10.1136/gutjnl-2016-313615
101. A-Gonzalez N, Bensinger SJ, Hong C, et al. Apoptotic Cells Promote Their Own Clearance and Immune Tolerance through Activation of the Nuclear Receptor LXR. *Immunity.* 2009;31(2):245-258. doi:10.1016/j.immuni.2009.06.018
102. Liu W, Bai F, Wang H, et al. Tim-4 Inhibits NLRP3 Inflammasome via the LKB1/AMPK $\alpha$  Pathway in Macrophages. *J Immunol.* 2019;203(4):990-1000. doi:10.4049/jimmunol.1900117
103. Lee SJ, Park SY, Jung MY, Bae SM, Kim IS. Mechanism for phosphatidylserine-dependent erythrophagocytosis in mouse liver. *Blood.* 2011;117(19):5215-5223. doi:10.1182/blood-2010-10-313239
104. Mori K, Kanemura Y, Fujikawa H, et al. Brain-specific angiogenesis inhibitor 1 (BAI1) is expressed in human cerebral neuronal cells. *Neurosci Res.* 2002;43(1):69-74. doi:10.1016/S0168-0102(02)00018-4

## References

---

105. Park D, Tosello-Trampont AC, Elliott MR, et al. BAI1 is an engulfment receptor for apoptotic cells upstream of the ELMO/Dock180/Rac module. *Nature*. 2007;450(7168):430-434. doi:10.1038/nature06329
106. Trahtemberg U, Mevorach D. Apoptotic cells induced signaling for immune homeostasis in macrophages and dendritic cells. *Front Immunol*. 2017;8(OCT). doi:10.3389/fimmu.2017.01356
107. Zeiss CJ. The apoptosis-necrosis continuum: Insights from genetically altered mice. *Vet Pathol*. 2003;40(5):481-495. doi:10.1354/vp.40-5-481
108. Savill J, Fadok V. Corpse clearance defines the meaning of cell death [In Process Citation]. *Nature*. 2000;407(6805):784-788.
109. Kurosaka K, Takahashi M, Watanabe N, Kobayashi Y. Silent Cleanup of Very Early Apoptotic Cells by Macrophages. *J Immunol*. 2003;171(9):4672-4679. doi:10.4049/jimmunol.171.9.4672
110. Saelens X, Festjens N, Vande Walle L, Van Gurp M, Van Loo G, Vandenameele P. Toxic proteins released from mitochondria in cell death. *Oncogene*. 2004;23(16 REV. ISS. 2):2861-2874. doi:10.1038/sj.onc.1207523
111. Garrido C, Galluzzi L, Brunet M, Puig PE, Didelot C, Kroemer G. Mechanisms of cytochrome c release from mitochondria. *Cell Death Differ*. 2006;13(9):1423-1433. doi:10.1038/sj.cdd.4401950
112. Chinnaiyan AM. The apoptosome: heart and soul of the cell death machine. *Neoplasia*. 1999;1(1):5-15. doi:10.1038/sj.neo.7900003
113. Hill MM, Adrain C, Duriez PJ, Creagh EM, Martin SJ. Analysis of the composition, assembly kinetics and activity of native Apaf-1 apoptosomes. *EMBO J*. 2004;23(10):2134-2145. doi:10.1038/sj.emboj.7600210
114. Du C, Fang M, Li Y, Li L, Wang X. Smac, a mitochondrial protein that promotes cytochrome c-dependent caspase activation by eliminating IAP inhibition. *Cell*. 2000;102(1):33-42. doi:10.1016/S0092-8674(00)00008-8
115. van Loo G, van Gurp M, Depuydt B, et al. The serine protease Omi/HtrA2 is released from mitochondria during apoptosis. Omi interacts with caspase-inhibitor XIAP and induces enhanced caspase activity. *Cell Death Differ*. 2002;9(1):20-26. doi:10.1038/sj.cdd.4400970
116. Cory S, Adams JM. The BCL2 family: Regulators of the cellular life-or-death switch. *Nat Rev Cancer*. 2002;2(9):647-656. doi:10.1038/nrc883
117. Locksley RM, Killeen N, Lenardo MJ. The TNF and TNF receptor superfamilies: Integrating mammalian biology. *Cell*. 2001;104(4):487-501. doi:10.1016/S0092-8674(01)00237-9
118. Chicheportiche Y, Bourdon PR, Xu H, et al. TWEAK, a new secreted ligand in the tumor necrosis factor family that weakly induces apoptosis. *J Biol Chem*. 1997;272(51):32401-32410. doi:10.1074/jbc.272.51.32401
119. Ashkenazi A, Dixit VM. Death receptors: Signaling and modulation. *Science (80- )*. 1998;281(5381):1305-1308. doi:10.1126/science.281.5381.1305
120. Walczak H, Krammer PH. The CD95 (APO-1/Fas) and the TRAIL (APO-2L) apoptosis systems. *Exp Cell Res*. 2000;256(1):58-66. doi:10.1006/excr.2000.4840
121. Wajant H. The Fas signaling pathway: More than a paradigm. *Science (80- )*. 2002;296(5573):1635-1636. doi:10.1126/science.1071553
122. Hsu H, Xiong J, Goeddel D V. The TNF receptor 1-associated protein TRADD signals cell death and NF- $\kappa$ B activation. *Cell*. 1995;81(4):495-504. doi:10.1016/0092-8674(95)90070-5
123. Kischkel FC, Hellbardt S, Behrmann I, et al. Cytotoxicity-dependent APO-1 (Fas/CD95)-associated proteins form a death-inducing signaling complex (DISC) with the receptor. *EMBO J*. 1995;14(22):5579-5588. doi:10.1002/j.1460-2075.1995.tb00245.x



## References

---

124. Slee EA, Adrain C, Martin SJ. Executioner Caspase-3, -6, and -7 Perform Distinct, Non-redundant Roles during the Demolition Phase of Apoptosis. *J Biol Chem*. 2001;276(10):7320-7326. doi:10.1074/jbc.M008363200
125. Emlen W. JN and RK. Accelerated in vitro apoptosis of lymphocytes from patients with systemic lupus erythematosus. *J Immunol*. 1994;152(7):3685-3692.
126. U.S. Gaipia, A. Kuhn, A. Sheriffa, L.E. Munoz, S. Franza, R.E. Volle, J.R. Kaldena MH. Clearance of Apoptotic Cells in. *Curr Dir Autoimmun*. 2006;9:2006. doi:doi: 10.1159/000090781.
127. Asahara H, Hasumuna T, Kobata T, et al. Expression of Fas antigen and Fas ligand in the rheumatoid synovial tissue. *Clin Immunol Immunopathol*. 1996;81(1):27-34. doi:10.1006/clin.1996.0153
128. Nakajima T, Aono H, Hasunuma T, et al. Apoptosis and functional fas antigen in rheumatoid arthritis synoviocytes. *Arthritis Rheum*. 1995;38(4):485-491. doi:10.1002/art.1780380405
129. Lumsden AB, Michael J, Kutner H. Endotoxin Levels Measured by a Chromogenic Assay in Portal, Hepatic and Peripheral Venous Blood in Patients with. *Hepatology*. 1988;8(2):232-236.
130. Kubes P, Jenne C, Snyder J. Annual review of immunology immune responses in the liver. *Annu Rev Immunol*. 2018;36(9):1-31. <https://doi.org/10.1146/annurev-immunol->
131. Tabibian JH, Masyuk AI, Masyuk T V., O'Hara SP, LaRusso NF. Physiology of cholangiocytes. *Compr Physiol*. 2013;3(1):541-565. doi:10.1002/cphy.c120019
132. Racanelli V, Rehmann B. The liver as an immunological organ. *Hepatology*. 2006;43(2 SUPPL. 1). doi:10.1002/hep.21060
133. Aizarani N, Saviano A, Mailly L, et al. A Human Liver Cell Atlas reveals Heterogeneity and Epithelial Progenitors. *Nature*. 2019;572(7768):199-204. doi:10.1038/s41586-019-1373-2.A
134. Bonnardel J, T'Jonck W, Gaubomme D, et al. Stellate Cells, Hepatocytes, and Endothelial Cells Imprint the Kupffer Cell Identity on Monocytes Colonizing the Liver Macrophage Niche. *Immunity*. 2019;51(4):638-654.e9. doi:10.1016/j.immuni.2019.08.017
135. Guidotti LG, Chisari F V. To kill or to cure: Options in host defense against viral infection. *Curr Opin Immunol*. 1996;8(4):478-483. doi:10.1016/S0952-7915(96)80034-3
136. Schneider KM, Albers S, Trautwein C. Role of bile acids in the gut-liver axis. *J Hepatol*. 2018;68(5):1083-1085. doi:10.1016/j.jhep.2017.11.025
137. Chiang JYL. Bile acid metabolism and signaling. *Compr Physiol*. 2013;3(3):1191-1212. doi:10.1002/cphy.c120023
138. Francis GA, Fayard E, Picard F, Auwerx J. Nuclear Receptors and the Control of Metabolism. *Annu Rev Physiol*. 2003;65:261-311. doi:10.1146/annurev.physiol.65.092101.142528
139. Thomas C, Pellicciari R, Pruzanski M, Auwerx J, Schoonjans K. Targeting bile-acid signalling for metabolic diseases. *Nat Rev Drug Discov*. 2008;7(8):678-693. doi:10.1038/nrd2619
140. Zollner G, Marschall HU, Wagner M, Trauner M. Role of nuclear receptors in the adaptive response to bile acids and cholestasis: Pathogenetic and therapeutic considerations. *Mol Pharm*. 2006;3(3):231-251. doi:10.1021/mp060010s
141. Moschetta A, Bookout AL, Mangelsdorf DJ. Prevention of cholesterol gallstone disease by FXR agonists in a mouse model. *Nat Med*. 2004;10(12):1352-1358. doi:10.1038/nm1138
142. Kawamata Y, Fujii R, Hosoya M, et al. A G protein-coupled receptor responsive to bile acids. *J Biol Chem*. 2003;278(11):9435-9440. doi:10.1074/jbc.M209706200
143. Keitel V, Reinehr R, Gatsios P, et al. The G-protein coupled bile salt receptor TGR5 is expressed in liver sinusoidal endothelial cells. *Hepatology*. 2007;45(3):695-704. doi:10.1002/hep.21458
144. Hylemon PB, Zhou H, Pandak WM, Ren S, Gil G, Dent P. Bile acids as regulatory molecules. *J Lipid Res*. 2009;50(8):1509-1520. doi:10.1194/jlr.R900007-JLR200

## References

---

145. Bilzer M, Roggel F, Gerbes AL. Role of Kupffer cells in host defense and liver disease. *Liver Int.* 2006;26(10):1175-1186. doi:10.1111/j.1478-3231.2006.01342.x
146. Soucie EL, Weng Z, Geirsdóttir L, et al. Lineage-specific enhancers activate self-renewal genes in macrophages and embryonic stem cells. *Science (80- )*. 2016;351(6274). doi:10.1126/science.aad5510.Lineage-specific
147. Naito M, Hasegawa G, Takahashi K. Development, differentiation, and maturation of kupffer cells. *Microsc Res Tech.* 1997;39(4):350-364. doi:10.1002/(SICI)1097-0029(19971115)39:4<350::AID-JEMT5>3.0.CO;2-L
148. Scott CL, Zheng F, De Baetselier P, et al. Bone marrow-derived monocytes give rise to self-renewing and fully differentiated Kupffer cells. *Nat Commun.* 2016;7:1-10. doi:10.1038/ncomms10321
149. Hoedemakers RMJ, Morselt HWM, Scherphof GL, Daemen T. Heterogeneity in secretory responses of rat liver macrophages of different size. *Liver.* 1995;15(6):313-319. doi:10.1111/j.1600-0676.1995.tb00691.x
150. David BA, Rezende RM, Antunes MM, et al. Combination of Mass Cytometry and Imaging Analysis Reveals Origin, Location, and Functional Repopulation of Liver Myeloid Cells in Mice. *Gastroenterology.* 2016;151(6):1176-1191. doi:10.1053/j.gastro.2016.08.024
151. Helmy KY, Katschke KJ, Gorgani NN, et al. CR1g: A macrophage complement receptor required for phagocytosis of circulating pathogens. *Cell.* 2006;124(5):915-927. doi:10.1016/j.cell.2005.12.039
152. Grozovsky R, Hoffmeister KM, Falet H. Novel clearance mechanisms of platelets. *Curr Opin Hematol.* 2010;17(6):585-589. doi:10.1097/MOH.0b013e32833e7561
153. Shi J, Gilbert GE, Kokubo Y, Ohashi T. Role of the liver in regulating numbers of circulating neutrophils. *Blood.* 2001;98(4):1226-1230. doi:10.1182/blood.V98.4.1226
154. Fadok V BD and HP. Phagocyte receptors for apoptotic cells: recognition, uptake, and consequences. *J Clin Invest.* 2001;108(7):957-962. doi:10.1172/jci14122
155. MacParland SA, Liu JC, Ma XZ, et al. Single cell RNA sequencing of human liver reveals distinct intrahepatic macrophage populations. *Nat Commun.* 2018;9(1):1-21. doi:10.1038/s41467-018-06318-7
156. Krenkel O, Tacke F. Liver macrophages in tissue homeostasis and disease. *Nat Rev Immunol.* 2017;17(5):306-321. doi:10.1038/nri.2017.11
157. Ju C, Tacke F. Hepatic macrophages in homeostasis and liver diseases: From pathogenesis to novel therapeutic strategies. *Cell Mol Immunol.* 2016;13(3):316-327. doi:10.1038/cmi.2015.104
158. Sierro F, Evrard M, Rizzetto S, et al. A Liver Capsular Network of Monocyte-Derived Macrophages Restricts Hepatic Dissemination of Intraperitoneal Bacteria by Neutrophil Recruitment. *Immunity.* 2017;47(2):374-388.e6. doi:10.1016/j.immuni.2017.07.018
159. Miura K, Yang L, van Rooijen N, Ohnishi H, Seki E. Hepatic recruitment of macrophages promotes nonalcoholic steatohepatitis through CCR2. *Am J Physiol - Gastrointest Liver Physiol.* 2012;302(11):1310-1321. doi:10.1152/ajpgi.00365.2011
160. Krenkel O, Puengel T, Govaere O, et al. Therapeutic inhibition of inflammatory monocyte recruitment reduces steatohepatitis and liver fibrosis. *Hepatology.* 2018;67(4):1270-1283. doi:10.1002/hep.29544
161. Cai B, Dongiovanni P, Corey KE, et al. Macrophage MerTK Promotes Liver Fibrosis in Nonalcoholic Steatohepatitis. *Cell Metab.* 2020;31(2):406-421.e7. doi:10.1016/j.cmet.2019.11.013
162. Ju C, Reilly TP, Bourdi M, et al. Protective role of kupffer cells in acetaminophen-induced hepatic injury in mice. *Chem Res Toxicol.* 2002;15(12):1504-1513. doi:10.1021/tx0255976

## References

---

163. Ramachandran P, Iredale JP. Macrophages: Central regulators of hepatic fibrogenesis and fibrosis resolution. *J Hepatol.* 2012;56(6):1417-1419. doi:10.1016/j.jhep.2011.10.026
164. Karlmark KR, Zimmermann HW, Roderburg C, et al. The fractalkine receptor CX3CR1 protects against liver fibrosis by controlling differentiation and survival of infiltrating hepatic monocytes. *Hepatology.* 2010;52(5):1769-1782. doi:10.1002/hep.23894
165. Seidman JS, Troutman TD, Sakai M, et al. Niche-Specific Re-Programming of Epigenetic Landscapes Drives Myeloid Cell Diversity in Nonalcoholic Steatohepatitis. *Immunity.* 2021;52(6):1057-1074. doi:10.1016/j.immuni.2020.04.001.Niche-Specific
166. Sato K, Hall C, Glaser S, Francis H, Meng F, Alpini G. Pathogenesis of Kupffer Cells in Cholestatic Liver Injury. *Am J Pathol.* 2016;186(9):2238-2247. doi:10.1016/j.ajpath.2016.06.003
167. Karlsen TH, Folseraas T, Thorburn D, Vesterhus M. Primary sclerosing cholangitis – a comprehensive review. *J Hepatol.* 2017;67(6):1298-1323. doi:10.1016/j.jhep.2017.07.022
168. Molodecky NA, Kareemi H, Parab R, et al. Incidence of primary sclerosing cholangitis: A systematic review and meta-analysis. *Hepatology.* 2011;53(5):1590-1599. doi:10.1002/hep.24247
169. Wee A, Ludwig J, Coffey RJ, LaRusso NF, Wiesner RH. Hepatobiliary carcinoma associated with primary sclerosing cholangitis and chronic ulcerative colitis. *Hum Pathol.* 1985;16(7):719-726. doi:10.1016/S0046-8177(85)80158-1
170. Broomé U, Lindberg G, Löfberg R. Primary sclerosing cholangitis in ulcerative colitis-A risk factor for the development of dysplasia and DNA aneuploidy? *Gastroenterology.* 1992;102(6):1877-1880. doi:10.1016/0016-5085(92)90308-L
171. Dutta AK, Khimji AK, Kresge C, et al. Identification and functional characterization of TMEM16A, a Ca<sup>2+</sup>-activated Cl<sup>-</sup> channel activated by extracellular nucleotides, in biliary epithelium. *J Biol Chem.* 2011;286(1):766-776. doi:10.1074/jbc.M110.164970
172. Hohenester S, Maillette de Buy Wenniger L, Paulusma CC, et al. A biliary HCO<sub>3</sub><sup>-</sup> umbrella constitutes a protective mechanism against bile acid-induced injury in human cholangiocytes. *Hepatology.* 2012;55(1):173-183. doi:10.1002/hep.24691
173. Beuers U, Spengler U, Kruis W, et al. Ursodeoxycholic acid for treatment of primary sclerosing cholangitis: A placebo-controlled trial. *Hepatology.* 1992;16(3):707-714. doi:10.1002/hep.1840160315
174. Smit JJM, Groen K, Mel CAAM, et al. Homozygous disruption of the murine MDR2 P-glycoprotein gene leads to a complete absence of phospholipid from bile and to liver disease. *Cell.* 1993;75(3):451-462.
175. Guicciardi ME, Gores GJ. Apoptosis: A mechanism of acute and chronic liver injury. *Gut.* 2005;54(7):1024-1033. doi:10.1136/gut.2004.053850
176. Marchioni Beery RM, Vaziri H, Forouhar F. Primary biliary cirrhosis and primary sclerosing cholangitis: A review featuring a women's health perspective. *J Clin Transl Hepatol.* 2014;2(4):266-284. doi:10.14218/JCTH.2014.00024
177. Trottier J, Białek A, Caron P, et al. Metabolomic profiling of 17 bile acids in serum from patients with primary biliary cirrhosis and primary sclerosing cholangitis: A pilot study. *Dig Liver Dis.* 2012;44(4):303-310. doi:10.1016/j.dld.2011.10.025
178. Alvaro D, Gigliozzi A, Attili AF. Regulation and deregulation of cholangiocyte proliferation. *J Hepatol.* 2000;33(2):333-340. doi:10.1016/S0168-8278(00)80377-3
179. Ji SG, Juran BD, Mucha S, et al. Genome-wide association study of primary sclerosing cholangitis identifies new risk loci and quantifies the genetic relationship with inflammatory bowel disease. *Nat Genet.* 2017;49(2):269-273. doi:10.1038/ng.3745
180. Liu JZ, Hov JR, Folseraas T, et al. Dense genotyping of immune-related disease regions identifies nine new risk loci for primary sclerosing cholangitis. *Nat Genet.* 2013;45(6):670-675.

- doi:10.1038/ng.2616
181. Trivedi PJ, Adams DH. Mucosal immunity in liver autoimmunity: A comprehensive review. *J Autoimmun.* 2013;46:97-111. doi:10.1016/j.jaut.2013.06.013
  182. Folseraas T, Melum E, Rausch P, et al. Extended analysis of a genome-wide association study in primary sclerosing cholangitis detects multiple novel risk loci. *J Hepatol.* 2012;57(2):366-375. doi:10.1016/j.jhep.2012.03.031
  183. Lichtman SN, Sartor RB, Keku J, Schwab JH. Hepatic inflammation in rats with experimental small intestinal bacterial overgrowth. *Gastroenterology.* 1990;98(2):414-423. doi:10.1016/0016-5085(90)90833-M
  184. Terjung B, Söhne J, Lechtenberg B, et al. p-ANCA in autoimmune liver disorders recognise human  $\beta$ -tubulin isotype 5 and cross-react with microbial protein FtsZ. *Gut.* 2010;59(6):808-816. doi:10.1136/gut.2008.157818
  185. Grant AJ, Lalor PF, Hübscher SG, Briskin M, Adams DH. MAdCAM-1 expressed in chronic inflammatory liver disease supports mucosal lymphocyte adhesion to hepatic endothelium (MAdCAM-1 in chronic inflammatory liver disease). *Hepatology.* 2001;33(5):1065-1072. doi:10.1053/jhep.2001.24231
  186. Rossen NG, Fuentes S, Boonstra K, et al. The mucosa-associated microbiota of PSC patients is characterized by low diversity and low abundance of uncultured Clostridiales II. *J Crohn's Colitis.* 2015;9(4):342-348. doi:10.1093/ecco-jcc/jju023
  187. Jacquemin E. Role of multidrug resistance 3 deficiency in pediatric and adult liver disease: One gene for three diseases. *Semin Liver Dis.* 2001;21(4):551-562. doi:10.1055/s-2001-19033
  188. Popov Y, Patsenker E, Fickert P, Trauner M, Schuppan D. Mdr2 (Abcb4)<sup>-/-</sup> mice spontaneously develop severe biliary fibrosis via massive dysregulation of pro- and antifibrogenic genes. *J Hepatol.* 2005;43(6):1045-1054. doi:10.1016/j.jhep.2005.06.025
  189. Fickert P, Fuchsbichler A, Wagner M, et al. Regurgitation of bile acids from leaky bile ducts causes sclerosing cholangitis in Mdr2 (Abcb4) knockout mice. *Gastroenterology.* 2004;127(1):261-274. doi:10.1053/j.gastro.2004.04.009
  190. Potikha T, Stoyanov E, Pappo O, et al. Interstrain differences in chronic hepatitis and tumor development in a murine model of inflammation-mediated hepatocarcinogenesis. *Hepatology.* 2013;58(1):192-204. doi:10.1002/hep.26335
  191. Gucciardi ME, Trussoni CE, Krishnan A, et al. Macrophages Contribute to the Pathogenesis of Sclerosing Cholangitis in Mice. *J Hepatol.* 2018;69(3):676-686. doi:10.1016/j.jhep.2018.05.018.Macrophages
  192. Guillot A, Guerri L, Feng D, et al. Bile acid-activated macrophages promote biliary epithelial cell proliferation through integrin  $\alpha\beta 6$  upregulation following liver injury. *J Clin Invest.* 2021;131(9). doi:10.1172/JCI132305
  193. Ravichandran G, Neumann K, Berkhout LK, et al. Interferon- $\gamma$ -dependent immune responses contribute to the pathogenesis of sclerosing cholangitis in mice. *J Hepatol.* 2019;71(4):773-782. doi:10.1016/j.jhep.2019.05.023
  194. Tedesco D, Thapa M, Chin CY, et al. Alterations in Intestinal Microbiota Lead to Production of Interleukin 17 by Intrahepatic  $\gamma\delta$  T-Cell Receptor-Positive Cells and Pathogenesis of Cholestatic Liver Disease. *Gastroenterology.* 2018;154(8):2178-2193. doi:10.1053/j.gastro.2018.02.019
  195. Berkhout L, Barikbin R, Schiller B, et al. Deletion of tumour necrosis factor  $\alpha$  receptor 1 elicits an increased TH17 immune response in the chronically inflamed liver. *Sci Rep.* 2019;9(1):1-11. doi:10.1038/s41598-019-40324-z
  196. Lin R, Zhang J, Zhou L, Wang B. Altered function of monocytes/macrophages in patients with autoimmune hepatitis. *Mol Med Rep.* 2016;13(5):3874-3880. doi:10.3892/mmr.2016.4998
  197. Li P zhi, Li J zheng, Li M, Gong J ping, He K. An efficient method to isolate and culture mouse

## References

---

- Kupffer cells. *Immunol Lett.* 2014;158(1-2):52-56. doi:10.1016/j.imlet.2013.12.002
198. Wegner K, Just S, Gau L, et al. Rapid analysis of bile acids in different biological matrices using LC-ESI-MS/MS for the investigation of bile acid transformation by mammalian gut bacteria. *Anal Bioanal Chem.* 2017;409(5):1231-1245. doi:10.1007/s00216-016-0048-1
199. Dugast AS, Tonelli A, Berger CT, et al. Decreased Fc receptor expression on innate immune cells is associated with impaired antibody-mediated cellular phagocytic activity in chronically HIV-1 infected individuals. *Virology.* 2011;415(2):160-167. doi:10.1016/j.virol.2011.03.012
200. Yin X-M, Ding W-X. Death Receptor Activation-Induced Hepatocyte Apoptosis and Liver Injury. *Curr Mol Med.* 2005;3(6):491-508. doi:10.2174/1566524033479555
201. Faubion WA, Guicciardi ME, Miyoshi H, et al. Toxic bile salts induce rodent hepatocyte apoptosis via direct activation of Fas. *J Clin Invest.* 1999;103(1):137-145. doi:10.1172/JCI4765
202. Wammers M, Schupp AK, Bode JG, et al. Reprogramming of pro-inflammatory human macrophages to an anti-inflammatory phenotype by bile acids. *Sci Rep.* 2018;8(1):1-15. doi:10.1038/s41598-017-18305-x
203. Trottier J, Białek A, Caron P, Straka RJ, Milkiewicz P, Barbier O. Profiling circulating and urinary bile acids in patients with biliary obstruction before and after biliary stenting. *PLoS One.* 2011;6(7). doi:10.1371/journal.pone.0022094
204. Chiang JYL. Bile acids: Regulation of synthesis. *J Lipid Res.* 2009;50(10):1955-1966. doi:10.1194/jlr.R900010-JLR200
205. Fiorucci S, Biagioli M, Zampella A, Distrutti E. Bile acids activated receptors regulate innate immunity. *Front Immunol.* 2018;9(AUG):1-17. doi:10.3389/fimmu.2018.01853
206. Cipriani S, Mencarelli A, Chini MG, et al. The bile acid receptor GPBAR-1 (TGR5) modulates integrity of intestinal barrier and immune response to experimental colitis. *PLoS One.* 2011;6(10). doi:10.1371/journal.pone.0025637
207. Vavassori P, Mencarelli A, Renga B, Distrutti E, Fiorucci S. The Bile Acid Receptor FXR Is a Modulator of Intestinal Innate Immunity. *J Immunol.* 2009;183(10):6251-6261. doi:10.4049/jimmunol.0803978
208. Cai S-Y, Boyer JL. The role of bile acids in cholestatic liver injury. *Ann Transl Med.* 2021;9(8):737-737. doi:10.21037/atm-20-5110
209. Wong KL, Tai JJY, Wong WC, et al. Gene expression profiling reveals the defining features of the classical, intermediate, and nonclassical human monocyte subsets. *Blood.* 2011;118(5):16-31. doi:10.1182/blood-2010-12-326355
210. Kapellos TS, Bonaguro L, Gemünd I, et al. Human monocyte subsets and phenotypes in major chronic inflammatory diseases. *Front Immunol.* 2019;10(AUG):1-13. doi:10.3389/fimmu.2019.02035
211. Liu Z, Davidson A. Taming lupus—a new understanding of pathogenesis is leading to clinical advances. *Nat Med.* 2012;18(6):871-882. doi:10.1038/nm.2752
212. Kawane K, Ohtani M, Miwa K, et al. Chronic polyarthritis caused by mammalian DNA that escapes from degradation in macrophages. *Nature.* 2006;443(7114):998-1002. doi:10.1038/nature05245
213. Vives-Pi M, Rodríguez-Fernández S, Pujol-Autonell I. How apoptotic  $\beta$ -cells direct immune response to tolerance or to autoimmune diabetes: A review. *Apoptosis.* 2015;20(3):263-272. doi:10.1007/s10495-015-1090-8
214. Cohen PL, Caricchio R, Abraham V, et al. Delayed apoptotic cell clearance and lupus-like autoimmunity in mice lacking the c-mer membrane tyrosine kinase. *J Exp Med.* 2002;196(1):135-140. doi:10.1084/jem.20012094
215. Hanayama R, Tanaka M, Miyasaka K, et al. Autoimmune Disease and Impaired Uptake of

## References

---

- Apoptotic Cells in MFG-E8–Deficient Mice. *Annu Rev Ecol Syst.* 2004;304(1147):873. <http://podaac.jpl.nasa.gov/www.sciencemag.org/cgi/content/full/304/5674/1144/>
216. Rodriguez-Manzanet R, Sanjuan MA, Wu HY, et al. T and B cell hyperactivity and autoimmunity associated with niche-specific defects in apoptotic body clearance in TIM-4-deficient mice. *Proc Natl Acad Sci U S A.* 2010;107(19):8706-8711. doi:10.1073/pnas.0910359107
217. Mochida S, Ogata I, Ohta Y, Yamada S, Fujiwara K. In situ evaluation of the stimulatory state of hepatic macrophages based on their ability to produce superoxide anions in rats. *J Pathol.* 1989;158(1):67-71. doi:10.1002/path.1711580113
218. Naito M, Hasegawa G, Ebe Y, Yamamoto T. Differentiation and function of Kupffer cells. *Med Electron Microsc.* 2004;37(1):16-28. doi:10.1007/s00795-003-0228-x
219. Horst AK, Tiegs G, Diehl L. Contribution of Macrophage Efferocytosis to Liver Homeostasis and Disease. *Front Immunol.* 2019;10(November). doi:10.3389/fimmu.2019.02670
220. Guicciardi ME, Trussoni CE, Krishnan A, et al. Macrophages contribute to the pathogenesis of sclerosing cholangitis in mice. *J Hepatol.* 2018;69(3):676-686. doi:10.1016/j.jhep.2018.05.018
221. Wang M, You Q, Lor K, Chen F, Gao B, Ju C. Chronic alcohol ingestion modulates hepatic macrophage populations and functions in mice. *J Leukoc Biol.* 2014;96(4):657-665. doi:10.1189/jlb.6a0114-004rr
222. Wynn TA, Vannella KM. Macrophages in Tissue Repair, Regeneration, and Fibrosis. *Immunity.* 2016;44(3):450-462. doi:10.1016/j.immuni.2016.02.015
223. Jiang Y, Tang Y, Hoover C, et al. Kupffer cell receptor CLEC4F is important for the destruction of desialylated platelets in mice. *Cell Death Differ.* 2021;28(11):3009-3021. doi:10.1038/s41418-021-00797-w
224. Truman LA, Ford CA, Pasikowska M, et al. CX3CL 1/fractalkine is released from apoptotic lymphocytes to stimulate macrophage chemotaxis. *Blood.* 2008;112(13):5026-5036. doi:10.1182/blood-2008-06-162404
225. Mass E, Ballesteros I, Farlik M, et al. Specification of tissue-resident macrophages during organogenesis. *Science* (80- ). 2016;353(6304):1-32. doi:10.1126/science.aaf4238.Specification
226. Zagórska A, Través PG, Jiménez-García L, et al. Differential regulation of hepatic physiology and injury by the TAM receptors Axl and Mer. *Life Sci Alliance.* 2020;3(8):1-15. doi:10.26508/LSA.202000694
227. Shao WH, Kuan AP, Wang C, et al. Disrupted Mer receptor tyrosine kinase expression leads to enhanced MZ B-cell responses. *J Autoimmun.* 2010;35(4):368-374. doi:10.1016/j.jaut.2010.08.001
228. Scott RS, McMahon EJ, Pop SM, et al. Phagocytosis and clearance of apoptotic cells is mediated by MER. *Nature.* 2001;411(6834):207-211. doi:10.1038/35075603
229. Pei-Chin Chuang, Meng-Hsing Wu YS and S-JT. Downregulation of CD36 results in reduced phagocytic ability of peritoneal macrophages of women with endometriosis. *J Pathol.* 2009;(June):232–241. doi:10.1002/path.2588
230. Min C, Park J, Kim G, et al. Tim-4 functions as a scavenger receptor for phagocytosis of exogenous particles. *Cell Death Dis.* 2020;11(7). doi:10.1038/s41419-020-02773-7
231. Lee J, Park B, Moon B, et al. A scaffold for signaling of Tim-4-mediated efferocytosis is formed by fibronectin. *Cell Death Differ.* 2019;26(9):1646-1655. doi:10.1038/s41418-018-0238-9
232. Meyers JH, Chakravarti S, Schlesinger D, et al. TIM-4 is the ligand for TIM-1, and the TIM-1-TIM-4 interaction regulates T cell proliferation. *Nat Immunol.* 2005;6(5):455-464. doi:10.1038/ni1185
233. Beattie L, Sawtell A, Mann J, et al. Bone marrow-derived and resident liver macrophages display

## References

---

- unique transcriptomic signatures but similar biological functions. *J Hepatol.* 2016;65(4):758-768. doi:10.1016/j.jhep.2016.05.037
234. Chen YY, Arndtz K, Webb G, et al. Intrahepatic macrophage populations in the pathophysiology of primary sclerosing cholangitis. *JHEP Reports.* 2019;1(5):369-376. doi:10.1016/j.jhepr.2019.10.003
235. Cameron RG, Blendis LM, Neuman MG. Accumulation of macrophages in primary sclerosing cholangitis. *Clin Biochem.* 2001;34(3):195-201. doi:10.1016/S0009-9120(01)00215-6
236. Thepen T, Van Vuuren AJH, Kiekens RCM, Damen CA, Vooijs WC, Van De Winkel JGJ. Resolution of cutaneous inflammation after local elimination of macrophages. *Nat Biotechnol.* 2000;18(1):48-51. doi:10.1038/71908
237. Van Roon JAG, Van Vuuren AJ, Wijngaarden S, et al. Selective elimination of synovial inflammatory macrophages in rheumatoid arthritis by an Fc $\gamma$  receptor I-directed immunotoxin. *Arthritis Rheum.* 2003;48(5):1229-1238. doi:10.1002/art.10940
238. van Vuuren AJ, van Roon JAG, Walraven V, et al. CD64-Directed Immunotoxin Inhibits Arthritis in a Novel CD64 Transgenic Rat Model. *J Immunol.* 2006;176(10):5833-5838. doi:10.4049/jimmunol.176.10.5833
239. Matsumoto K, Miyake Y, Umeda Y, et al. Serial changes of serum growth factor levels and liver regeneration after partial hepatectomy in healthy humans. *Int J Mol Sci.* 2013;14(10):20877-20889. doi:10.3390/ijms141020877
240. Holt MP, Cheng L, Ju C. Identification and characterization of infiltrating macrophages in acetaminophen-induced liver injury. *J Leukoc Biol.* 2008;84(6):1410-1421. doi:10.1189/jlb.0308173
241. Bartocci A, Mastrogiannis DS, Migliorati G, Stockert RJ, Wolkoff AW, Stanley ER. Macrophages specifically regulate the concentration of their own growth factor in the circulation. *Proc Natl Acad Sci USA.* 1987;84(17):6179-6183. doi:10.1073/pnas.84.17.6179
242. Botto M, Dell' Agnola C, Bygrave AE, et al. Homozygous C1q deficiency causes glomerulonephritis associated with multiple apoptotic bodies. *Nat Genet.* 1998;18(3):231-236.
243. Ramirez-Ortiz ZG, Pendergraft WF, Prasad A, et al. The scavenger receptor SCARF1 mediates the clearance of apoptotic cells and prevents autoimmunity. *Nat Immunol.* 2013;14(9):917-926. doi:10.1038/ni.2670
244. Lewis MJ, Botto M. Complement deficiencies in humans and animals: Links to autoimmunity. *Autoimmunity.* 2006;39(5):367-378. doi:10.1080/08916930600739233
245. Henson PM, Tuder RM. Apoptosis in the lung: Induction, clearance and detection. *Am J Physiol - Lung Cell Mol Physiol.* 2008;294(4):601-611. doi:10.1152/ajplung.00320.2007
246. Mattson MP. Apoptosis in neurodegenerative disorders. *Nat Rev Mol Cell Biol.* 2000;1(2):120-129. doi:10.1038/35040009
247. Cardona AE, Pioro EP, Sasse ME, et al. Control of microglial neurotoxicity by the fractalkine receptor. *Nat Neurosci.* 2006;9(7):917-924. doi:10.1038/nn1715
248. Bolognesi M, Merkel C, Sacerdoti D, Nava V, Gatta A. Role of spleen enlargement in cirrhosis with portal hypertension. *Dig Liver Dis.* 2002;34(2):144-150. doi:10.1016/S1590-8658(02)80246-8
249. Liangpunsakul S, Ulmer BJ, Chalasani N. Predictors and implications of severe hypersplenism in patients with cirrhosis. *Am J Med Sci.* 2003;326(3):111-116. doi:10.1097/00000441-200309000-00001
250. Akahoshi T, Hashizume M, Tanoue K, et al. Role of the spleen in liver fibrosis in rats may be mediated by transforming growth factor  $\beta$ -1. *J Gastroenterol Hepatol.* 2002;17(1):59-65. doi:10.1046/j.1440-1746.2002.02667.x

## References

---

251. Cai X, Li Z, Zhang Q, et al. CXCL6-EGFR-induced kupffer cells secrete TGF- $\beta$ 1 promoting hepatic stellate cell activation via the SMAD2/BRD4/C-MYC/ EZH2 pathway in liver fibrosis. *J Cell Mol Med*. 2018;22(10):5050-5061. doi:10.1111/jcmm.13787
252. Li A, Li Z, Ma S, et al. Dysfunction of splenic macrophages in cirrhotic patients with hypersplenism and HBV infection. *Am J Med Sci*. 2008;336(1):32-38. doi:10.1097/MAJ.0b013e31815b69e7
253. Ren S, Zhang S, Li M, et al. NF- $\kappa$ B p65 and c-Rel subunits promote phagocytosis and cytokine secretion by splenic macrophages in cirrhotic patients with hypersplenism. *Int J Biochem Cell Biol*. 2013;45(2):335-343. doi:10.1016/j.biocel.2012.11.012
254. Jiang A, Zhang S, Li Z, et al. miR-615-3p promotes the phagocytic capacity of splenic macrophages by targeting ligand-dependent nuclear receptor corepressor in cirrhosis-related portal hypertension. *Exp Biol Med*. 2011;236(6):672-680. doi:10.1258/ebm.2011.010349
255. Flannagan RS, Canton J, Furuya W, Glogauer M, Grinstein S. The phosphatidylserine receptor TIM4 utilizes integrins as coreceptors to effect phagocytosis. *Mol Biol Cell*. 2014;25(9):1511-1522. doi:10.1091/mbc.E13-04-0212
256. Kim S, Park S-Y, Kim S-Y, et al. Cross Talk between Engulfment Receptors Stabilin-2 and Integrin  $\alpha$ v $\beta$ 5 Orchestrates Engulfment of Phosphatidylserine-Exposed Erythrocytes. *Mol Cell Biol*. 2012;32(14):2698-2708. doi:10.1128/mcb.06743-11
257. Coburn CT, Hajri T, Ibrahim A, Abumrad NA. Role of CD36 in membrane transport and utilization of long-chain fatty acids by different tissues. *J Mol Neurosci*. 2001;16(2-3):117-121. doi:10.1385/JMN:16:2-3:117
258. Febbraio M, Hajjar DP, Silverstein RL. CD36: a class B scavenger receptor involved in angiogenesis, atherosclerosis, inflammation, and lipid metabolism. *J Clin Invest*. 2001;108(6):785-791. doi:10.1172/jci200114006
259. Fadok VA, Warner ML, Bratton DL, Henson PM. CD36 is required for phagocytosis of apoptotic cells by human macrophages that use either a phosphatidylserine receptor or the vitronectin receptor ( $\alpha$ v $\beta$ 3). *J Immunol*. 1998;161(11):6250-6257.
260. Greenberg ME, Sun M, Zhang R, Febbraio M, Silverstein R, Hazen SL. Oxidized phosphatidylserine-CD36 interactions play an essential role in macrophage-dependent phagocytosis of apoptotic cells. *J Exp Med*. 2006;203(12):2613-2625. doi:10.1084/jem.20060370
261. Fadok VA, De Cathelineau A, Daleke DL, Henson PM, Bratton DL. Loss of phospholipid asymmetry and surface exposure of phosphatidylserine is required for phagocytosis of apoptotic cells by macrophages and fibroblasts. *J Biol Chem*. 2001;276(2):1071-1077. doi:10.1074/jbc.M003649200
262. Tait JF, Smith C. Phosphatidylserine receptors: Role of CD36 in binding of anionic phospholipid vesicles to monocytic cells. *J Biol Chem*. 1999;274(5):3048-3054. doi:10.1074/jbc.274.5.3048
263. Fabisiak JP, Tyurina YY, Tyurin VA, Lazo JS, Kagan VE. Random versus selective membrane phospholipid oxidation in apoptosis: Role of phosphatidylserine. *Biochemistry*. 1998;37(39):13781-13790. doi:10.1021/bi9808262
264. Kagan VE, Gleiss B, Tyurina YY, et al. A Role for Oxidative Stress in Apoptosis: Oxidation and Externalization of Phosphatidylserine Is Required for Macrophage Clearance of Cells Undergoing Fas-Mediated Apoptosis. *J Immunol*. 2002;169(1):487-499. doi:10.4049/jimmunol.169.1.487
265. Champion JA, Mitragotri S. Role of target geometry in phagocytosis. *Proc Natl Acad Sci U S A*. 2006;103(13):4930-4934. doi:10.1073/pnas.0600997103
266. Gratton SEA, Ropp PA, Pohlhaus PD, et al. The effect of particle design on cellular internalization pathways. *Proc Natl Acad Sci U S A*. 2008;105(33):11613-11618. doi:10.1073/pnas.0801763105



## References

---

267. Pratten MK, Lloyd JB. Pinocytosis and phagocytosis: the effect of size of a particulate substrate on its mode of capture by rat peritoneal macrophages cultured in vitro. *BBA - Gen Subj*. 1986;881(3):307-313. doi:10.1016/0304-4165(86)90020-6
268. Tabata Y, Ikada Y. Effect of the size and surface charge of polymer microspheres on their phagocytosis by macrophage. *Biomaterials*. 1988;9(4):356-362. doi:10.1016/0142-9612(88)90033-6
269. Ahsan F, Rivas IP, Khan MA, Torres Suárez AI. Targeting to macrophages: Role of physicochemical properties of particulate carriers - Liposomes and microspheres - On the phagocytosis by macrophages. *J Control Release*. 2002;79(1-3):29-40. doi:10.1016/S0168-3659(01)00549-1
270. Beningo KA, Wang Y. Fc-receptor-mediated phagocytosis is regulated by mechanical properties of the target. *J Cell Sci*. 2002;115:849-856. doi:10.1242/jcs.115.4.849.
271. Lefebvre P, Cariou B, Lien F, Kuipers F, Staels B. Role of bile acids and bile acid receptors in metabolic regulation. *Physiol Rev*. 2009;89(1):147-191. doi:10.1152/physrev.00010.2008
272. Chiang JYL, Ferrell JM. Bile Acids as Metabolic Regulators and Nutrient Sensors. *Annu Rev Nutr*. 2019;39:175-200. doi:10.1146/annurev-nutr-082018-124344
273. Fiorucci S, Distrutti E, Carino A, Zampella A, Biagioli M. Bile acids and their receptors in metabolic disorders. *Prog Lipid Res*. 2021;82(December 2020):101094. doi:10.1016/j.plipres.2021.101094
274. Xia X, Francis H, Glaser S, Alpini G, LeSage G. Bile acid interactions with cholangiocytes TOPIC HIGHLIGHT. *World J Gastroenterol World J Gastroenterol ISSN*. 2006;12(1222):3553-3563.
275. Jansen PLM, Ghallab A, Vartak N, et al. The ascending pathophysiology of cholestatic liver disease. *Hepatology*. 2017;65(2):722-738. doi:10.1002/hep.28965
276. Chen W, Owsley E, Yang Y, Stroup D, Chiang JYL. Nuclear receptor-mediated repression of human cholesterol 7  $\alpha$ -hydroxylase gene transcription by bile acids. *J Lipid Res*. 2001;42(9):1402-1412. doi:10.1016/s0022-2275(20)30272-8
277. Allen K, Jaeschke H, Copple BL. Bile acids induce inflammatory genes in hepatocytes: A novel mechanism of inflammation during obstructive cholestasis. *Am J Pathol*. 2011;178(1):175-186. doi:10.1016/j.ajpath.2010.11.026
278. Drivas G, James O, Wardle N. Study of reticuloendothelial phagocytic capacity in patients with cholestasis. *Br Med J*. 1976;1(6025):1568-1569. doi:10.1136/bmj.1.6025.1568
279. Cooksley WGE, Powell LW, Halliday JW. Reticuloendothelial Phagocytic Function in Human Liver Disease and its Relationship to Haemolysis. *Br J Haematol*. 1973;25(2):147-164. doi:10.1111/j.1365-2141.1973.tb01725.x
280. Keitel V, Donner M, Winandy S, Kubitz R, Häussinger D. Expression and function of the bile acid receptor TGR5 in Kupffer cells. *Biochem Biophys Res Commun*. 2008;372(1):78-84. doi:10.1016/j.bbrc.2008.04.171
281. Fiorucci S, Antonelli E, Rizzo G, et al. The nuclear receptor SHP mediates inhibition of hepatic stellate cells by FXR and protects against liver fibrosis. *Gastroenterology*. 2004;127(5):1497-1512. doi:10.1053/j.gastro.2004.08.001
282. Cariello M, Peres C, Zerlotin R, et al. Long-term Administration of Nuclear Bile Acid Receptor FXR Agonist Prevents Spontaneous Hepatocarcinogenesis in Abcb4<sup>-/-</sup> Mice. *Sci Rep*. 2017;7(1):1-11. doi:10.1038/s41598-017-11549-7
283. Spatz M, Ciocan D, Merlen G, et al. Bile acid-receptor TGR5 deficiency worsens liver injury in alcohol-fed mice by inducing intestinal microbiota dysbiosis. *JHEP Reports*. 2021;3(2):100230. doi:10.1016/j.jhepr.2021.100230
284. Ferrell JM, Pathak P, Boehme S, Gilliland T, Chiang JYL. Deficiency of Both Farnesoid X Receptor and Takeda G Protein-Coupled Receptor 5 Exacerbated Liver Fibrosis in Mice.

## References

---

- Hepatology*. 2019;70(3):955-970. doi:10.1002/hep.30513
285. Yazen Alnouti, Iván L. Csanaky and CDK. Quantitative-Profilng of Bile Acids and their Conjugates in Mouse Liver, Bile, Plasma, and Urine Using LC-MS/MS. *J Chromatogr B Anal Technol Biomed Life Sci*. 2008;873(2):209-217. doi:10.1016/j.jchromb.2008.08.018. Quantitative-Profilng
286. Fuchs CD, Paumgartner G, Mlitz V, et al. Colesevelam attenuates cholestatic liver and bile duct injury in *Mdr2*<sup>-/-</sup> mice by modulating composition, signalling and excretion of faecal bile acids. *Gut*. 2018;67(9):1683-1691. doi:10.1136/gutjnl-2017-314553
287. Tian X, Wang Y, Lu Y, et al. Conditional depletion of macrophages ameliorates cholestatic liver injury and fibrosis via lncRNA-H19. *Cell Death Dis*. 2021;12(7):1-13. doi:10.1038/s41419-021-03931-1
288. El Kasmi KC, Vue PM, Anderson AL, et al. Macrophage-derived IL-1 $\beta$ /NF- $\kappa$ B signaling mediates parenteral nutrition-associated cholestasis. *Nat Commun*. 2018;9(1). doi:10.1038/s41467-018-03764-1
289. Soderborg TK, Clark SE, Mulligan CE, et al. The gut microbiota in infants of obese mothers increases inflammation and susceptibility to NAFLD. *Nat Commun*. 2018;9(1):1-12. doi:10.1038/s41467-018-06929-0
290. Ikenaga N, Liu SB, Sverdllov DY, et al. A new *Mdr2*<sup>-/-</sup> mouse model of sclerosing cholangitis with rapid fibrosis progression, early-onset portal hypertension, and liver cancer. *Am J Pathol*. 2015;185(2):325-334. doi:10.1016/j.ajpath.2014.10.013
291. Li J, Dawson PA. Animal models to study bile acid metabolism. *Biochim Biophys Acta - Mol Basis Dis*. 2019;1865(5):895-911. doi:10.1016/j.bbadis.2018.05.011
292. Dueland S, Reichen J, Everson GT, Davis RA. Regulation of cholesterol and bile acid homeostasis in bile-obstructed rats. *Biochem J*. 1991;280(2):373-377. doi:10.1042/bj2800373
293. Gustafsson J. Effect of biliary obstruction on 26-hydroxylation of C27-steroids in bile acid synthesis. *J Lipid Res*. 1978;19(2):237-243. doi:10.1016/s0022-2275(20)41563-9
294. Johansson H, Svensson JF, Almström M, et al. *Regulation of Bile Acid Metabolism in Biliary Atresia: Reduction of FGF19 by Kasai Portoenterostomy and Possible Relation to Early Outcome*. Vol 287.; 2020. doi:10.1111/joim.13028
295. Schaap FG, van der Gaag NA, Gouma DJ, Jansen PLM. High expression of the bile salt-homeostatic hormone fibroblast growth factor 19 in the liver of patients with extrahepatic cholestasis. *Hepatology*. 2009;49(4):1228-1235. doi:10.1002/hep.22771
296. Inagaki T, Choi M, Moschetta A, et al. Fibroblast growth factor 15 functions as an enterohepatic signal to regulate bile acid homeostasis. *Cell Metab*. 2005;2(4):217-225. doi:10.1016/j.cmet.2005.09.001
297. Kunzmann LK, Schoknecht T, Poch T, et al. Monocytes as Potential Mediators of Pathogen-Induced T-Helper 17 Differentiation in Patients With Primary Sclerosing Cholangitis (PSC). *Hepatology*. 2020;72(4):1310-1326. doi:10.1002/hep.31140
298. Liaskou E, Zimmermann HW, Li KK, et al. Monocyte subsets in human liver disease show distinct phenotypic and functional characteristics. *Hepatology*. 2013;57(1):385-398. doi:10.1002/hep.26016
299. Zimmermann HW, Seidler S, Nattermann J, et al. Functional contribution of elevated circulating and hepatic non-classical CD14<sup>+</sup>CD16<sup>+</sup> monocytes to inflammation and human liver fibrosis. *PLoS One*. 2010;5(6). doi:10.1371/journal.pone.0011049
300. Gleeson D, Ruppin DC, Saunders A, Murphy GM, Dowling RH. Final outcome of ursodeoxycholic acid treatment in 126 patients with radiolucent gallstones. *Qjm*. 1990;76(1):711-729. doi:10.1093/oxfordjournals.qjmed.a068477
301. Sinakos E, Marschall HU, Kowdley K V., Befeler A, Keach J, Lindor K. Bile acid changes after

## References

---

- high-dose ursodeoxycholic acid treatment in primary sclerosing cholangitis: Relation to disease progression. *Hepatology*. 2010;52(1):197-203. doi:10.1002/hep.23631
302. Thorp E, Vaisar T, Subramanian M, Mautner L, Blobel C, Tabas I. Shedding of the Mer tyrosine kinase receptor is mediated by ADAM17 protein through a pathway involving reactive oxygen species, protein kinase C $\delta$ , and p38 Mitogen-activated Protein Kinase (MAPK). *J Biol Chem*. 2011;286(38):33335-33344. doi:10.1074/jbc.M111.263020